
[All ETDs from UAB](#)

[UAB Theses & Dissertations](#)

2014

Development of a Patient-Derived Xenograft Model of Ovarian Cancer to Characterize the Chemotherapy Resistant Population

Zachary Christopher Dobbin
University of Alabama at Birmingham

Follow this and additional works at: <https://digitalcommons.library.uab.edu/etd-collection>



Part of the [Medical Sciences Commons](#)

Recommended Citation

Dobbin, Zachary Christopher, "Development of a Patient-Derived Xenograft Model of Ovarian Cancer to Characterize the Chemotherapy Resistant Population" (2014). *All ETDs from UAB*. 1534.
<https://digitalcommons.library.uab.edu/etd-collection/1534>

This content has been accepted for inclusion by an authorized administrator of the UAB Digital Commons, and is provided as a free open access item. All inquiries regarding this item or the UAB Digital Commons should be directed to the [UAB Libraries Office of Scholarly Communication](#).

DEVELOPMENT OF A PATIENT-DERIVED XENOGRAFT MODEL OF OVARIAN
CANCER TO CHARACTERIZE THE CHEMOTHERAPY RESISTANT
POPULATION

by

ZACHARY C. DOBBIN

CHARLES N. LANDEN, CHAIR
ROBIN LORENZ, MSTP ADVISOR
RONALD D. ALVAREZ
MARY-ANN BJORNSTI
MICHAEL CONNER
G. YANCEY GILLESPIE

A DISSERTATION

Submitted to the graduate faculty of The University of Alabama at Birmingham,
in partial fulfillment of the requirements for the degree of
Doctor of Philosophy

BIRMINGHAM, ALABAMA

2014

Copyright by
ZACHARY CHRISTOPHER DOBBIN
2014

DEVELOPMENT OF A PATIENT-DERIVED XENOGRAFT MODEL OF OVARIAN
CANCER TO CHARACTERIZE THE CHEMOTHERAPY RESISTANT
POPULATION

ZACHARY C. DOBBIN

CANCER BIOLOGY

ABSTRACT

Ovarian cancer while the second most common gynecologic malignancy is the most common cause of death due to a gynecologic malignancy and the fifth most common cause of death to cancer in women. In 2014, there will be an expected 21,980 cases and 14,270 deaths. Unfortunately, the five-year survival for ovarian cancer is only 40% and this has barely increased over the past 30 years. New approaches need to be developed in order to study ovarian cancer and identify methods of overcoming chemotherapy resistance. This dissertation presents the work conducted in the development of a patient-derived xenograft model of ovarian cancer to characterize the chemotherapy resistant population and identify novel methods of targeting ovarian cancer. The ovarian cancer patient-derived xenograft model recapitulates the heterogeneity of the patients' tumor and has demonstrated clinical relevance in response to primary therapy. Using RNA-seq, it was identified that ribosomal synthesis was up-regulated and targeting RNA Polymerase I is a potential method of overcoming chemotherapy resistance. Using a patient-derived xenograft model provides a novel platform for understanding chemotherapy resistance and recurrence in ovarian cancer.

Keywords: Ovarian Cancer, Patient-derived xenograft, RNA Polymerase I

DEDICATION

This dissertation is dedicated first and foremost to my lovely wife, Johanna. I could not have completed this work without her support and love through both the frustrations and successes. She kept me focused on the goal of finishing my degree and making sure I did the best work I could do.

Second, I dedicate this dissertation to my parents. Their love, support, and encouragement throughout my schooling have driven me to challenge myself and reach new heights.

Lastly, I dedicate this dissertation to my undergraduate mentor Dr. Ayesha Shajahan who was a driving force in convincing me to pursue my PhD and MD.

ACKNOWLEDGMENTS

First, I must acknowledge my PhD dissertation committee. Their guidance has taught me to be a better scientist and always strive to answer the next question. Also, I must acknowledge the UAB Medical Scientist Training Program led by Dr. Robin Lorenz. Their support both financial and moral was imperative to my success. Finally, I must thank my mentor, Dr. Charles Landen for showing me the true meaning of being a physician-scientist and providing a model that I wish to emulate when I have completed my training. With his guidance and support, I have been given the tools needed to be successful in my future endeavors.

TABLE OF CONTENTS

	<i>Page</i>
ABSTRACT	iii
DEDICATION	iv
ACKNOWLEDGMENTS	v
LIST OF TABLES	viii
LIST OF FIGURES	ix
INTRODUCTION	1
Ovarian Cancer	1
Incidence, presentation, and standard of care	1
Pathogenesis of epithelial ovarian cancer	3
Cancer Stem Cells	4
Definition of Cancer Stem Cells and the Cancer Stem Cell Hypothesis	4
Evidence of Cancer Stem Cells in Ovarian Cancer	8
Markers of ovarian cancer stem cells	11
Clinical significant of ovarian cancer stem cells	12
Patient-Derived Xenograft Models	13
THE IMPORTANCE OF THE PI3K/AKT/MTOR PATHWAY IN THE PROGRESSION OF OVARIAN CANCER	19
USING HETEROGENETIY OF THE PATIENT-DERIVED XENOGRAFT MODEL TO IDENTIFY THE CHEMORESISTANT POPULATION IN OVARIAN CANCER	46
TARGETING RNA-POLYMERASE I USING CX-5461 AS A MECHANISM FOR TREATING CHEMOTHERAPY RESISTANT EPITHELIAL OVARIAN CANCER	86
DISCUSSION	107
Summary of Key Findings	107

TABLE OF CONTENTS (Continued)

Current and Future Directions 109
 Development of a fully chemotherapy resistant ovarian cancer PDX..... 109
 Targeting cancer stem cells in the chemotherapy resistant PDX 111
 Identifying novel pathways to target chemotherapy resistance in ovarian
 cancer..... 113
 Autophagy in ovarian cancer PDX..... 116
 Conflict between induction of autophagy and ribosome translation 118

Final Conclusions 120

GENERAL REFERENCES 122

APPENDIX A: INSTITUTIONAL REVIEW BOARD APPROVAL FORM 130

APPENDIX B: INSTITUTIONAL ANIMAL CARE AND USE COMMITTEE
APPROVAL FORM..... 131

LIST OF TABLES

<i>Table</i>	<i>Page</i>
USING HETEROGENEITY OF THE PATIENT-DERIVED XENOGRAFT MODEL TO IDENTIFY THE CHEMORESISTANT POPULATION IN OVARIAN CANCER	
1	Patient demographics of implanted and growing patient-derived xenograft lines 66
2	RNAseq analysis on PDX comparing 6 pairs of treated and untreated samples 67
3	RNAseq revealed 299 genes that had significantly ($p < 0.05$) higher expression in the treated PDX samples versus the untreated PDX lines 77
TARGETING RNA-POLYMERASE I USING CX-5461 AS A MECHANISM FOR TREATING CHEMOTHERAPY RESISTANT EPITHELIAL OVARIAN CANCER	
1	Mutational status and IC_{50} of CX-5461 in the ovarian cancer cell lines tested 99

LIST OF FIGURES

<i>Figures</i>	<i>Page</i>
INTRODUCTION	
1 Model of clonal evolution of a tumor	5
2 Initial model of the cancer stem cell theory	6
3 The fluid model of the CSC hypothesis	9
4 Ovarian cancer patient-derived xenograft model	17
USING HETEROGENEITY OF THE PATIENT-DERIVED XENOGRAFT MODEL TO IDENTIFY THE CHEMORESISTANT POPULATION IN OVARIAN CANCER	
1 Take rates of different sites of implantation and maintenance of PDX histology	68
2 Establishment of the PDX line does not enrich for the tumorigenic cell population and human stroma is replaced in the implanted PDX	69
3 Cancer drug targets are maintained in the PDX line and the PDX response to treatment correlates to the patient's response to primary chemotherapy	70
4 Chemotherapy treatment reduces proliferation and enriches the PDX for cancer stem cells	71
5 RNAseq comparing the treated PDX lines to the untreated PDX lines	72
6 The SABiosciences RT ² qPCR array for cancer drug targets was run on the patient's tumor and their matched untreated PDX tumor	85
TARGETING RNA-POLYMERASE I USING CX-5461 AS A MECHANISM FOR TREATING CHEMOTHERAPY RESISTANT EPITHELIAL OVARIAN CANCER	
1 Expression of RNA Polymerase I initiation factors in ovarian cancer PDX models	100
2 Response of ovarian cancer cell lines to CX-5461	101

LIST OF FIGURES (Continued)

<i>Figures</i>	<i>Page</i>
TARGETING RNA-POLYMERASE I USING CX-5461 AS A MECHANISM FOR TREATING CHEMOTHERAPY RESISTANT EPITHELIAL OVARIAN CANCER (continued)	

3	Treatment of ovarian cancer PDX with CX-5461 102
4	Response of ribosomal translation factors after CX-5461 treatment 103

DISCUSSION

1	Model of development for a chemotherapy-resistant PDX 110
2	Comparison between chemotherapy sensitive and resistant PDX 112
3	Treatment of PDX-136-Resistant with 673A and chemotherapy 114
4	Treatment of pDX-136-Sensitive with 673A and chemotherapy 115
5	Analysis of autophagy induction in treated PDX tumors 117

GENERAL INTRODUCTION

Ovarian Cancer

Incidence, presentation, and standard of care

Ovarian cancer, while the second most common gynecologic malignancy, is the most common cause of death due to a gynecologic malignancy and the fifth most common cause of death due to cancer [1]. In 2014, there will be an expected 21,980 cases and 14,270 deaths [1]. While ovarian cancer encompasses multiple subtype such as epithelial, stromal, and germ cell varieties, the most common and most deadly are the epithelial. Along with primary peritoneal and fallopian tube cancer, this group accounts for approximately 80% of “ovarian” malignancies[2, 3].

In women that are diagnosed with ovarian cancer, the average 5-year survival is only 40% and this has barely increased over the past 30 years [4]. In patients that are diagnosed with localized disease or regional disease, 5-year survival is 93.8% and 72.8% respectively, while the 5-year survival of metastatic disease, the survival is ~28% [5]. Unfortunately, 70% of patients present with advanced disease. The high mortality rate of ovarian cancer is primarily due to two factors: (1) the high incidence of patients presenting with advanced disease and (2) the high rate of recurrence, despite successful initial therapy. Clinically, the symptoms of ovarian cancer are non-descript as a patient or physician is unlikely to palpate a mass when the disease is still localized. Clinical symptoms of ovarian cancer are bloating, urinary urgency and frequency, difficulty eating or early satiety, and pelvic or abdominal pain [6, 7]. These symptoms are typically sub-acute and nonspecific, and so frequently are downplayed by patients or physicians, allowing for the disease to develop to a more advanced stage. Acute symptoms of ovarian cancer can in-

clude a pleural effusion or bowel obstruction, though when patients present with these symptoms they have advanced disease [8]. With these ambiguous symptoms, there have been efforts to develop methods of early detection; such as following serum CA-125 levels prior to diagnosis in combination with transvaginal ultrasound. Unfortunately, these methods have not resulted in early detection of ovarian cancer [9].

After diagnosis of ovarian cancer, the primary treatment is a surgical tumor reduction surgery followed by chemotherapy treatment, although administration of chemotherapy prior to surgery is become more common. The primary tumor reductive surgery should consists of a thorough exploratory laparotomy with staging, a total abdominal hysterectomy, and bilateral salpingo-oophorectomy [3]. The goal of surgery is to bring the patient to no residual disease, as patients that have an optimal cytoreduction have a median survival of 39 months compared to patients with a suboptimal cytoreduction who have a median survival of 17 months [10-12]. Following surgical management, patients typically undergo six cycles of a platinum and taxane-based chemotherapy regimen. Interestingly, approximately 50% of patients treated with platinum/taxane-based therapy will achieve a complete clinical response. However, if those patients undergo a second-look laparotomy, 50% will be positive for residual disease, and the 50% with no detectable disease will eventually relapse [5]. This leads to the somber fact that 75% of patients will eventually have a recurrence, and these recurrences become less and less responsive to current chemotherapy regimens [13]. These features lead to the hypothesis that there is a residual surviving population of cells that result in recurrence and eventual chemotherapy resistance [14, 15]. For advances to be made in survival of ovarian cancer, new therapies have to be developed that target the chemotherapy resistant population of cells.

Pathogenesis of Epithelial Ovarian Cancer

Despite its name, it is believed that all not ovarian cancers arise from the ovary. Research suggests that many epithelial “ovarian” cancers arises from the ovary or the fallopian tube and occasionally from the peritoneal lining of the abdominal and pelvic cavity [16]. Tumors that are believed to arise from the ovary proper tend to have the following histologies: endometrioid, mucinous, clear cell, borderline, and low grade serous. Tumors arising from the fallopian tubes or the peritoneal lining are typically of a high-grade serous histology. Traditionally, epithelial ovarian cancer was classified based on histological subtype. However, with the advent of genomic sequencing, and the recently complete Cancer Genome Atlas (TCGA) for ovarian cancer, it has been proposed that it is more accurate to classify epithelial ovarian cancer into Type I and Type II [17]. Type I is considered low-grade, and while relatively resistant to platinum-based therapy, it presents at an early stage and is easily managed through surgical intervention [17, 18]. Type II encompasses high grade serous and undifferentiated cancers that present at more advanced stages, and while more aggressive in growth tend to respond to platinum-based therapy initially [18]. Analysis by the TCGA has indicated that high-grade serous ovarian cancer (Type II) is defined predominately by *TP53* mutations in 96% of tumors [19]. In addition, one heavily mutated pathway in epithelial ovarian cancer is the PI3K/Akt/mTOR pathway which is described in *Section 2: The importance of the PI3K/AKT/MTOR pathway in the progression of ovarian cancer* (pp 19 – pp. 46) of this dissertation.

Cancer Stem Cells

Definition of Cancer Stem Cells and the Cancer Stem Cell Hypothesis

As mentioned above, while most patients present with advanced disease, a majority of patients will have a complete clinical response to primary chemotherapy only to later develop recurrence and resistance. This scenario of high initial response, followed by high recurrence and resistance indicates the presence of a cell population that survives initial therapy and repopulates the tumor. This population of cells has been hypothesized to be so-called tumor-initiating-cells (TICs), cancer stem cells (CSC), or therapy-resistant cells, however for consistency, only CSC will be used in this section.

In the last two decades, there has been a resurgence of the CSC model when describing tumor growth as opposed to the clonal evolution model that precedes it. Clonal evolution of cancer is the theory that each cell of a tumor possesses the ability to acquire genetic changes that would give the cell the ability to form a tumor (Figure 1)[20, 21]. However evidence was found in the 1970s that only a limited sub-population of cells in a tumor have the ability to form a tumor, self-renew, and differentiate (Figure 2)[22, 23], at least in mouse xenograft models. It was theorized that CSC had the ability to self-renew and undergo differentiation while their offspring had limited ability to self-renew and proliferate. This hypothesis then led to speculation that this was also the population most resistant to therapy. In the CSC hypothesis, it is accepted that there are two key observations that must be observed for defining a potential CSC population. First, only a minority of cancer cells within the heterogeneous tumor have tumorigenic potential when implanted into immunocompromised animals.



Figure 1: *Model of clonal evolution of a tumor.* In the clonal evolution model, where all cells are derived from a single cell and are divided into subpopulations resulting from specific mutations and selection fitness. Each subclone population is able to divide and form a new tumor.

Adapted from: O'Connor, ML. *Cancer Stem Cells: A Contentious hypothesis now moving forward.* Cancer Letters, Volume 344, Issue 2, 180-187. Used with permission from Elsevier Ireland, LTD.

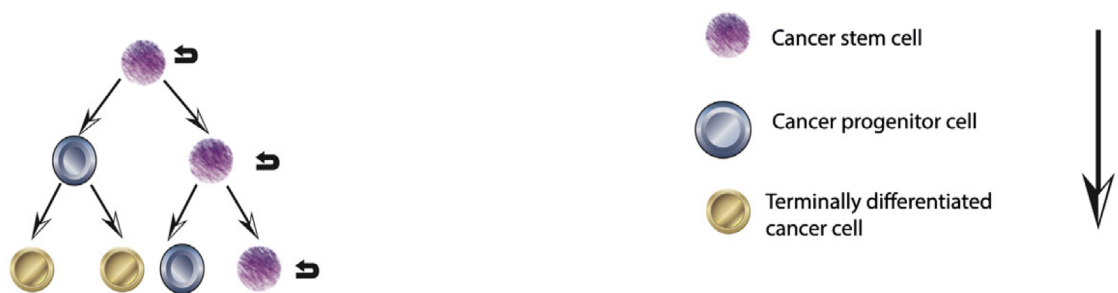


Figure 2: *Initial model of the cancer stem cell theory.* The original CSC model, a mirage to the cellular hierarchy in normal tissue, with the exception of unregulated control of CSC driving tumorigenesis.

Adapted from: O'Connor, ML. *Cancer Stem Cells: A Contentious hypothesis now moving forward.* Cancer Letters, Volume 344, Issue 2, 180-187. Used with permission from Elsevier Ireland, LTD.

This is investigated by injecting in serial dilutions isolated single cell populations of cells into animals. CSCs are more tumorigenic and able to form tumors at much lower numbers than injecting non-CSC cells [20, 24, 25]. While this is considered the gold-standard for functionally identifying CSC populations, some researchers argue that this method just measures the ability of human tumors cells to grow in mice [26, 27]. The second feature of a CSC refers to its ability to differentiate into CSC and non-CSC populations. This demonstrates enhanced differentiating capacity [28].

Evidence describing CSCs was first reported in 1994 by Lapidot *et al* in an model of human acute myeloid leukemia (AML). They were able to identify a subpopulation of cells that were CD34⁺ and CD38⁻ and that were the only cells that were tumorigenic and were able to fully re-capitulate the AML disease phenotype in mice [29]. In this study, a malignant phenotype could be created with the injection of a single cell. With this discovery, research quickly moved in the direction of identifying CSC in solid tumors. However, studying CSC in solid tumors had the added complexity of having to reduce a tumor mass to a single-cell population while also maintaining cell viability. CSCs were identified in gliomas by the observation of the formation of “neurospheres” that had properties of stem cells [30] which led to the identification of CD133⁺ subpopulation in glioblastoma meeting the definition of CSC [24, 31]. These studies showed that as few as 100 CD133⁺ cells needed to be injected for a tumor that recapitulated the entire heterogeneity of a human glioblastoma [24]. Since these first studies, CSCs have been identified in breast, colon, ovarian, and multiple other cancers using the same methods of serial dilution of a putative population and tumorsphere growth [32-35]. In cancer treatment, resistance to available chemotherapies and even molecularly targeted therapies is a major

cause of treatment failure [36]. There have been studies that suggest CSCs are the reason for tumor relapse and are the cause of chemotherapy resistance [20]. Reasons for CSC resistance to chemotherapy include increased expression of drug transporters, up-regulation of anti-apoptotic proteins, increased efficiency of DNA repair, and alterations in cell cycle kinetics [37]. Current chemotherapy treatment options results in elimination of the non-CSC population, therefore durable cures can only be completed if therapy targets both the CSC and non-CSC population. When comparing the CSC model to the clonal evolution model and the evidence supporting both, it is entirely possible that the actual evolution and development of cancer is a hybrid of the two models (Figure 3). While CSC do make up a population of cells responsible for the recurrence and growth of a tumor, it is equally likely that some differentiated tumor cells have the ability to de-differentiate to a more CSC-like format in the face of evolutionary pressures.

Evidence of Cancer Stem Cells in Ovarian Cancer

While it is possible that the CSC hypothesis doesn't fully apply to every solid cancer, in ovarian cancer the CSC hypothesis fits well with the clinical progression over the course of treatment. As mentioned above, in ovarian cancer, while approximately 70% of patients will have a complete clinical response to surgery and chemotherapy [5], eventually 80% will have recurrence and a five-year survival rate of 40-50% [13]. This type of clinical response isn't observed in other cancers such as colorectal or prostate when the patient presents with advanced disease [38]. This clinical course for ovarian cancer indicates that there is a population of tumor cells that survived initial therapy to later cause recurrence and eventual chemotherapy resistance. In addition to the clinical



Figure 3: *The fluid model of the CSC hypothesis.* In the fluid CSC model, both progenitor cells and differentiated cells are able to re-acquire self-renewal potential.

Adapted from: O'Connor, ML. *Cancer Stem Cells: A Contentious hypothesis now moving forward.* Cancer Letters, Volume 344, Issue 2, 180-187. Used with permission from Elsevier Ireland, LTD.

course of response, recurrence, diminished response, resistance, there is other evidence that helps fit ovarian cancer pathogenesis within the CSC hypothesis. First, ovarian surface epithelium is more mesenchymal in appearance and usually less differentiated than other epithelial cells [38-40]. The CSC hypothesis becomes more applicable when considering the fallopian tubes as a source of ovarian cancer, as the cells in the fallopian tube represent tissue with a high turnover and the presence of normal stem cells that give rise to differentiated cells [41, 42].

While ovarian cancer histologically presents with multiple subtypes including papillary serous, endometrioid, clear cell, and mucinous that could arise from different cells of origins, it is the rate of “mixed histology” lesions that provides evidence that potential ovarian CSC have the ability to be multipotent and differentiate. Ovarian cancer is extremely heterogeneous, and it is not known if the CSCs are present in the initial tumor or induced by chemotherapy. There have been studies that have isolated putative CSC from primary tumors that were therapy naïve and demonstrated the properties of CSC such as chemotherapy resistance, and ability to differentiate [38]. One group used lineage tracing in colonic adenomas to provide support for the initial existence of CSC prior to therapeutic intervention [43]. Humphries *et al* found that while initially in a quiescent state, the CSC were activated and stochastically expand in response to stressors, such as chemotherapy after primary surgery. Some studies have shown that chemotherapy can induce a stem-like quality to tumor cells, but it is unlikely that this is the sole method for generation of chemotherapy-resistant CSC [38]. Other gynecologic malignancies, such as gestational trophoblastic disease and ovarian germ cell tumors can have durable cures with the same chemotherapy regimens that are used in ovarian cancer. While the origin of CSC

can be debated for ovarian cancer, the reality is that there is a significant body of evidence that CSC, in some form, do exist in ovarian cancer and they are likely the cell population responsible for recurrence and eventual chemotherapy resistance. Therefore, developing methods to target this population is necessary in order to combat recurrence and improve outcomes for patients.

Markers of ovarian cancer stem cells.

Initial experiments that identified ovarian cancer stem cells focused on markers that were used in other malignancies, such as CD133 in glioblastoma [24]. In ovarian cancer, the primary markers that have been widely accepted as markers for CSC in ovarian cancer are CD133, CD44, ALDH1A1, and ABCG2. ALDH1A1 is aldehyde dehydrogenase, which is responsible for processing toxic aldehydes produced in metabolic processes. It is identified using a functional assay called the ALDEFLUOR assay, which is also used to isolate stem cells from bone marrow to be used in stem-cell transplantations [44]. Outside of ovarian cancer, ALDH1A1 has been used as a marker for CSC and is usually an indicator of poor prognosis in head and neck cancer, breast cancer, and rectal cancer [45-47]. ALDH1A1 has been found to not only to be up-regulated in ovarian cancer cell lines that have developed chemoresistance, but targeting ALDH1A1 with siRNA results in a restoration of sensitivity to cisplatin [48]. ALDH1A1 expression has also been correlated with a poor prognosis, pluripotency, self-renewal, and increased tumorigenesis [48-50].

CD44 is a receptor for the extracellular matrix component hyaluronic acid that has been shown to activate several survival pathways via activation of ERBB2-ERBB3 and via activation of survival aspects of the PI3K/Akt/mTOR pathway [51]. In addition, cells

with CD44 expression have an increase in tumorigenesis, the ability to form spheroids, and recapitulate the parental tumor [35, 52-54]. CD133 is an interesting marker because while it has been identified in CSC for multiple malignancies, it is unknown what its exact function is. While a surface marker, in some studies it has been associated with a poor prognosis [48, 49, 55], and in other studies it has been correlated to a good prognosis [56]. However, studies have shown that CD133 marks a population of cells that have an increase in tumorigenicity and is related to chemotherapy resistance [57, 58]. While these are the most common CSC markers for ovarian cancer, it takes multiple studies using multiple methods to confirm a marker and even then the result can be contradictory. As presented in *Section 3 (pp. 47 – pp. 86)*, these markers do not represent the entire surviving population after chemotherapy treatment indicating that more markers need to be elucidated.

Clinical significance of ovarian cancer stem cells

Traditionally the discovery and characterization of putative CSCs takes place in the laboratory with techniques that result in the dissociation and separation of the tumor [25]. Once a CSC is identified, it is imperative that it is validated using clinical specimens. There have been studies that have shown CSC expression at diagnosis is correlated with poor outcome in CD44[56], in CD133 [49, 59], or ALDH1A1 [48]. In addition, if CSCs are mediating the development of recurrence and chemoresistance, they should be more prevalent in recurrent and resistant tumors in patients. One study that examined the ascites of patients after recurrence following first-line platinum therapy found they were enriched for side-population cells [60]. When tumors are compared pre- and post-treatment, CD133 was found to be more highly expressed in the post-treatment tumors

and still expressed tumor-initiating properties [61]. In a study that looked at matched primary, recurrent and resistant tumors, recurrent-chemoresistant tumors were significantly more enriched in ALDH1A1 and CD133 [62]. Interestingly, the tumors at presentation and first recurrence were remarkably similar in density of CSC, while tumors analyzed at the persistent stage and chemoresistant stage had a significant increase for at least one CSC marker [62]. These data demonstrates that the cells surviving chemotherapy after surgery are heavily enriched for CSC that must then divide and differentiate into the heterogeneous mass that presents at first recurrence. The Steg *et al* study also identified pathways believed to be involved in “stemness” to be upregulated in the recurrent samples including TGF-beta, Notch, Wnt, and Hedgehog. While currently accepted CSC markers for ovarian cancer may not represent the definitive guide, it is important for research to identify methods to target these populations in order for durable cures to be developed.

Patient-Derived Xenograft Models

The primary method of pre-clinical research for drug discovery has been the use of clonal cell lines. While cell lines provide many benefits including the ability to replicate experiments, identify and interrogate individual genes and proteins in a pathway, they have limitations as well. Cancer cell lines lack the heterogeneity of the patients’ tumors, and some cases have been maintained in plastic for over 30 years with little resemblance to the original tumor [63]. With the advent of full genomic sequencing, there have been examples of ovarian cancer cell lines having more in common to other cell lines of other tumor types than primary ovarian cancer tumor cells [64]. More recently after the

publishing of the TCGA for ovarian cancer, the most commonly used ovarian cancer cell lines were found to be very dissimilar from papillary serous carcinoma, the disease responsible for most ovarian cancer deaths [65]. These problems have led to a high rate of failure for drugs in the clinical trial setting after seeing success in pre-clinical experiments [66].

Attempts to solve the problems of cancer cell lines have led to the development of genetic-engineered mouse models that develop spontaneous tumors and the patient-derived xenograft model (PDX). Genetically engineered mice are useful for studying the origins and biology of disease; they still pose the problem of having to understand the genetic initiating events of a cancer and furthermore are still murine tumors and not comprised of human cells. PDX models on the other hand are established by the direct implantation of a patient's tumor into immunodeficient mice [67]. When a tumor is implanted into the mice, it can either be in a heterotopic location or an orthotopic location. Heterotopic, such as the flank of the animal, allows for technical ease in terms of implantation and following tumor growth [68]. Orthotopic, while more complex depending on location implanted allows for the tumor to grow in its "natural" environment [69]. Unfortunately, PDX models have some limitations that have made them used sparingly in large scale pre-clinical studies. First, PDX models are very time intensive, with the first generation of tumor growth after implantation not occurring from anywhere from two to twelve months [70-73]. Another problem with the PDX model is that engraftment rates varies widely with cancers, and historically has been reported to be anywhere from 23% to 75% depending on tumor type. Interestingly, higher engraftment rates are typically seen with more aggressive tumors [74]. However, the advantages of the PDX model can-

not be ignored. PDX models, when established, allow for a tumor that recapitulates the original patient's tumor heterogeneity. This recapitulation of the various cellular components of a tumor have resulted in many PDX models having a high correlation to drug response as the patients do in the clinic [75-77]. In theory, this would allow for accurate pre-clinical trials regarding therapeutics and perhaps more importantly, the ability to study the natural progression of a cancer as it is treated and re-treated with various chemotherapeutics. Using the PDX model in this capacity could allow for the unearthing of mechanisms of chemotherapy resistance that have been elusive to identify in clonal cell lines.

Goals of Dissertation

To date, ovarian cancer is in desperate need of novel therapeutics and a greater understanding of the eventual development of chemotherapy resistance. The use of PDX models in ovarian cancer to date has been limited to a few models established with either characterization of the genetics of the tumor or response to a pre-clinical drug target. Recently, there was a published cohort of 168 ovarian PDX models engrafted in the intra-peritoneal cavity with the primary goal of testing novel therapeutics [71]. For this dissertation, the goal was to establish a PDX model of ovarian cancer that could be used to study the development of chemotherapy resistance in order to gain a better understanding of the pathways involved in chemotherapy resistance.

In Section 2 (pp. 19 – pp. 45), a thorough review of the potential role of the PI3K/Akt/mTOR pathway's role in ovarian cancer is described. The recent release of the Cancer Genome Atlas for ovarian cancer showed that the PI3K/Akt/mTOR pathway was

one of the most frequently mutated or altered pathway in patient's tumors. In this section, a review of the normal role of the PI3K/Akt/mTOR pathway is discussed. The PI3K/Akt/mTOR pathway has been implicated in the tumorigenesis of ovarian cancer, with many members of the pathway, such as PTEN, being shown to be key initial driver mutations. In addition to tumorigenesis, the PI3K/Akt/mTOR pathway has active roles in tumor progression and proliferation.

Section 3 (pp. 46 – pp. 85) focuses on research in the development of the ovarian cancer PDX model and its use to identify potential pathways involved in survival of chemotherapy. The ovarian PDX model was established by first comparing the optimal growth site: subcutaneous (SQ), mammary fat pad (MFP), intraperitoneal (IP), and sub-renal capsule (SRC). The SQ and MFP sites were used in initial studies as they represent heterotopic sites that could be easily followed using caliper measurements. In addition, growth of tumor in these locations caused minimal complications for the animal during tumor growth and development. IP was tested as this would represent the orthotopic site and could potentially provide a more appropriate environment for tumor development. Finally the SRC was tested as previous reports in the literature found an engraftment rate of greater than 90% in this location [78]. After establishment of the model, the ovarian cancer PDX mice were subjected to a combination therapy of carboplatin and paclitaxel to simulate what the patient would receive in the clinic (Figure 4). This was done to allow for clinical relevance of the model to be established. In addition PDX tumors were profiled using RNA-Seq and oncogene cancer panels to show genetic similarities to the patient tumor and gain a global understanding of what pathways are being activated in response to chemotherapy treatment. The prevalence of CSCs was also assessed in the PDX

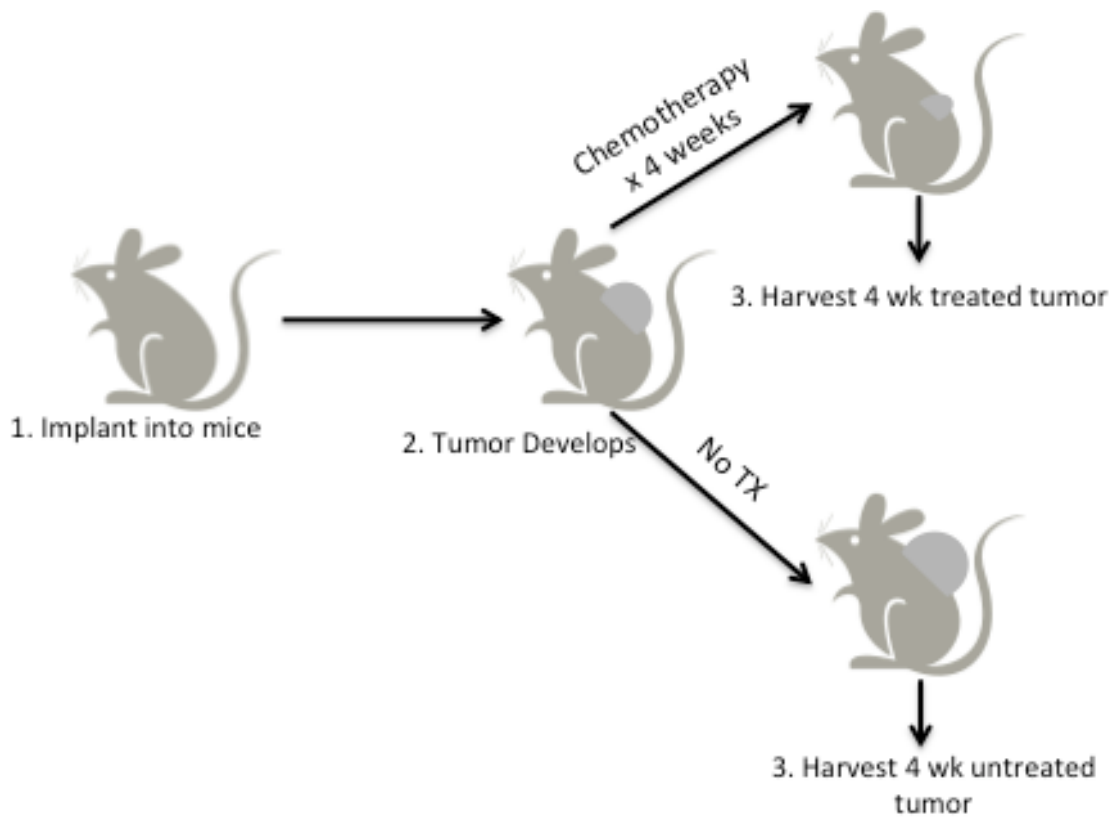


Figure 4: *Ovarian Cancer Patient-Derived Xenograft Model.* The ovarian cancer PDX model is established by first implanting tumors into mice. After the tumor develops, PDX mice are stratified into two groups: (1) Chemotherapy treatment with carboplatin and paclitaxel for 4 weeks or (2) No treatment for 4 weeks. At the end of treatment, tumor is collected for analysis.

model to determine if they are the cells responsible for chemotherapy resistance.

In Section 4 (pp. 86- pp. 106), data from the RNA-Seq on the chemotherapy ovarian cancer PDX models indicated the prevalence of ribosomal machinery up-regulation in response to chemotherapy. Specifically, there was an increase in gene expression that was related to RNA Polymerase I (Pol I) in the treated ovarian cancer PDX samples. This led to an investigation into the use of a Pol I inhibitor, CX-5461, to evaluate its usefulness in chemotherapy resistant ovarian cancer and the potential use in ovarian cancer patients. In cancer, an increase in the size and number of nucleoli is a marker of an aggressive tumor [79, 80]. An enlarged nucleolus correlates with accelerated ribosomal RNA synthesis. Our studies confirmed that after chemotherapy treatment there was an increase in the total number of ribosomes, chemotherapy resistant ovarian cancer cell lines were more sensitive to Pol I inhibition, and that there is potential utility in targeting ribosomal translation in patients with ovarian cancer as responses were noted in the ovarian cancer PDX model. Finally in Section 5 (Page 107-121), general conclusions and potential future directions are explored.

THE IMPORTANCE OF THE PI3K/AKT/MTOR PATHWAY IN THE PROGRES-
SION OF OVARIAN CANCER

by

ZACHARY C. DOBBIN AND CHARLES N. LANDEN

International Journal of Molecular Sciences

Copyright

2013

by

Multidisciplinary Digital Publishing Institute

Used by permission under the Creative Common Attribution License 3.0

Format adapted and errata corrected for dissertation

ABSTRACT

Ovarian cancer is the fifth most common cause of death due to cancer in women despite being the tenth in incidence. Unfortunately the five-year survival rate is only 45%, which has not improved much in the past 30 years. The reason for such a low rate of survival is even though the majority of women have successful initial therapy; eventually they develop recurrence and succumb to their disease. With the recent release of the Cancer Genome Atlas for ovarian cancer, it was shown that the PI3K/AKT/mTOR pathway was one of the most frequently mutated or altered pathways in patients' tumors. Researching how the PI3K/AKT/mTOR pathway affects the progression and tumorigenesis of ovarian cancer will hopefully lead to new therapies that will increase the survival for women. This review focuses on recent research on the PI3K/AKT/mTOR pathway and its role in the progression and tumorigenesis of ovarian cancer.

INTRODUCTION

Ovarian cancer is the fifth most common cause of death due to cancer in women, despite ranking tenth in incidence [1]. In ovarian cancer, primary treatment is surgical resection of visible disease followed by adjuvant chemotherapy usually consisting of a combination of platinum-based and taxane-based chemotherapy. Currently the five-year survival rate for ovarian cancer is only 45% [1]. This high mortality rate is due to the high incidence of patients presenting with advanced stage disease and the high rate of recurrence despite successful initial therapy. Approximately 50% of all patients treated with 1st-line chemotherapy will achieve a complete clinical response; however, if those

patients undergo a secondary laparotomy 50% of the complete clinical response patients will be positive for residual disease, and rarely ever be disease free[2]. Importantly, even among patients who have no visible or pathologically-detected disease, 50% of those will eventually relapse. This leads to the somber fact that more than 70% of patients will ultimately develop recurrent disease [2].

In order to reduce the high mortality rate seen in ovarian cancer, research is being conducted in early detection [3-5] and in development of new therapeutics to treat recurrence and chemoresistance in ovarian cancer. In terms of treatment of ovarian cancer, many clinical trials have focused on changing the dosing, scheduling, and combination of available chemotherapies in order to improve survival. While there have been moderate improvements, such as using intraperitoneal delivery of chemotherapy, or dose-dense Taxol regimens, cure rates have not changed significantly. Therefore, in order to improve survival, new therapeutics need to be developed that will target the chemoresistant population of ovarian cancers.

In ovarian cancer, numerous targeted therapies have been developed and tested with limited success. This indicates that identification of an advanced ovarian cancer depending on a single gene or on oncogene addiction that can be targeted by a single agent is rare [6]. Furthermore, there is prevailing evidence that ovarian cancers can be broadly classified into two groups, Type I and Type II. Type I ovarian cancer is considered low-grade that will more often present in an early stage but still have relative resistance to platinum-based therapy. Type II ovarian cancers are represented by high grade serous and undifferentiated cancers that present at a late stage and while aggressive, normally initially respond to platinum-based therapy [6].

The Cancer Genome Atlas has identified numerous activating mutations, DNA copy number changes and inactivating mutations in ovarian cancer that demonstrate the complex heterogeneity seen in ovarian cancer. While this complexity indicates that there will likely never be one molecular-targeted therapy that will cure all ovarian cancer, several pathways are frequently abnormal. One such pathway is the PI3K/AKT/mTOR pathway, with mutations or amplifications in 34% of samples analyzed [7]. These include mutations in *PIK3CA*, deletion in *PTEN*, amplification of *AKT1*, *AKT2*, and *AKT3*, which all lead to an aberrant functioning PI3K/AKT/mTOR pathway. In this review, the focus will be on recent research implicating the PI3K/AKT/mTOR pathway in ovarian cancer progression and tumorigenesis.

OVERVIEW OF THE PI3K/AKT/MTOR PATHWAY

The PI3K/Akt/mTOR pathway is a central regulator in both normal cell physiology and in cancer proliferation, tumorigenesis, and metastasis. The pathway is comprised of three main driving molecules: PI3 kinase (PI3K), AKT, and mammalian Target of Rapamycin (mTOR).

The PI3K are a family of lipid kinases that phosphorylate the 3-hydroxyl group of phosphoinositides [8]. There are three classes that make up the PI3K family: Class I, Class II, and Class III [9]. Class I are heterodimers of PI3K consisting of a catalytic p110 subunit and a regulatory p85 subunit. The p110 has 3 isoforms (α , β , and δ). A combination of the p85 subunit and the p110 (α , β , or δ) make up the group known as Class IA PI3K. Class IB is made up of a p101 and 110- γ subunit [8]. Together, the role of Class I PI3K is involved in cell proliferation, insulin signaling, immune function and inflammation [8, 9]. Class II PI3Ks are monomeric catalytic isoforms involved in the regulation of

membrane trafficking, while Class III, solely made up of Vps34, has a role in autophagy [10] It is primarily Class IA PI3K that has been implicated in cancer and have numerous targeted pharmaceuticals being developed or currently in clinical trials.

After PI3K is fully activated, the kinase converts the substrate phosphatidylinositol 4,5-bisphosphate (PI(4,5)-P₂) into PIP(3,4,5)₃. This conversion of PIP₂ to PIP₃ allows for AKT and PDK1 to be brought together near the inside of the cell membrane. This results in AKT, a serine/threonine kinase, being phosphorylated at threonine-308 in its kinase domain. AKT can also be activated by phosphorylation at serine-473 by mTOR-Rictor (MTORC2) which is in the helical domain of AKT [11]. AKT is the central molecule in the PI3K/AKT/mTOR pathway, activating and modulating numerous downstream targets. AKT can stimulate protein synthesis and cell growth by activating mTOR through inhibition of the TSC1/2 complex and modulating cell proliferation by inactivating cell cycle inhibitors [9, 12, 13].

TOR1 and TOR2 were originally discovered in the yeast *Saccharomyces cerevisiae* by the observation that this protein was inhibited by the macrolide rapamycin [14]. Later a structurally and functionally conserved mammalian version was discovered and designated mTOR [15, 16]. mTOR is a 289 kDa serine/threonine kinase that actually belongs to the PI3K-related protein kinase family as its C-terminus shares strong homology to the catalytic domain of PI3K [16]. In the mammalian cell it was discovered that mTOR actually exists in two complexes, mTORC1 and mTORC2 [17, 18]. mTORC1 is made up of Raptor, mTOR, PRAS40, mLST8/GβL, and dector, while mTORC2 contains Rictor, mTOR, mLST8/GβL, Sin1, protor-1, and dector [17, 19]. mTORC2 is unique from mTORC1 not only because of the slight difference in molecules that make up the com-

plex but because it is not sensitive to rapamycin. [17] mTORC1 is sensitive to growth factor stimulation, oxygen levels, or nutrient availability and functions by regulating the phosphorylation of rS6K and 4E-BP1, two proteins involved in the control of protein synthesis, translation initiation, and cell mass. mTORC2 participates in cell survival and proliferation in part through its ability to control AKT activity by phosphorylation of AKT at serine-473 [11].

The role of the PI3K/Akt/mTOR pathway in ovarian cancer is foreshadowed by its role in protecting the primordial follicles from destruction during normal oocyte maturation. Polycyclic aromatic hydrocarbons, which are environmental toxins, are known reproductive toxins that result in primordial follicle atresia causing premature ovarian failure [20]. One polycyclic aromatic hydrocarbon that has been shown to induce ovotoxicity is 3-methylcholanthrene (3MC) [20, 21]. However, until recently the mechanism was not well understood. When murine ovaries are treated with 3MC, follicular atresia is documented, [22] that can be prevented with treatment LY294002, a PI3K inhibitor. In the face of insult by an ovotoxin, the follicles attempt cell survival via up-regulation of the PI3K/AKT/mTOR pathway that paradoxically leads to an increase in follicular proliferation, depleting the reserve of primordial ovarian follicles [22]. This results in the phenotype of premature ovarian failure in 3MC treatment. As in cancer, the PI3K/Akt/mTOR pathway has a key role in promoting cell survival in the normal ovary.

The role of the PI3K/AKT/mTOR pathway in ovarian cancer is extremely complex, arising from two main sources: (1) the diverse alterations found with PI3K/AKT/mTOR pathway itself and (2) the diverse alterations in inputs into the PI3K/AKT/mTOR pathway. Through these various changes, the PI3K/AKT/mTOR

pathway has demonstrated to play a key role in ovarian cancer tumorigenesis, progression, and chemotherapy resistance.

TUMORIGENESIS OF OVARIAN CANCER AND PI3K/AKT/MTOR PATHWAY

Historically, the subtypes of epithelial ovarian cancer have been defined by histology and are primarily classified into papillary serous, endometrioid, mucinous, and clear cell [23, 24]. Recent evidence is leading to the idea that the disease of epithelial ovarian cancer is actually comprised of a spectrum of cancer types that originate from different pelvic organs, most notably from the fallopian tube [6, 25], [26].

While Kim *et al* identified a role for PI3K/AKT/mTOR in the tumorigenesis of Type II ovarian cancer arising from the fallopian tube, other groups have implicated the pathway in the tumorigenesis of Type I ovarian cancer arising from the ovarian bursa. Type I ovarian cancer is considered lower grade than Type II and typically less responsive to traditional chemotherapy [27]. In addition, Type I has frequent cell signaling pathway mutations in KRAS, BRAF, CTNNB1, and PTEN and comprises most endometrioid, clear cell, and mucinous histologies [28] [29]. When *Apc* and *Pten* are conditionally inactivated in the ovarian bursa of a mouse, an endometrioid ovarian carcinoma develops that has nuclear expression of β -catenin and absence of PTEN expression [27].

While the above models required one mutation in PI3K/Akt/mTOR coupled with a mutation in another pathway, if a double knock-out is present with alterations to two members of the PI3K/AKT/mTOR pathway, ovarian tumorigenesis can occur. Using a genetically engineered mouse that was bred to have an activating *PIK3CA*^{H1047R} mutation and be *Pten*^{WT/del}, Kinross *et al* noticed that the mice only had hyperplasia of the ovarian surface epithelium [30]. However, when a second deletion of *Pten* was introduced direct-

ly into the ovarian bursa, the mice developed ovarian serous adenocarcinomas and granulosa cell tumors. This indicates that a secondary defect in a co-regulator of PI3K activity is sufficient in conjunction with a mutant *PIK3CA* for tumorigenesis to occur [30]. Mutations in the PI3K/AKT/mTOR pathway clearly result in the generation of ovarian tumors; however, what type they relate to clinically depends on the type of the genetic loss and the combination of genetic mutations.

PI3K/AKT/MTOR IN THE PROLIFERATION AND PROGRESSION OF OVARIAN CANCER

The role of the PI3K/AKT/mTOR pathway in terms of proliferation and progression of ovarian cancer is extremely complex. Many perturbations have been shown to contribute to carcinogenesis, with the endpoint the same: activation of the pathway results in an increase in cell proliferation, migration, invasion, and chemotherapy resistance.

The complexity begins with how deregulation of PI3K/AKT/mTOR can occur as a result of over-activation, mutations in the catalytic domains, mutations in the regulatory domain, or modifications to the downstream targets of PI3K. As demonstrated by the TCGA, the most prevalent mutational alterations are those affecting *PIK3CA* and *PTEN* [7]. *PTEN* is located on chromosome 10q23 and functional loss of *PTEN* impairs its lipid phosphatase activity, which is critical for tumor suppressor activity [31]. For *PIK3CA*, its dysfunction arises as a mutation on chromosome 3 that is predominately observed in endometrial, breast, and colorectal cancers or by gene amplification in ovarian cancer [32].

Robust pre-clinical models have been established for studying the PI3K/AKT/mTOR pathway in ovarian cancer. For example, SKOV3 has an activating

mutation in *PIK3CA* [33] and the A2780 cell line has deletion of *PTEN* [34]. By targeting the individual members of the PI3K/AKT/mTOR pathway with siRNA, the role of each component can be easily elucidated.

If the p100 subunit of PI3K, which is encoded for by *PIK3CA*, is targeted with siRNA in OVCAR-3 cells, there is a decrease in migration, decreased invasion, and a decrease in proliferation [35]. The decrease in proliferation has also been replicated in OVCAR-8 (*AKT2* copy number gain), UPN251 (*PIK3CA* DNA copy number gain) and A2008 (*PIK3CA* mutation) cell lines that are treated with siRNA against *PIK3CA* [36]. However, one report was not able to reduce proliferation in OVCAR-3 cells treated with the PI3K inhibitor LY29400 [37]. The difference might be accounted for given molecular targeted therapies require the over-activation of the target in order for the therapy to have a target. While OVCAR-3 may have low basal AKT activity, targeting it via siRNA will still knock-out any expression [35, 37]. This leads to the complexity in designing treatments that take advantage of the pathway in ovarian cancer. Overall targeting of *PIK3CA* results in the decrease of proliferation markers CyclinD1, CDK4, CyclinE, CDK2 and p21 and an increase in expression of p27. As G1 cell cycle progression is regulated by the CDK inhibitor p27, the release from its inhibition seems to account for the decrease in cell proliferation [35].

Proliferation and invasion is also affected when AKT is directly targeted as well. SiRNA against the AKT1 isoform of reduces proliferation of OVCAR-3 cells, but to a lesser degree than inhibition of *PIK3CA* [35]. Targeting the AKT2 isoform has been shown to increase the activation of apoptosis [36]. This increase in apoptosis activation is not seen when *PIK3CA* is targeted. Invasion of ovarian cancer cells is reduced with

AKT1 knockout but to a lesser extent than PIK3CA knockout [35, 36]. When p110- α or AKT1 are targeted with siRNA, there is also a decrease in the downstream molecule p70S6K1. Directly targeting p70S6K1 also reduces proliferation and invasion in ovarian cancer cells, though there is no rescue of expression of the CDK-inhibitor p27^{KIP1} that is seen in targeting p110- α or AKT1 [35]. This indicates the cell cycle is not being inhibited as strongly as when molecules higher in the PI3K/AKT/mTOR pathway are targeted.

Targeting mTOR directly can also decrease ovarian cancer cell proliferation and migration. However, the complexity of mTOR in the pathway contributes to the difficulty in elucidating mTOR's exact role in proliferation. As mentioned earlier, mTOR can be found in two complexes: mTORC1 and mTORC2 [17-19]. It is important to study each complex independently as treating with rapamycin shows a differential response in each complex. When mTORC1 was targeted using siRNA against Raptor, there was a decrease in pS6 and p4E-BP1 levels [17]. Raptor knockdown also provokes an increase in pS⁴⁷³-AKT indicating compensatory activation of AKT by mTORC2 in response to loss of mTORC1 signaling. Conversely, Rictor knockdown decreases pS⁴⁷³-AKT and pS6 levels. In terms of proliferation, knockdown of Raptor has a greater inhibitory effect than knockdown of Rictor. Raptor has a similar effect on proliferation as mTOR siRNA knockdown indicating that mTORC1 is more important in cell proliferation for ovarian cancer [17]. Though mTORC1 signaling has the more important role in ovarian cancer cell proliferation than mTORC2, therapeutically, both molecules will need to be targeted to prevent the compensatory activation of AKT via mTORC2 when mTORC1 is inhibited alone [17, 38].

While the activation of PI3K/AKT/mTOR leads to an increase in proliferation, invasion, and migration, the mechanism of how this occurs appears to be regulated through essential matrix metalloproteinase (MMPs). MMPs are zinc dependent endopeptidases with the ability to degrade various extracellular matrix proteins. They are involved in cleavage of cell surface receptors and releasing apoptotic signals and by targeting Collagen IV in the basement help allow a cell to migrate [39, 40]. Tissue inhibitor of matrix metalloproteinases (TIMP) are naturally occurring inhibitors of MMPs, except for TIMP1 and TIMP2 which help activate MMP-2 and MMP-9, [41]thereby playing a role in migration and invasion in ovarian cancer [42]. Research in other malignancies has identified that activation of PI3K leads to an increase in MMP-2 activity and an increase in cell motility [43, 44]. Treating ovarian cancer cell lines SKOV3, OVCAR5 and IGROV1 with a PI3K inhibitor, LY294002, there is a reduction in gonadotropin induced MMP-2 activity with little change in MMP-9 activity [42]. However migration and invasion are significantly decreased when cells are treated with LY294002 and cisplatin. This can be occurring due to TIMP1 and TIMP2 expression decreased by LY294002 hence preventing migration through a decrease in MMP-2 activity [42].

Other studies have found that MMP-9 activity and not MMP-2 activity is responsible for migration and invasion. The flavonoid apigenin, which can inhibit tumor growth [45], is able to reduce the amount of metastases in the abdominal organs of a orthotopic xenograft model [46]. Mechanistically the reduction in metastases is due to apigenin inhibiting AKT phosphorylation and subsequently caused a decrease in MMP-9 activity though not MMP-2. While these results are opposite of what Karam *et al* [42] who saw a decrease in MMP-2 activity in the presence of a decrease in AKT phosphorylation, over-

all the observed phenotype is identical. Whether through a decrease in MMP-2 or MMP-9 activity, inhibiting AKT phosphorylation results in a decrease in invasion, migration, and metastasis of ovarian cancer cells.

When brought together, a picture begins to emerge on how the PI3K/AKT/mTOR pathway is playing a key role in invasion for ovarian cancer. PI3K activation leads to the phosphorylation of AKT, which in turn activates p70S6K1. This downstream activation results in TIMP1 and TIMP2 expression activating MMP-2 or MMP-9 allowing for invasion and migration.

OUTSIDE INFLUENCES ON THE PI3K/AKT/MTOR PATHWAY

Numerous different inputs into the PI3K/AKT/mTOR pathway add to the complexity of the picture. One input involves the normal stress response pathway. The AMP-activated protein kinase (AMPK) is a metabolic stress-related and energy sensor kinase that plays a role in monitoring the AMP/ATP ratio. Activation of AMPK ultimately results in downstream signals that control processes important for regulation of metabolism including fatty acid oxidation and mRNA translation/protein synthesis [47]. AMPK can suppress the activation of the mTOR pathway via indirect inhibitory effects on the mTORC1 complex by the phosphorylation and activation of the TSC2-TSC1 complex [47]. Normally AMPK physiologically inhibits mTOR in the context of decreased energy sources to the cell. However in cancer, there is evidence that AMPK signaling is reduced allowing the cancer cell to escape normal proliferation controls. [47] While AMPK signaling is reduced in ovarian cancer cells, it can be restored through the use of metformin. Metformin is used in therapy for diabetes and can modulate AMPK activation [48]. With metformin treatment, AMPK activation inhibits protein biosynthesis and decrease phos-

phorylation of mTOR [48]. This results in a modulation of p21, p27, and Cyclin D1, reducing proliferation [48].

Alternatively, PI3K/AKT/mTOR can be activated by the loss of sMEK1 without affecting individual members of the PI3K/AKT/mTOR pathway. sMEK1 is a tumor suppressor of the protein phosphatase 4 regulatory subunit 3 (PP4R3) and the PP2A subfamily, which are conserved serine/threonine phosphatase [49]. Interestingly, sMEK1 is down regulated in ovarian and cervical tumor tissue [49]. However, re-expression of sMEK1 in the OVCAR-3 cell line results in a suppression of cell proliferation by inducing cell cycle arrest at G₁/G₀ phase with an increase in CDK inhibitor p16, and p27 [49]. In addition, sMEK1 expression induces PI3K and AKT dephosphorylation and reduction of expression of the mTOR/p70S6K proteins [49].

The PI3K/AKT/mTOR pathway can also be activated via alternative phosphorylation of AKT. PI3K will activate AKT through phosphorylation on a Threonine-308 residue. However, EGFR can phosphorylate AKT independent of PI3K change at the Serine-473 residue resulting in AKT over-activation [50] and an increase in angiogenesis, metastasis and anti-apoptosis properties. Reduction of EGFR phosphorylation and AKT phosphorylation results in apoptosis induction and the dissociation of Rictor and Raptor from mTOR, causing a decrease in proliferation [50]. The activation of the EGFR-AKT axis may also be further upstream involving G protein-coupled receptor 30 (GPR30). GPR30, a 7-transmembrane estrogen receptor, is widely expressed in cancer cell lines [51, 52] and is strongly associated with proliferation, invasion, metastasis, and drug resistance of various cancer cell lines [53-55]. GPR30 can phosphorylate EGFR and thus activate AKT

in ovarian cancer cell [56], and at least one study has demonstrated a poor prognosis with high GPR30 expression.[57]

Another example of mutations outside the pathway impacting mTOR is hyper activation of fatty acid synthase (FASN). FASN is an enzyme responsible for *de novo* synthesis of lipids from sugars, is overexpressed in 80% of ovarian carcinomas [58], and has been shown to be a predictor of poor survival [59]. Inhibition of FASN results in PI3K and downstream mediators to be targeted for degradation by ubiquitination, leading to cytoreduction and growth arrest in A2780, SKOV3, OVCAR-3 ovarian cancer cell lines [60]. This is unique, as pathway inhibitors usually result in a reduction of phosphorylation and not an actual decrease in measurable protein.

These outside pathways that result in activation of the PI3K/AKT/mTOR pathway will make it difficult to identify which patients would benefit the most from target therapy. If only the mutation status of PI3K/AKT/mTOR members is analyzed, potential candidates for treatment would be missed if their pathway aberration is the result of an outside influence.

MICRORNA, OVARIAN CANCER, AND THE PI3K/AKT/MTOR PATHWAY

The discovery of miRNAs in 1993 and later in functional roles in cancer as tumor suppressors or oncogenes opened up a new understanding of tumorigenesis and possible therapeutic options [61, 62]. Work by Zhang et al in 2008 [63] brought some of the first research implicating miRNA in the pathogenesis and tumorigenicity of epithelial ovarian cancer. miRNA in ovarian cancer play both oncogenic and tumor suppressive roles. miRNA-93 has been identified as a regulator of PTEN/AKT signaling with expression of miRNA-93 inversely correlating with PTEN expression [64]. In addition miRNA-93 has

been shown to decrease cisplatin chemosensitivity in ovarian cancer cells. miRNA-21 also acts on ovarian cancer via the PI3K/AKT/mTOR pathway by suppressing PTEN, and is even activated by AKT in hypoxic conditions to induce survival [65, 66]. Another oncogenic miRNA in ovarian cancer is miRNA-182, which has been shown to promote cell growth, invasion and chemoresistance by targeting programmed cell death 4 (PDCD4) and was able to reduce chemosensitivity of ovarian cancer cells to Taxol [67].

The role of miRNA in epithelial ovarian cancer is not always oncogenic. miRNA-152 and miRNA-185 co-contribute to cisplatin sensitivity in ovarian cancer cells [68]. Overexpressing miRNA-152 and miRNA-185 in cisplatin-resistant ovarian cancer cell lines results in restoring of chemosensitivity through suppressing DNA methyltransferase 1 [68]. Research has indicated that miR-204 has an important role in tumorigenesis [69, 70], and high-resolution custom miRNA comparative genomic hybridization has shown that there is frequent genomic loss in the chromosome containing miR-204 [71]. miR-204 is lost in 44.63% of ovarian tumors analyzed and its overexpression in SKOV3 ovarian cancer cells reduces colony forming capacity. It appears that miR-204 is targeting genes associated with tumorigenesis [71] by reducing p-AKT, p-4E-BP1 and p-S6. However, the regulation of p-AKT is outside of the known phosphorylated residues associated with the PI3K/AKT/mTOR pathway [71]. This indicates miR-204 is down regulating p-AKT outside of the two phosphorylated residues known in to be activated in the PI3K/AKT/mTOR pathway.

CLINICAL RELEVANCE OF THE PI3K/AKT/MTOR PATHWAY

While preclinical studies have contributed invaluable knowledge about the progression and tumorigenesis of ovarian cancer, the final step is finding a correlation in the

clinic. Not only are genetic alterations identified and observed in preclinical models present in clinical samples, but there is also prognostic and potential therapeutic value in understanding how a patient's tumor has a modified PI3K/AKT/mTOR pathway. Analyses of clinical samples have ranged from looking at mutational status of the regulator molecules of the pathway, changes in the activity of the downstream molecules, and the effect these changes have on survival and therapy options.

One molecule that is frequently mutated in ovarian cancer is *PIK3CA*. A mutational change here can result in over activation of PI3K kinase-activity. When there is a *PIK3CA*^{H1047R} mutation, which is in the kinase domain, it results in enhanced lipid kinase activity [30]. If an inactivating mutation occurs in *PIK3R1*, the p85 regulatory subunit of PI3K, PI3K/AKT/mTOR over activation occurs. In patients with a *PIK3CA* activating mutation, 40% also had an inactivating mutation in the regulatory genes *PIK3R1* or *PTEN* [30]. Mutations and alterations also occur in *AKT* resulting in an increased amount of activated AKT. Typically, ovarian cancer will have *AKT* amplification and at a lower frequency due to a missense mutation in *AKT* [35, 72].

In a more comprehensive analysis of 93 primary ovarian tumors, Comparative Genomic Hybridization (aCGH) was used to identify copy number changes. When looking at 9 canonical signaling pathways (PI3K/AKT/mTOR, MAPK, TGF- β , p38/MAPK, JNK, JAK/STAT, WNT/ β -Catenin, and NF κ B) and copy number variation in terms of patient survival, the PI3K/AKT/mTOR pathway was the most frequently altered cancer related pathway [36]. Similar to Kinross *et al*, 40% of patients had genetic aberrations in *PIK3CA*, with the most copy number gains seen in all the patient samples [36]. The second most copy number gains were seen in *PIK3CB* (27%) and *Cyclin-D2* (27%), which

would account for uncontrolled cell cycle progression in ovarian cancer [36]. Also *PIK3R4* and *PIK3R1*, genes for the regulatory subunit for PI3K, showed a decrease in copy number in 20% and 22% of patients respectively [36]. Importantly, the copy number variations identified in the PI3K/AKT/mTOR pathway were directionally concordant with the expected oncogenic activity. This was not the case in the other pathways examined. In the other pathways that showed a copy number variation, it was “non-directional” or against the observed oncogenic activation [36].

These data implicate that copy number variation is a feasible method for identifying alterations in the PI3K/AKT/mTOR pathway in patients. The copy number variations observed in the PI3K/AKT/mTOR pathway also correlated with survival. Patients with 2 copies of wild-type *PIK3CA* vs. patients with a copy number gain or mutation in *PIK3CA* survived 59.3 months versus 28 months [36]. If a patient does not have any copy number variation or mutation in *PIK3CA*, *PIK3CB*, or *PIK3R4* median survival was 80.4 months compared to patients who have two or more alterations in different genes had a median survival of 18.2 months. The findings of this study indicate that not only can changes in the PI3K/AKT/mTOR pathway provide prognostic factors about survival, but also genetic activation of the PI3K/AKT/mTOR pathway is an important characteristic of ovarian cancer.

Increasingly, clinicians and researchers believe that while genetic information is informative regarding the genetic background of a patient’s tumor, functional read-outs of alterations in a patient’s tumor can provide more information in directing future therapies. Identifying which patients are expected to respond to first-line chemotherapy treat-

ment and future treatment can help guide therapy, avoiding therapies that will not benefit the patient.

In a study that analyzed the ascites fluid of eighty-eight patients with advanced ovarian cancer, the mutational status and phosphorylation status of members of the PI3K/AKT/mTOR pathway was analyzed. In patients that were chemotherapy naïve, there was a statistically significant increase in the level of phospho-p70S6K and p-AKT in the ascites fluid of patients who were classified as non-responders as compared to patients who had either a partial- or complete-response to first-line chemotherapy [73]. However, this increase in phosphorylated p70S6K and phosphorylated AKT did not correlate with corresponding mutations or amplifications in *PIK3CA*, mutations in *AKT2*, or loss of *PTEN*. While the study admits the lack of correlation could be the result of small sample size, it is also possible that there are other factors leading to over activation of the p70S6K and AKT. Interestingly, in patients that did not respond to subsequent chemotherapy compared to patients who did, only phosphorylated p70S6K was significantly elevated [73].

While there is no doubt that genetic alterations in *PIK3CA*, and *AKT*, or the loss of *PTEN* contribute to the role of the PI3K/AKT/mTOR pathway in the progression of ovarian cancer, this study suggests that there are additional important factors that drive the PI3K pathway [73]. Furthermore, it is important to look at functional readouts of pathway activation, as elevated phosphorylated p70S6K levels may be indicative of chemoresistance.

Further studies are highly warranted in identifying the best scenarios for administering PI3K/AKT/mTOR pathway inhibitors. While PI3K/AKT/mTOR inhibitors are in

trials for breast cancer and endometrial cancer, there have been limited clinical uses thus far in ovarian cancer. One of the first reports on clinical use of a PI3K/AKT/mTOR inhibitor in ovarian cancer looked at the utility of the dual-targeting strategy involving PI3K/AKT/mTOR and RAF/MEK/ERK pathways.[74] The PI3K/AKT/mTOR and RAF/MEK/ERK pathways are both heavily implicated in cancer progression. Also, both pathways have the ability to be activated by the RAS proteins and recent data have shown that when downstream AKT and mTOR are inhibited by pharmacologic agents, PI3K can activate mitogen-activation protein kinase (MAPK) via RAS [75]. There is concern that targeting one pathway will lead to quick resistance to that therapy as the other pathway will compensate and take over activation [76] In this study of 236 patients, 32.2% received a combination of PI3K-pathway inhibitor and MAPK-pathway inhibitor, where 52.5% received just a PI3K-pathway inhibitor and 15.3% received a MAPK-pathway inhibitor [74]. In patients that had co-activation of both PI3K/AKT/mTOR and RAS/MEK/ERK that were treated with dual-inhibitors, all patients showed regression of the tumors varying between 2% to 64%. However, if the patients had a *PI3KCA* mutation with KRAS activation and only received an inhibitor to one of the two pathways, there was no response to therapy[74]. Considering the complexities of the PI3K/AKT/mTOR pathway, single-agent treatment is unlikely to be successful.

CONCLUSION

In the development and progression of ovarian cancer, it is clear that the PI3K/AKT/mTOR pathway plays an instrumental role. This role manifests itself in many unique ways presenting a complex picture for ovarian cancer. Alterations in the pathway

can be the initializing event in aggressive high grade serous cancers or for low grade endometrioid type ovarian carcinoma. Mutations in the pathway can contribute to cellular proliferation, invasion and migration through modification of cell cycle inhibitors and MMPs. Additionally, changes in outside inputs, such as AMPK, sMEK, or FASN can result in pathway changes without initiating genetic alterations in PI3K/AKT/mTOR family members. Multiple miRNA's can suppress or promote pathway activation in the same way as outside molecules.

Clinically, expression of p70S6K can help determine if a patient will respond to chemotherapy and copy-number alterations can be prognostic for a patient's survival. The PI3K/AKT/mTOR is a diverse pathway that affects equally diverse aspects of tumor development, progression, and patient survival. While targeting of PI3K/AKT/mTOR for treatment would seem to be an ideal strategy due to its importance, it will be difficult. Therapies will have to be given in combination and specifically tailored to each patient in order to have the most effect.

Conflict of Interest

The authors declare no conflict of interest

Acknowledgements

Funding support provided in part by the University of Alabama at Birmingham Center for Clinical and Translational Science (5UL1RR025777), the Reproductive Scientist Development Program through the Ovarian Cancer Research Fund and the National Institutes of Health (K12 HD00849), and the Department of Defense Ovarian Cancer Research Academy (OC093443)

References and Notes

1. Siegel, R., et al., *Cancer statistics, 2011*. CA: A Cancer Journal for Clinicians, 2011. **61**(4): p. 212-236.
2. Armstrong, D.K., *Relapsed ovarian cancer: challenges and management strategies for a chronic disease*. Oncologist, 2002. **7 Suppl 5**: p. 20-8.
3. Badgwell, D. and R.C. Bast, Jr., *Early detection of ovarian cancer*. Dis Markers, 2007. **23**(5-6): p. 397-410.
4. Bast, R.C., Jr., et al., *Prevention and early detection of ovarian cancer: mission impossible?* Recent Results Cancer Res, 2007. **174**: p. 91-100.
5. Kobayashi, E., et al., *Biomarkers for screening, diagnosis and monitoring of ovarian cancer*. Cancer Epidemiol Biomarkers Prev, 2012.
6. Bast, R.C. and G.B. Mills, *Dissecting "PI3Kness": The Complexity of Personalized Therapy for Ovarian Cancer*. Cancer Discovery, 2012. **2**(1): p. 16-18.
7. Cancer Genome Atlas Research, N., *Integrated genomic analyses of ovarian carcinoma*. Nature, 2011. **474**(7353): p. 609-15.
8. Cantley, L.C., *The Phosphoinositide 3-Kinase Pathway*. Science, 2002. **296**(5573): p. 1655-1657.
9. Markman, B., R. Dienstmann, and J. Tabernero, *Targeting the PI3K/Akt/mTOR Pathway – Beyond Rapalogs*. 2010. Vol. 1. 2010.
10. Engelman, J.A., J. Luo, and L.C. Cantley, *The evolution of phosphatidylinositol 3-kinases as regulators of growth and metabolism*. Nat Rev Genet, 2006. **7**(8): p. 606-619.
11. Sarbassov, D.D., et al., *Phosphorylation and regulation of Akt/PKB by the rictor-mTOR complex*. Science, 2005. **307**(5712): p. 1098-101.
12. Brunet, A., et al., *Akt Promotes Cell Survival by Phosphorylating and Inhibiting a Forkhead Transcription Factor*. Cell, 1999. **96**(6): p. 857-868.
13. Diehl, J.A., et al., *Glycogen synthase kinase-3 β regulates cyclin D1 proteolysis and subcellular localization*. Genes & Development, 1998. **12**(22): p. 3499-3511.
14. Heitman, J., N.R. Movva, and M.N. Hall, *Targets for cell cycle arrest by the immunosuppressant rapamycin in yeast*. Science, 1991. **253**(5022): p. 905-9.

15. Sabatini, D.M., et al., *RAFT1: A mammalian protein that binds to FKBP12 in a rapamycin-dependent fashion and is homologous to yeast TORs*. Cell, 1994. **78**(1): p. 35-43.
16. Brown, E.J., et al., *A mammalian protein targeted by G1-arresting rapamycin-receptor complex*. Nature, 1994. **369**(6483): p. 756-758.
17. Montero, J.C., et al., *Predominance of mTORC1 over mTORC2 in the Regulation of Proliferation of Ovarian Cancer Cells: Therapeutic Implications*. Molecular Cancer Therapeutics, 2012. **11**(6): p. 1342-1352.
18. Zoncu, R., A. Efeyan, and D.M. Sabatini, *mTOR: from growth signal integration to cancer, diabetes and ageing*. Nat Rev Mol Cell Biol, 2011. **12**(1): p. 21-35.
19. Peterson, T.R., et al., *DEPTOR Is an mTOR Inhibitor Frequently Overexpressed in Multiple Myeloma Cells and Required for Their Survival*. Cell, 2009. **137**(5): p. 873-886.
20. Borman, S.M., et al., *Ovotoxicity in Female Fischer Rats and B6 Mice Induced by Low-Dose Exposure to Three Polycyclic Aromatic Hydrocarbons: Comparison through Calculation of an Ovotoxic Index*. Toxicology and Applied Pharmacology, 2000. **167**(3): p. 191-198.
21. Shiromizu, K. and D.R. Mattison, *Murine oocyte destruction following intraovarian treatment with 3-methylcholanthrene or 7,12-dimethylbenz(a)anthracene: Protection by alpha-naphthoflavone*. Teratogenesis, Carcinogenesis, and Mutagenesis, 1985. **5**(6): p. 463-472.
22. Sobinoff, A.P., et al., *Staying Alive: PI3K Pathway Promotes Primordial Follicle Activation and Survival in Response to 3MC-Induced Ovotoxicity*. Toxicological Sciences, 2012. **128**(1): p. 258-271.
23. Kaku, T., et al., *Histological classification of ovarian cancer*. Med Electron Microsc, 2003. **36**(1): p. 9-17.
24. McCluggage, W.G., *Morphological subtypes of ovarian carcinoma: a review with emphasis on new developments and pathogenesis*. Pathology, 2011. **43**(5): p. 420-32.
25. Dubeau, L., *The cell of origin of ovarian epithelial tumours*. The Lancet Oncology, 2008. **9**(12): p. 1191-1197.
26. Kim, J., et al., *High-grade serous ovarian cancer arises from fallopian tube in a mouse model*. Proceedings of the National Academy of Sciences, 2012.

27. Wu, R., et al., *Preclinical Testing of PI3K/AKT/mTOR Signaling Inhibitors in a Mouse Model of Ovarian Endometrioid Adenocarcinoma*. *Clinical Cancer Research*, 2011. **17**(23): p. 7359-7372.
28. Kurman, R.J. and I.-M. Shih, *Pathogenesis of Ovarian Cancer: Lessons From Morphology and Molecular Biology and Their Clinical Implications*. *International Journal of Gynecologic Pathology*, 2008. **27**(2): p. 151-160
10.1097/PGP.0b013e318161e4f5.
29. Shih Ie, M. and R.J. Kurman, *Ovarian tumorigenesis: a proposed model based on morphological and molecular genetic analysis*. *Am J Pathol*, 2004. **164**(5): p. 1511-8.
30. Kinross, K.M., et al., *An activating *Pik3ca* mutation coupled with *Pten* loss is sufficient to initiate ovarian tumorigenesis in mice*. *The Journal of Clinical Investigation*, 2012. **122**(2): p. 553-557.
31. Myers, M.P., et al., *The lipid phosphatase activity of PTEN is critical for its tumor suppressor function*. *Proceedings of the National Academy of Sciences*, 1998. **95**(23): p. 13513-13518.
32. Markman, B., et al., *Status of PI3K inhibition and biomarker development in cancer therapeutics*. *Annals of Oncology*, 2010. **21**(4): p. 683-691.
33. Ihle, N.T., et al., *Mutations in the Phosphatidylinositol-3-Kinase Pathway Predict for Antitumor Activity of the Inhibitor PX-866 whereas Oncogenic Ras Is a Dominant Predictor for Resistance*. *Cancer Research*, 2009. **69**(1): p. 143-150.
34. Santiskulvong, C., et al., *Dual Targeting of Phosphoinositide 3-Kinase and Mammalian Target of Rapamycin Using NVP-BEZ235 as a Novel Therapeutic Approach in Human Ovarian Carcinoma*. *Clinical Cancer Research*, 2011. **17**(8): p. 2373-2384.
35. Meng, Q., et al., *Role of PI3K and AKT specific isoforms in ovarian cancer cell migration, invasion and proliferation through the p70S6K1 pathway*. *Cell Signal*, 2006. **18**(12): p. 2262-2271.
36. Huang, J., et al., *Frequent genetic abnormalities of the PI3K/AKT pathway in primary ovarian cancer predict patient outcome*. *Genes, Chromosomes and Cancer*, 2011. **50**(8): p. 606-618.
37. Altomare, D.A., et al., *AKT and mTOR phosphorylation is frequently detected in ovarian cancer and can be targeted to disrupt ovarian tumor cell growth*. *Oncogene*, 2004. **23**(34): p. 5853-7.

38. Itamochi, H., et al., *Inhibiting the mTOR Pathway Synergistically Enhances Cytotoxicity in Ovarian Cancer Cells Induced by Etoposide through Upregulation of c-Jun*. *Clinical Cancer Research*, 2011. **17**(14): p. 4742-4750.
39. Curran, S. and G.I. Murray, *Matrix metalloproteinases: molecular aspects of their roles in tumour invasion and metastasis*. *European Journal of Cancer*, 2000. **36**(13): p. 1621-1630.
40. Stamenkovic, I., *Matrix metalloproteinases in tumor invasion and metastasis*. *Seminars in Cancer Biology*, 2000. **10**(6): p. 415-433.
41. Brew, K., D. Dinakarpanthian, and H. Nagase, *Tissue inhibitors of metalloproteinases: evolution, structure and function*. *Biochimica et Biophysica Acta (BBA) - Protein Structure and Molecular Enzymology*, 2000. **1477**(1-2): p. 267-283.
42. Karam, A.K., et al., *Cisplatin and PI3kinase inhibition decrease invasion and migration of human ovarian carcinoma cells and regulate matrix-metalloproteinase expression*. *Cytoskeleton*, 2010. **67**(8): p. 535-544.
43. Vasko, V., et al., *Akt activation and localisation correlate with tumour invasion and oncogene expression in thyroid cancer*. *Journal of Medical Genetics*, 2004. **41**(3): p. 161-170.
44. Furuya, F., J.A. Hanover, and S.-y. Cheng, *Activation of phosphatidylinositol 3-kinase signaling by a mutant thyroid hormone β receptor*. *Proceedings of the National Academy of Sciences of the United States of America*, 2006. **103**(6): p. 1780-1785.
45. Fang, J., et al., *Apigenin inhibits tumor angiogenesis through decreasing HIF-1 α and VEGF expression*. *Carcinogenesis*, 2006. **28**(4): p. 858-864.
46. He, J., et al., *Oral Administration of Apigenin Inhibits Metastasis through AKT/P70S6K1/MMP-9 Pathway in Orthotopic Ovarian Tumor Model*. *International Journal of Molecular Sciences*, 2012. **13**(6): p. 7271-7282.
47. Vakana, E., J.K. Altman, and L.C. Plataniias, *Targeting AMPK in the treatment of malignancies*. *J Cell Biochem*, 2012. **113**(2): p. 404-409.
48. Rattan, R., et al., *Metformin suppresses ovarian cancer growth and metastasis with enhancement of cisplatin cytotoxicity in vivo*. *Neoplasia*, 2011. **13**(5): p. 483-91.
49. Byun, H.J., et al., *sMEK1 enhances gemcitabine anti-cancer activity through inhibition of phosphorylation of Akt/mTOR*. *Apoptosis*, 2012.

50. Loganathan, S., et al., *Inhibition of EGFR-AKT Axis Results in the Suppression of Ovarian Tumors <italic>In Vitro</italic> and in Preclinical Mouse Model*. PLoS One, 2012. 7(8): p. e43577.
51. Prossnitz, E.R. and M. Barton, *The G-protein-coupled estrogen receptor GPER in health and disease*. Nat Rev Endocrinol, 2011. 7(12): p. 715-726.
52. Smith, H.O., et al., *GPR30: a novel indicator of poor survival for endometrial carcinoma*. American Journal of Obstetrics and Gynecology, 2007. 196(4): p. 386.e1-386.e11.
53. Albanito, L., et al., *G Protein–Coupled Receptor 30 (GPR30) Mediates Gene Expression Changes and Growth Response to 17 β -Estradiol and Selective GPR30 Ligand G-1 in Ovarian Cancer Cells*. Cancer Research, 2007. 67(4): p. 1859-1866.
54. He, Y.-Y., et al., *Estrogenic G protein-coupled receptor 30 signaling is involved in regulation of endometrial carcinoma by promoting proliferation, invasion potential, and interleukin-6 secretion via the MEK/ERK mitogen-activated protein kinase pathway*. Cancer Science, 2009. 100(6): p. 1051-1061.
55. Pandey, D.P., et al., *Estrogenic GPR30 signalling induces proliferation and migration of breast cancer cells through CTGF*. EMBO J, 2009. 28(5): p. 523-532.
56. Fujiwara, S., et al., *GPR30 regulates the EGFR-Akt cascade and predicts lower survival in patients with ovarian cancer*. Journal of Ovarian Research, 2012. 5(1): p. 35.
57. Smith, H.O., et al., *GPR30 predicts poor survival for ovarian cancer*. Gynecologic Oncology, 2009. 114(3): p. 465-471.
58. Alo, P.L., et al., *Immunohistochemical study of fatty acid synthase in ovarian neoplasms*. Oncol Rep, 2000. 7(6): p. 1383-8.
59. Gansler, T.S., et al., *Increased expression of fatty acid synthase (OA-519) in ovarian neoplasms predicts shorter survival*. Hum Pathol, 1997. 28(6): p. 686-92.
60. Tomek, K., et al., *Blockade of Fatty Acid Synthase Induces Ubiquitination and Degradation of Phosphoinositide-3-Kinase Signaling Proteins in Ovarian Cancer*. Molecular Cancer Research, 2011. 9(12): p. 1767-1779.
61. Lee, R.C., R.L. Feinbaum, and V. Ambros, *The C. elegans heterochronic gene lin-4 encodes small RNAs with antisense complementarity to lin-14*. Cell, 1993. 75(5): p. 843-854.

62. Calin, G.A., et al., *Frequent deletions and down-regulation of micro- RNA genes miR15 and miR16 at 13q14 in chronic lymphocytic leukemia*. Proceedings of the National Academy of Sciences, 2002. **99**(24): p. 15524-15529.
63. Zhang, L., et al., *Genomic and epigenetic alterations deregulate microRNA expression in human epithelial ovarian cancer*. Proceedings of the National Academy of Sciences, 2008. **105**(19): p. 7004-7009.
64. Fu, X., et al., *Involvement of microRNA-93, a new regulator of PTEN/Akt signaling pathway, in regulation of chemotherapeutic drug cisplatin chemosensitivity in ovarian cancer cells*. FEBS Letters, 2012. **586**(9): p. 1279-1286.
65. Polytarchou, C., et al., *Akt2 Regulates All Akt Isoforms and Promotes Resistance to Hypoxia through Induction of miR-21 upon Oxygen Deprivation*. Cancer Research, 2011. **71**(13): p. 4720-4731.
66. Lou, Y., et al., *MicroRNA-21 promotes the cell proliferation, invasion and migration abilities in ovarian epithelial carcinomas through inhibiting the expression of PTEN protein*. Int J Mol Med, 2010. **26**(6): p. 819-27.
67. Wang, Y.-Q., et al., *MicroRNA-182 promotes cell growth, invasion and chemoresistance by targeting programmed cell death 4 (PDCD4) in human ovarian carcinomas*. J Cell Biochem, 2012: p. n/a-n/a.
68. Xiang, Y., et al., *MiR-152 and miR-185 co-contribute to ovarian cancer cells cisplatin sensitivity by targeting DNMT1 directly: a novel epigenetic therapy independent of decitabine*. Oncogene, 2013.
69. Gong, M., et al., *MicroRNA-204 critically regulates carcinogenesis in malignant peripheral nerve sheath tumors*. Neuro-Oncology, 2012. **14**(8): p. 1007-1017.
70. Chung, T.K.H., et al., *Dysregulation of microRNA-204 mediates migration and invasion of endometrial cancer by regulating FOXC1*. International Journal of Cancer, 2012. **130**(5): p. 1036-1045.
71. Imam, J.S., et al., *Genomic Loss of Tumor Suppressor miRNA-204 Promotes Cancer Cell Migration and Invasion by Activating AKT/mTOR/Rac1 Signaling and Actin Reorganization*. PLoS One, 2012. **7**(12): p. e52397.
72. Bellacosa, A., et al., *Molecular alterations of the AKT2 oncogene in ovarian and breast carcinomas*. Int J Cancer, 1995. **64**(4): p. 280-5.
73. Carden, C.P., et al., *The Association of PI3 Kinase Signaling and Chemoresistance in Advanced Ovarian Cancer*. Molecular Cancer Therapeutics, 2012. **11**(7): p. 1609-1617.

74. Shimizu, T., et al., *The Clinical Effect of the Dual-Targeting Strategy Involving PI3K/AKT/mTOR and RAS/MEK/ERK Pathways in Patients with Advanced Cancer*. *Clinical Cancer Research*, 2012. **18**(8): p. 2316-2325.
75. Carracedo, A. and P.P. Pandolfi, *The PTEN-PI3K pathway: of feedbacks and cross-talks*. *Oncogene*, 2008. **27**(41): p. 5527-5541.
76. Hoeflich, K.P., et al., *In vivo Antitumor Activity of MEK and Phosphatidylinositol 3-Kinase Inhibitors in Basal-Like Breast Cancer Models*. *Clinical Cancer Research*, 2009. **15**(14): p. 4649-4664.

USING HETEROGENEITY OF THE PATIENT-DERIVED XENOGRAFT MODEL
TO IDENTIFY THE CHEMORESISTANT POPULATION IN OVARIAN CANCER

by

ZACHARY C. DOBBIN, ASHWINI A. KATRE, ADAM D. STEG, BRITT K. ERICK-
SON, MONJRI M. SHAH, RONALD D. ALVAREZ, MICHAEL G. CONNER, DAVID
SCHNEIDER, DONGQUAN CHEN, AND CHARLES N. LANDEN

Oncotarget , In Press

Copyright

2014

by

Impact Journals LLC

Used by permission

Format adapted and errata corrected for dissertation

ABSTRACT

A cornerstone of preclinical cancer research has been the use of clonal cell lines. However, this resource has underperformed in its ability to effectively identify novel therapeutics and evaluate the heterogeneity in a patient's tumor. The patient-derived xenograft (PDX) model retains the heterogeneity of patient tumors, allowing a means to not only examine efficacy of a therapy, but also basic tenets of cancer biology in response to treatment. Herein we describe the development and characterization of an ovarian-PDX model in order to study the development of chemoresistance. We demonstrate that PDX tumors are not simply composed of tumor-initiating cells, but recapitulate the original tumor's heterogeneity, oncogene expression profiles, and clinical response to chemotherapy. Combined carboplatin/paclitaxel treatment of PDX tumors enriches the cancer stem cell populations, but persistent tumors are not entirely composed of these populations. RNA-Seq analysis of six pairs of treated PDX tumors compared to untreated tumors demonstrates a consistently contrasting genetic profile after therapy, suggesting similar, but few, pathways are mediating chemoresistance. Pathways and genes identified by this methodology represent novel approaches to targeting the chemoresistant population in ovarian cancer.

INTRODUCTION

Although most ovarian cancer patients present with advanced-stage disease, response to front-line platinum-based chemotherapy is high, on the order of 75%. The combination of surgery and adjuvant chemotherapy will allow remission in most patients, and about 40% of advanced stage patients will live at least 5 years [1]. However, absolute

cures are uncommon, with 80% of patients eventually having a recurrence [2]. The clinical profile of high rates of positive responses yet high recurrence rates suggests the presence of a subpopulation of cells within the heterogeneous tumor that survives initial chemotherapy, to lie dormant and eventually regrow with chemoresistant disease. Only by targeting this subpopulation can we achieve durable cures [3, 4].

Pre-clinical models used in drug discovery have predominately used clonal ovarian cancer cell lines, which cannot account for tumor heterogeneity, and evolve through selective growth and time to become very different from tumors growing in patients. Recently some of the most commonly used ovarian cell lines used were reported to have profiles more like endometrioid than papillary serous carcinoma, as defined by TCGA expression profiling[5]. Studying tumors preclinically that more closely resemble human tumors may increase the likelihood that medications effective in preclinical studies are effective in clinical trials. The patient-derived xenograft (PDX) model, whereby tumors are collected from patients and immediately implanted into mice, has recently been characterized and may allow such an advantage [6-8].

We set out to further characterize the PDX model and determine whether the heterogeneity seen in ovarian cancer is recapitulated, in order to explore the cell populations responsible for chemoresistance. One potential subpopulation with chemotherapy resistance is the cancer stem cell (CSC) population. CSCs have been shown to have increased tumorigenicity in mice, chemotherapy resistance, and are enriched in recurrent ovarian cancer [9-11]. In developing and characterizing the PDX model our goals were to 1) optimize methods to allow a high success rate of implantation, 2) examine retention of heterogeneity, 3) determine if PDX tumors respond to chemotherapy similarly to patient

tumors, 4) assess whether treatment with chemotherapy results in survival of just CSC populations, and 5) identify pathways that are amplified in resistant tumors. We demonstrate that the PDX model can be established with a high success rate, have similar expression profiles and biologic activities as patient tumors, and can be used as a model to identify the chemoresistant population.

RESULTS

Implantation Success Rate and Establishment of the Ovarian PDX Model

Here we report outcomes on the first 34 patient samples implanted into SCID mice. Demographics for patients from whom tumors were collected are presented in Table 1. All patients had stage IIIc or IV high-grade epithelial ovarian cancers, and tumors were collected prior to any chemotherapy. Tumor collected and implanted into mice was either from an omental metastasis or peritoneal implant, since they are plentiful, composed of grossly-identifiable tumor, and most relevant to recurrent disease.

Different sites of implantation in the mouse were tested to identify the best location for growth. Subcutaneous (SQ) and mammary fat pad (MFP) sites were tested as their location allows for tumor growth to be monitored with caliper-measurements. Intraperitoneal (IP) injection was examined, to provide an orthotopic location for model establishment. The subrenal capsule (SRC) was evaluated given previous reports of high take rates in this site [12]. Implantation for all 4 sites was conducted as described in the methods. Therefore both site and method of processing were controlled for each patient. The rates for PDX tumor development in each site, including individual implants are presented in Figure 1A. In the first 34 patients, a PDX line was established in 85% of SQ implants. This is compared to 64% in the MFP, 22% IP, and 8% in the SRC. SQ xenografts

almost always visually disappeared in the weeks after implantation before regrowing and being detectable at a mean of 78.4 days after implantation (range 17-174 days, Figure 1C) compared to 77.3 days for the MFP (range 29 to 129 days, NS). The success of a PDX being established is highest in the SQ site in part due to the increased number of implants per patient sample. Based on these data, and subsequent studies showing similar expression profiles in tumors from the SQ site and original patient tumors (described below), continued development of the PDX model was done in the SQ site. PDX tumors were examined for histologic characteristics by a gynecologic pathologist. In all cases and in up to six generations of re-implantation, the original histology was maintained (Figure 1D). Interestingly, in the few cases where a mixed epithelial-type ovarian cancer was implanted, both histologies were present in each of the subsequent PDX generations.

Heterogeneity of PDX Tumors

One potential advantage of the PDX model is that it may maintain patient heterogeneity, as opposed to the clonality that ultimately characterizes cell lines. However, a growing body of evidence suggests that certain cell subpopulations have enhanced ability to initiate tumors, often termed tumor-initiating cells (TIC's) or sometimes CSCs if additional attributes are demonstrated [10]. We examined whether resulting PDX tumors maintained tumor heterogeneity from a tumor-initiating cell standpoint. PDX tumors and original patient tumors were subjected to IHC for the TIC markers ALDH1A1 [11, 13, 14], CD133 [15-17], and CD44 [18, 19]. For ALDH1A1, CD44, and CD133, the patient samples averaged expression of 19.95%, 5.56%, and 3.27% respectively. The PDX tumors had similar expression of ALDH1A1 and CD133 at 17.4%, and 7.1% respectively (p=0.80 and 0.49, Figure 2A, 2B). There was a significant change in expression of CD44,

but it was actually a decrease, from 5.54% to 2.36% ($p=0.014$). If TICs in ovarian cancer are indeed the cells mediating xenograft formation, these data suggests that they subsequently differentiate into marker-positive and -negative cells and recapitulate tumor heterogeneity, in keeping with the CSC hypothesis[10, 20].

Related to heterogeneity, the human/murine component of PDX tumor would have implications to the biologic relevance of this model. IHC for human HLA antigen was conducted to identify the species-specific composition of the PDX tumor. Interestingly, all stromal cells in the PDX tumors were of murine origin (Figure 2C). This was consistent across 100% of the tumor specimen, and in all of the first 15 PDX tumors established.

Biological and Clinical Characterization of PDX tumors

To begin to evaluate the biologic characteristics of PDX tumors compared to original patient tumors, we examined oncogenic expression, proliferation, and response to chemotherapy. Weroha *et al* have previously demonstrated similar amplification and deletion patterns between PDX and patient tumors using aCGH [6]. To characterize whether expression of key oncogenes are similarly expressed in PDX tumors, an RT² PCR array on four pairs of patient samples and matched PDX tumors was used. This array quantifies mRNA levels of 84 genes that are recognized targetable oncogenes[21]. There was a strong correlation of expression in 79 of the cancer drug targets, with an overall R²-value of .744 (Figure 3A). This correlation was also present in individual samples (Supplemental Figure 1). The five genes that exhibited the poorest correlation had expression in the patient with near-zero mRNA expression in the PDX. These genes were platelet-derived growth factor receptor, alpha and beta polypeptide (PDGFRA, PDGFRB) and

vascular endothelial growth factor receptor one, two, and three (VEGFR1, VEGFR2, VEGFR3). These genes were expected to be decreased in the PDX tumor, since they are produced by the host, and the primers are human-specific. Therefore, there is strong consistency in expression of targetable oncogenes intrinsic to malignant cells, despite the fact that these tumors are growing in the subcutaneous compartment. In addition, we profiled the genetic difference of oncogene expression using the RT² PCR array comparing PDX tumors from the IP location versus the SQ implant. There was a strong correlation of expression among the 84 genes in the oncogene drug target array, with an overall R²-value of .8895 (Figure 3B). This indicates that the SQ tumor has similar expression to a tumor growing in the orthotopic location.

While expression at the single-gene level is important, biologic similarity regarding response to treatment is equally important. Mice with measurable tumors from 19 PDX models were treated with IP carboplatin (90 mg/kg/week) and paclitaxel (20 mg/kg/week) in combination for 4 weeks. After 4 weeks, percent-reduction in tumor volume was calculated and compared to the patient's response to therapy, categorized as complete (CR, no evidence of disease at completion of 6 cycles of primary chemotherapy) or partial (PR, residual disease present at completion of 6 cycles of primary therapy). Patients that had a CR to therapy had an average reduction in volume of 63.73% (range 95.04% to 24.87%) compared to an average reduction of just 1.53% (range 57.77% reduction to 107.9% increase) in patients that had a PR ($p = 0.0009$, Figure 3C). There was also a differential, but not significant, response between patients who had an optimal or suboptimal tumor reductive surgery (Figure 3D). While not definitive, this suggests that

patients presenting with disease unable to be optimally debulked are more aggressive and resistant to chemotherapy.

Biologic Mediators of Chemotherapy Resistance in the PDX

With evidence showing that the PDX model accurately replicates the biology and clinical properties of the original patient tumor, we sought to explore differences between matched untreated and treated tumors. Mice were treated as described above, with tumors harvested 6 days after the 4th weekly dose, to minimize acute tumoral effects that might occur after chemotherapy administration. Ki-67 was examined to measure proliferation, and was not significantly different in untreated PDX tumors compared to the original patient tumor (Figure 4A,B). However, treated tumors had significant decrease in Ki-67 positivity (33.6% compared to 64.9% in untreated tumors $p=0.0013$). Examining the trend of each tumor individually (Figure 4C), two pairs actually showed an increase in Ki-67, one of which had a 107% increase in tumor size on therapy, but the other with a 70.9% reduction. Despite these aberrations, the overall decrease in proliferating fraction suggests that dormancy is either being induced by chemotherapy, or some cells are already in a dormant state at presentation, and have intrinsic resistance to chemotherapy.

For analysis of which subpopulations have enhanced survival with chemotherapy, we assessed the density of the CSC populations expressing ALDH1A1, CD44, and CD133. If these populations were important to survival in the presence of chemotherapy, they should be more densely present after treatment, as noted in human specimens [11]. Treatment resulted in the significant enrichment of ALDH1A1-positive cells (increased from 16.2 to 36.1%, $p=0.002$) and CD133-positive cells (increased from 9.5% to 33.8%, $p=0.011$) (Figure 4D). Mean CD44 expression increased, but this was driven by two

samples, and was not significant. These data suggests treated tumors are enriched in CSC populations.

Differential Expression of Genes Due to Chemotherapy Treatment

Although cells with CSC properties were increased in treated specimens, they did not make up the entirety of the tumor. To globally examine which other genes and pathways are significantly altered during chemotherapy treatment, RNA-Seq was conducted on 6 pairs of treated and untreated PDX tumors. Across all six pairs, 299 genes were found to be significantly differentially expressed in the treated PDX samples compared to untreated (Supplementary Table 1), 137 of which have known roles in cancer. The top up-regulated and down-regulated genes are listed in Table 2. When Principal Component Analysis was performed, an interesting trend emerged. Four of the samples clustered together, and the remaining two were separated in the 3D space. All the treated samples showed a shift in the same direction away from their untreated PDX pair (Figure 5). This indicates that while the majority of genes are similar before and after treatment, all six tumors were affected similarly by therapy. Ingenuity Pathway Analysis identified 5 major pathways that were significantly altered with treatment and key changes in molecular and cellular function (Table 2). Changes in these biological functions and pathways are consistent with the visualized phenotype of tumors responding to chemotherapy and reorganizing cellular function to adapt for survival.

DICUSSION

We demonstrated the feasibility of an ovarian PDX model that closely models the heterogeneity of the original patient's tumor and maintains clinical relevance. Ovarian PDX tumors form at a high rate when placed in the subcutaneous location. Growing tu-

mors recapitulate the heterogeneity of the original patient tumor, and are not composed of just TICs, though the stromal component is murine. The PDX tumors have similar oncogene expression as the patient tumor, and respond to chemotherapy in a similar manner as the patients from which they were harvested. These similarities make the PDX model an attractive platform for pre-clinical testing of therapies that will hopefully correlate with a clinical response better than noted in cell lines. Finally, using this model has allowed identification of pathways mediating survival after chemotherapy that are attractive targets for future study.

In most malignancies, preclinical studies have primarily utilized cell lines to assess novel therapies and biologic processes. Cell lines are still ideal for carefully controlled studies on mechanisms and pathways. However, in terms of translating results to the clinic, these models have underperformed [22]. The clonal nature of cell lines limits the ability to study both intratumoral and interpatient heterogeneity [8, 23]. In addition, new genomic studies indicate that commonly-used ovarian cancer cell lines do not accurately represent high-grade serous ovarian cancers when compared to profiling performed on the TCGA dataset[5].

Development of PDX models have been demonstrated in a few malignancies, including ovarian, colorectal, medulloblastoma, pancreatic, breast, and non-small cell lung cancers [6, 24-29], and have consistently been found to be similar to patient samples. One well-established program in pediatric malignancies has demonstrated prediction of response in the clinic is higher when the PDX model is used [30]. However, there are drawbacks to the model. The time for PDX tumors to grow is variable, but usually on the order of months, making experiments slow and expensive. Historically, rates for success

of PDX establishment have been low, with the most successful models having 37% establishment rate [28, 31, 32], until Weroha's recent report of 74% overall success in ovarian cancer[6]. In this study, we had 85.29% success rate of establishing a PDX in the first 34 patients we implanted in the SQ. We believe the higher success rate is due to several factors. Given similar success of Weroha's report, this may be disease-specific. Strong working relationships with clinicians and pathologists allow for implantation within one hour of removal. We used two different processing methods that could be directly compared - one where solid tumors were implanted (SQ and SRC), and one where tumors were dissociated (MFP and IP). With both methods, the take rate was more dependent on the site implanted than the processing method. A crucial factor is the starting material. Other groups have reported that higher engraftment rates are associated with more aggressive tumors [6, 8, 29]. Instead of using the primary tumor from the ovary, we have implanted omental or peritoneal metastatic implants. The reasons for this are both biologic and practical. From a practical standpoint, omental implants are easily distinguished from normal tissue, reducing the risk of implanting normal tissue. A portion of "tumor" taken from the ovary, a complex tissue with normal solid components, may more likely be misinterpreted grossly as tumor, when in fact was benign. Because the omentum is well-vascularized, tumors are very "healthy", giving additional confidence that the portion implanted is not necrotic. Finally, it has been demonstrated that other factors produced in the omental microenvironment are pro-tumorigenic, and are likely implanted with these tumors[33]. The biologic rationale for using metastatic implants is that these sites are more relevant to the portions of tumors that recur. Therefore it may be more clinically relevant to characterize the metastatic site.

The site of implantation is an important consideration as there are benefits and drawbacks from using an orthotopic or heterotopic site. Heterotopic locations allows for easier monitoring of the tumor while orthotopic preserves the appropriate microenvironment [24]. However, in developing this model, use of the intraperitoneal orthotopic location had practical limitations of lower engraftment rates and difficulty in assessment of growth. In several instances mice become moribund with ascites before there was appreciable tumor volume, even when following with micro-CT imaging. This limits the ability to measure response to a therapy, and provides less tissue for analysis and propagation into the next generation of PDX. However, the Weroha study demonstrated an ability for high take rate using the intraperitoneal injection with large volumes of tumor-cells [6]. Like our study, their mice also demonstrated development of ascites but by using ultrasound, were able to more accurately follow tumor progression then using a micro-CT. By using the heterotopic location, tumor growth can be easily monitored for establishment, growth, and response to therapy [8]. However, biologic relevance has to be demonstrated. With our findings that subcutaneous tumors have similar oncogene expression profiles to patient tumors and the orthotopic intraperitoneal PDX tumors, and respond to chemotherapy similarly, the subcutaneous model appears relevant. This information helps alleviate the primary concern of not using the orthotopic location and provides a mechanism for decreasing the technical complexity of establishing and using a PDX model. While in our hands, not enough intraperitoneal tumors developed to evaluate their correlation to the clinical response, based on our oncogene data comparing SQ and IP tumors and the Weroha study, it appears both models are equivalent. Not enough intraperitoneal tumors developed to demonstrate whether they would be equivalent, or superior, to the

subcutaneous model. While previous groups have reported a high rate of success using the subrenal-capsule for tumor establishment [12], we did not see these successes. The ultimate proof of the importance of location in the PDX model will require testing numerous compounds, and relating the response in PDX tumors to responses in patients. PDX models in other malignancies have demonstrated a similar response rate between mice and the corresponding clinical trial [34-36]. Such studies in ovarian cancer are ongoing. But our analysis of the oncogene expression profiles, and their consistent similarity to patient tumors (Figure 3A), suggest that differences in targetable oncogenes between orthotopic PDX tumors and patient tumors are minimal.

We also demonstrate that the ovarian PDX model maintains the heterogeneity of the original patient tumor, at least from a TIC standpoint. Studies of CSC and TIC populations have shown that some cells are more capable of forming xenograft tumors than other[37]. Our analysis of density of ALDH1A1, CD44, and CD133 cells, the most consistent markers of TICs in ovarian cancer, demonstrates that PDX tumors are not only composed of these subpopulations (Figure 2B). It is possible that these subpopulations are the drivers of tumor formation, but as they grow they produce differentiated tumors with both CSC and non-CSC populations. This in fact would be predicted by the CSC model.

Potential limitations to the PDX model in ovarian cancer have been identified through our analysis. We saw that of 84 oncogenes examined, 5 were under-expressed in PDX tumors: receptors for platelet-derived growth factors and VEGF receptors. Analysis of the species making up tumor stroma showed it to be composed purely of murine origin. The fact that all members of these receptor families rely on tumor-stromal signal-

ing strengthens the validity of the association. The reduced content of human stromal genes is expected [38] as a result of the replacement of the human stroma with mouse stromal cells after implantation. Prior reports in pancreatic cancer have suggested that human stromal cells are maintained for several generations[39], although Weroha *et al* also found that IP ovarian PDX tumors had murine stroma. Whether murine stroma impacts the validity of the model will depend on the specific agent and pathway targeted.

The heterogeneity demonstrated in ovarian PDX tumors makes it uniquely positioned to investigate the key clinical problem of chemoresistance and recurrence. Ovarian cancer has a high rate of response to primary chemotherapy followed by an equally high rate of recurrence. One hypothesis is that this population is the same as the tumorigenic CSC population. While we have seen an increase in CSC density in the treated PDX tumors, and previously in treated patients[11], the persistent/recurrent tumors were by no means completely composed of these populations. Either the CSC populations had already begun to give rise to repopulating daughter cells negative for the CSC marker, or (more likely) other chemoresistant populations exist that cannot be identified by ALDH1A1, CD44, or CD133 alone. Going beyond CSCs, we have shown that surviving tumors have more cells in dormancy, decreasing from a baseline of 65% to 34%. RNA-seq analysis resulted in 299 genes being significantly different between the treated and untreated tumors with principal component analysis indicating that the changes in gene expression represent a small subset of the entire genetic makeup of the tumor (Figure 5, Supplementary Table 1). Most remarkable and encouraging is that the changes were similar in all pairs tested, providing hope that there may be common pathways to be targeted in most patients. One of the top up-regulated genes was ABCG1 (BCRP1), a member of

the White family of ATP-Binding cassette (ABC) transporters. Expression of ABCG1 has been shown to identify a side population of cancer cells that demonstrate CSC properties and chemoresistance [40]. Interestingly, one of the top activated pathways identified by Ingenuity Pathway Analysis was Sphingosine-1-phosphate signaling. This pathway has been shown to protect oocytes from apoptosis induced by chemotherapeutic agents *in vitro* and *in vivo* [41, 42]. Taken together, the enrichment of CSC markers in the treated population, decrease in cell proliferation, and increase in genes and signaling pathways predicted to play a role in chemoresistance, it appears that treatment of the ovarian PDX results in the survival of a cell population that is chemoresistant to primary therapy. The global analysis by RNAseq provides a snapshot of possible pathways that are responsible for the development of chemoresistance. These will be important targets for therapy in future studies. With the development of an ovarian PDX model that recapitulates the clinical response and the heterogeneity of ovarian cancer, investigators are positioned to more effectively evaluate novel therapeutics and use the model to improve our understanding of the mechanisms of chemotherapy resistance. Hopefully targeting these pathways will sensitize cells to chemotherapy and lead to more durable cures.

CONCLUSION

Development of an ovarian PDX model to study *de novo* chemotherapy resistance provides a unique use of the xenograft model beyond testing pre-clinical compounds, allowing for possible novel understandings of tumoral responses to therapy that may lead to new strategies for targeting the residual survival population after primary therapy.

MATERIALS AND METHODS

Collection and Implantation of Tumor Specimens

Under IRB and IACUC approval, patients with suspected ovarian cancer that were being treated by the Division of Gynecologic Oncology at UAB were consented for this study. At the time of primary tumor reductive surgery, a specimen from an omental metastasis or peritoneal implant that was not required for pathologic diagnosis was collected and transported to the laboratory for processing. Specimens were sectioned and a portion submitted for formalin-fixed-paraffin embedding; placed in RNAlater (Qiagen, Frederick, MD); snap frozen in liquid nitrogen, and slow freezing in Optimal Cutting Temperature (OCT) Medium, and stored at -80°C . Remaining tumor was isolated for implantation into SCID mice (NCI-Frederick, Frederick MD) into four sites: subcutaneous (SQ), subrenal capsule (SRC), intraperitoneally (IP), and mammary fat pad (MFP). To discover the optimal site for tumor growth, of the first 22 patients, 22 were implanted SQ and MFP, 18 IP, and 12 SRC. When enough tumor was available, all four sites were implanted to allow direct comparison of growth rates. After it was evident that the subcutaneous implantation site was optimal, an additional 11 patients had tumors implanted only SQ.

For SQ implants, 5mm^2 tumor pieces ($n=20$ per patient) adjacent to the slice used for confirmation of histology were sectioned. 5 mice were implanted with four tumors each. The dorsal surface of the mouse was shaved and prepped with betadine solution. A 1cm midline incision was made and with blunt dissection, four pockets were created in four quadrants of the flank of the SCID mouse. One 5mm^2 tumor implant was placed in each quadrant and the incision was closed with staples.

For SRC implantation, five 3mm² tumor sections were prepared for implantation into five mice, one kidney per mouse. An incision was made in the body wall along the long axis of the kidney. The kidney was gently exposed through the incision, a 4 mm incision was made in the renal capsule, and an implant was inserted.. The kidney was gently placed back into the body cavity and incision was closed with chromic gut sutures. For both SQ and SRC implantation, mice were anesthetized using isoflurane with 5% for induction of anesthesia and 1.5% for maintenance. Mice were administered carprofen (7mg/kg, Pfizer) prior to incision to reduce post-operative pain.

For injection into the MFP and IP sties, an adjacent portion of tumor was manually dissociated until fine enough to pass through a 21g needle. Prior to injection, the suspension was added to an equal volume of BD Matrigel (BD Biosciences, Cat#356234), mixed, and injected intraperitoneally (500,000 cells) or into bilateral MFPs (250,000 cells). Five mice were injected IP, and five mice had cells injected into the left and right MFP.

Treatment of PDX Lines With Chemotherapy

Once SQ or MFP tumors reached 500 mm² in volume, chemotherapy treatment was initiated in mice from 21 patients. Mice were injected IP with 90 mg/kg of carboplatin and 20 mg/kg of paclitaxel weekly or with vehicle, doses which approximate the maximal tolerated dose used in weekly dose-dense schedule of carboplatin and paclitaxel in patients. Tumors were measured biweekly using calipers. Volume of tumor was calculated using the formula (Length x Width²)/2. After 5 weeks of treatment (4 weekly doses, then one week after last chemotherapy dose in order to minimize acute tumor effects of chemotherapy), mice were euthanized by CO₂ asphyxiation and cervical dislocation.

Samples of treated and mice treated with vehicle were stored for future analysis. Any remaining tumor was reimplanted for maintenance of the PDX.

Immunohistochemistry of Patient Samples and Tumors From PDX tumors

Samples in FFPE were cut into 5 μm sections and placed on positively-charged slides. Hematoxylin and eosin stained tissue was analyzed by a gynecologic pathologist to confirm histology. For IHC of ALDH1A1, CD133, CD44, Ki-67 and human-HLA, slides were deparaffinized and rehydrated. Antigen retrieval was with 10 mM sodium citrate at pH 6.0 under pressure. Slides were washed in PBS. Endogenous peroxidases were blocked with 3% H_2O_2 in methanol. For ALDH1, CD133, and CD44, slides were blocked with Ctyo-Q immune-diluent (Innovex Biosciences Cat#NB307) followed by primary antibody incubation in Ctyo-Q immune diluent. Antibody concentrations were as follows: ALDH1A – 1:500 (BD Biosciences, Cat#611195) CD133 – 1:500 (Cell Signaling, Cat#3663S), CD44 – 1:500 (Cell Signaling, Cat# 3570S). After primary antibody, slides were washed in PBS. Primary antibody detection was achieved with Mach 4 HRP polymer (Biocare Medical), followed by 3,3'-diaminobenzidine incubation. Slides were counterstained with Gill's Hematoxylin then washed in water and PBS. Slides were sealed with Universal Mount (Open Biosystems, Cat#MBI1232). For Ki-67 (Abgent cat# AJ1427b) and human HLA (Proteintech Group Cat#15240-1), primary antibodies were used at concentrations of 1:200 in 10% normal goat serum. After incubation, slides were washed and blocked with 5% goat serum in 1X PBS. Primary antibody detection was visualized using an anti-rabbit HRP secondary at 1:500 in 5% goat serum (Vector Labs, Cat# PI-1000) and DAB substrate. Slides were counterstained as described above.

Scoring of IHC for TIC Makers and Ki67

Two examiners (AK and CNL) visually estimated the percent of cancer cells staining for ALDH1A1, CD133, CD44, and Ki-67. A 3rd examiner (MGC) was included if there was a >20% discrepancy. The examiners were blinded to the experimental condition for each slide, and a 4th investigator (ZCD) averaged the scores for each specimen and decoded samples for analysis. To be consistent with prior identification of CSCs with flow cytometry, for CD133 and CD44 only expression at the surface membrane was considered. The average number of positive tumor cells for each marker was compared between the untreated PDX tumor and the patient's tumor, and between the treated and untreated PDX, with Student's t-test.

RT²-qPCR Arrays

RNA extracted from stored samples was converted to cDNA and amplified using the RT² First Strand cDNA Synthesis Kit (SABiosciences). Gene expression was then analyzed using the Cancer Drug Targets RT² Profiler PCR Array (SABiosciences), which profiles the expression of 84 genes that are potential oncogenic targets for anticancer therapeutics [21]. PCR amplification was conducted on an ABI Prism 7900HT and gene expression was calculated using the comparative C_T method as previously described [43].

High Throughput Sequencing of Untreated and Treated PDX Tumors

Sample preparation, raw data processing, quality control were conducted in UAB Genomics Core and preliminary analysis was conducted in the UAB Biostatistics Core. For RNA-seq, total RNA quality was assessed and the rRNA depleted and concentrated. The RNA-Seq libraries were prepared, validated and quantified. The raw fastq files were aligned to human genome hg19 of a local instance of Partek Flow software package

(Saint Louis, MO). Pre-alignment was conducted to determine if trimming is needed based on reads quality score. Aligner STAR was used for best recovery[44]. The BAM files were loaded into Partek Genomics Suite 6.6 (Saint Louis, MO) for further analysis [45]. The reads per kilobase of exon model per million mapped reads (RPKM)-normalized reads were calculated and the expression levels of genes were estimated [46]. Additional filter was applied to exclude genes of low expression. The differential expressions were determined by using paired t-test [47]. Further functional analysis was conducted by using Ingenuity Pathway Analysis (IPA, Redwood City, CA).

ACKNOWLEDGEMENTS

Funding support provided in part by UAB Medical Scientist Training Program (NIGMS T32GM008361) to ZCD; and by the Norma Livingston Ovarian Cancer Foundation, the University of Alabama at Birmingham Center for Clinical and Translational Science (5UL1RR025777), and the Department of Defense Ovarian Cancer Research Academy (OC093443) to CNL.

Table 1: Patient demographics of implanted and growing patient-derived xenograft (PDX) lines

Characteristic	Percent or Average (range)
Age at diagnosis	61.7 (47-87)
Stage	
Stage IIIC	83%
Stage IV	17%
Race	
Caucasian	76%
African American	24%
Procedure	
Tumor Reductive Surgery	
Optimal TRS	52%
Suboptimal TRS	45%
Laparoscopic Biopsy prior to neoadjuvant chemotherapy	3%
Histology	
Papillary Serous Adenocarcinoma	79%
Endometrioid	3%
Mixed Epithelial	9%
Mucinous	3%
Extra-ovarian in origin	6%
Chemotherapy Treatment	
Carboplatin	4%
Carboplatin/Avastin	4%
Carboplatin/Paclitaxel	56%
Carboplatin/Paclitaxel/Avastin	7%
Carboplatin/Taxotere	19%
Cisplatin/Docetaxel	4%
Cisplatin/Paclitaxel	4%
Cisplatin/Taxotere	4%

Table 2: RNAseq analysis on PDX comparing 6 pairs of treated versus untreated samples.

Top Canonical Pathways	P-Value
Protein Kinase A Signaling	3.58E-05
GNRH Signaling	2.74E-04
Sphingosine-1-phosphate signaling	5.4E-04
α -Adrenergic signaling	9.39E-04
Cholecystokinin/Gastrin-mediated signaling	1.91E-03
Molecular and Cellular Functions	
Lipid Metabolism	1.33E-04 to 3.80E-02
Molecular Transport	1.33E-04 to 3.80E-02
Small Molecule Biochemistry	1.33E-04 to 3.80E-02
Cell Morphology	1.64E-04 to 3.80E-02
Cellular Assembly and Organization	1.64E-04 to 3.75E-02
Top Up-Regulated Molecules	Fold-Change Expression
ZNF750	2.441
ACP5	2.294
HIST2H2BE	2.141
CPEB3	2.117
DNM3	2.028
MPC1	1.980
ABCG1	1.938
MGLL	1.924
TLR5	1.884
Top Down-Regulated Molecules	Fold-Change Expression
APOC1	-2.488
GPHA2	-2.262
POLR3G	-1.862
TES	-1.759
PLCE1	-1.738
PUS7	-1.618
ARNT2	-1.607
MECOM	-1.570
CKAP4	-1.564
KLF5	-1.554

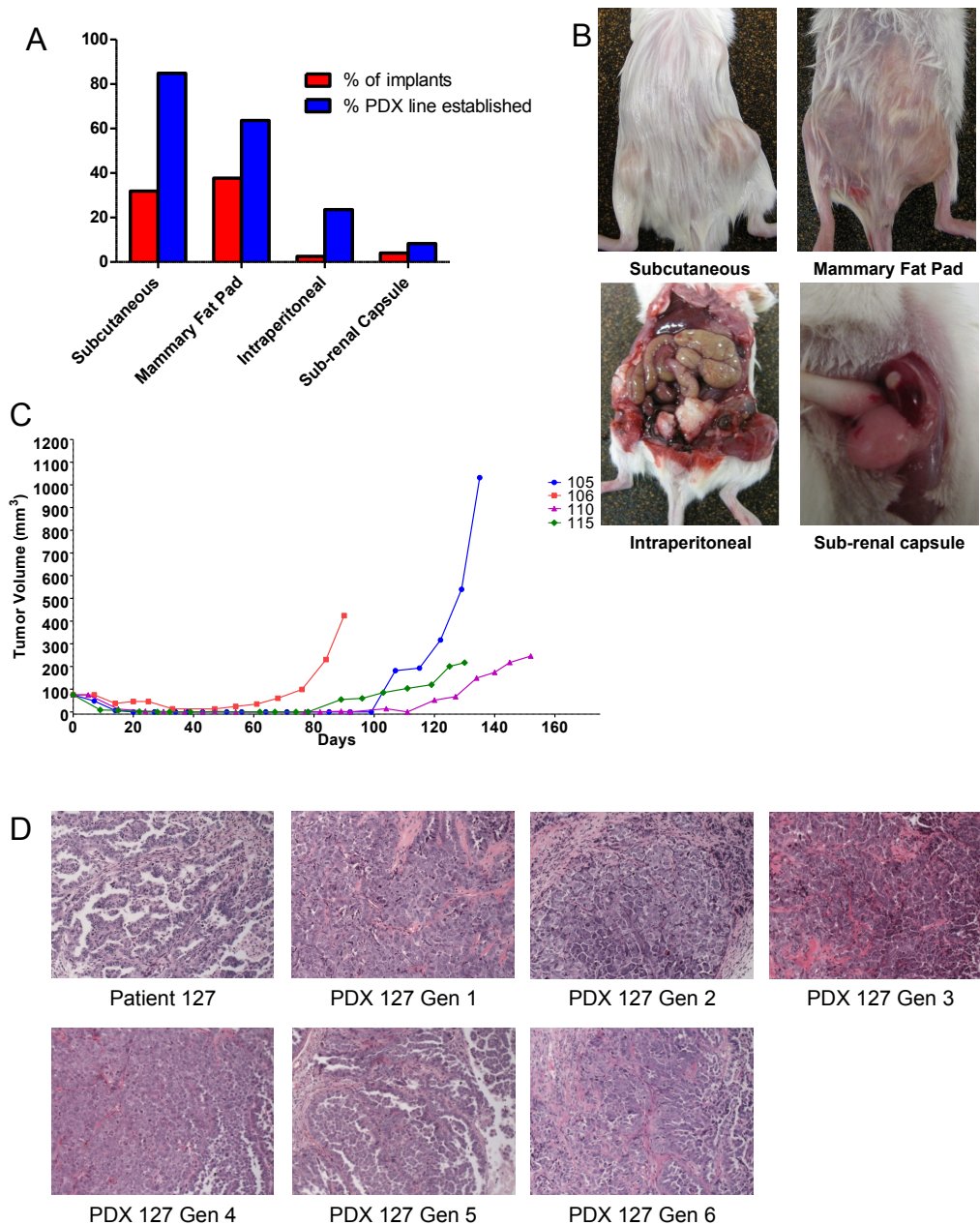


Figure 1: Take rates of different sites for implantation and maintenance PDX histology . (A) Tumors were implanted subcutaneously (SQ), in the mammary fat pad (MFP), intra-peritoneal (IP), or sub-renal capsule. The success of implantation was similar comparing SQ to MFP, however more PDX lines were established from SQ implant due to number of implants. IP and SRC implants are not effective for establishing a PDX line. (B) Representative pictures of implanted tumors at either SQ, MFP, IP, or SRC. (C) After implantation, tumor volume decreased to an undetectable size then re-grew after a dormancy period. This implicate the small population of tumorigenic cells survive and re-capitulate the tumor after implantation. Representative growth chart showed of 4 different PDX lines after implantation. (D) Histology of the original tumor is maintained throughout subsequent generations. Patient 127 had a histology of papillary serous adenocarcinoma that has been maintained for 6 generations in the corresponding PDX.

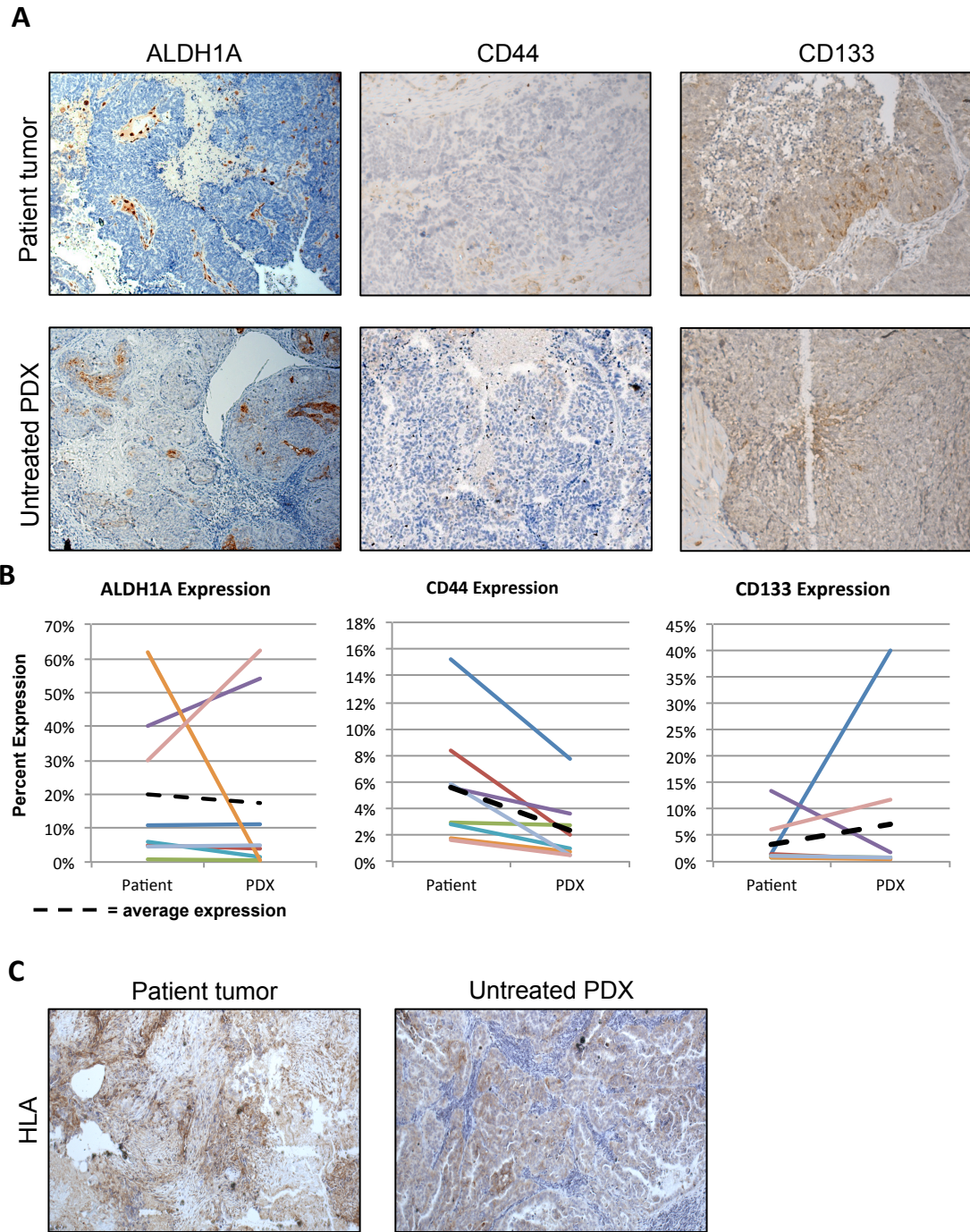


Figure 2: Establishment of the PDX line does not enrich for the tumorigenic cell population and human stroma is replaced in the implanted PDX. (A) Representative staining for ALDH1A1, CD133, and CD44 on the patient sample and untreated PDX. (B) Quantification of change in expression of ALDH1A1, CD133, and CD44 between the patient sample and the untreated PDX. Only CD44 had a significant decrease in expression (p -value < 0.05). ALDH1A1 and CD133 had no significant change in expression. (C) Human HLA expression in patient and untreated PDX tumors, demonstrating replacement of human stroma with murine cells.

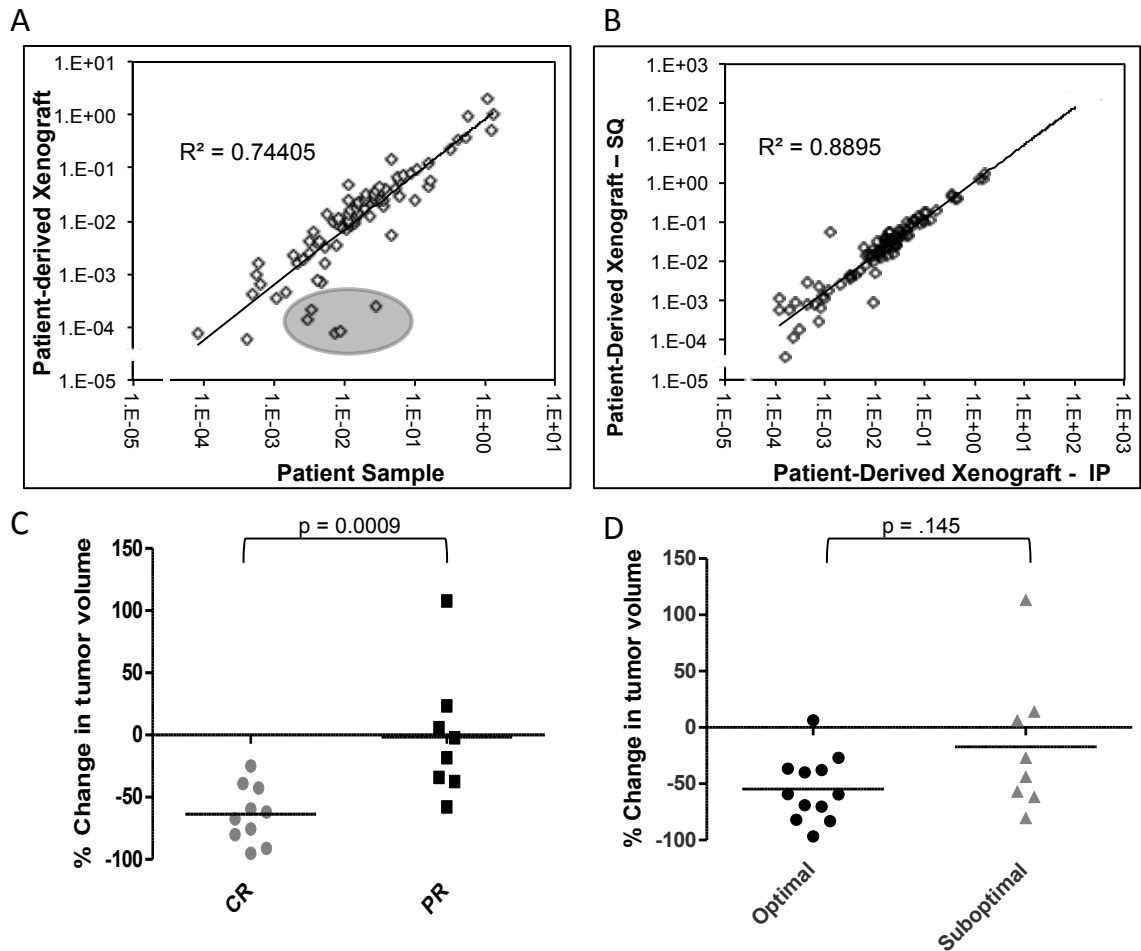


Figure 3: Cancer drug targets are maintained in the PDX line and the PDX response to treatment correlates to the patient's response to primary chemotherapy. (A) The SABiosciences RT² qPCR array for cancer drug targets was run on the patient's tumor and their matched untreated PDX tumor. Differences in relative gene expression for each target was calculated and the $2^{\Delta Ct}$ value was determined. Most of the 84 cancer drug target genes had similar expression in the PDX and the original patient sample. 5 gene were down-regulated in the PDX sample, though all 5 are related to VEGF and PDGF signaling (circled in grey). (B) The SABiosciences RT² qPCR array for cancer drug targets was run on matched subcutaneous PDX tumors and intraperitoneal PDX tumors. Differences in relative gene expression for each target was calculated and the $2^{\Delta Ct}$ value was determined. All 84 cancer drug target genes showed a strong correlation between the IP and SQ PDX tumors (C) PDX lines were treated with combination carboplatin and paclitaxel IP weekly. The percent change in tumor volume at 30 days was compared to the patient's response to primary therapy. PDX lines with the greatest decrease in volume significantly correlated to patients with a complete response to therapy ($p=0.0009$) (D) Classifying reduction in tumor volume by outcome of tumor reductive surgery (optimal debulking vs suboptimal) shows a trend towards PDX with the greatest reduction in volume correlating to optimal debulking for the patient (p -value = NS).

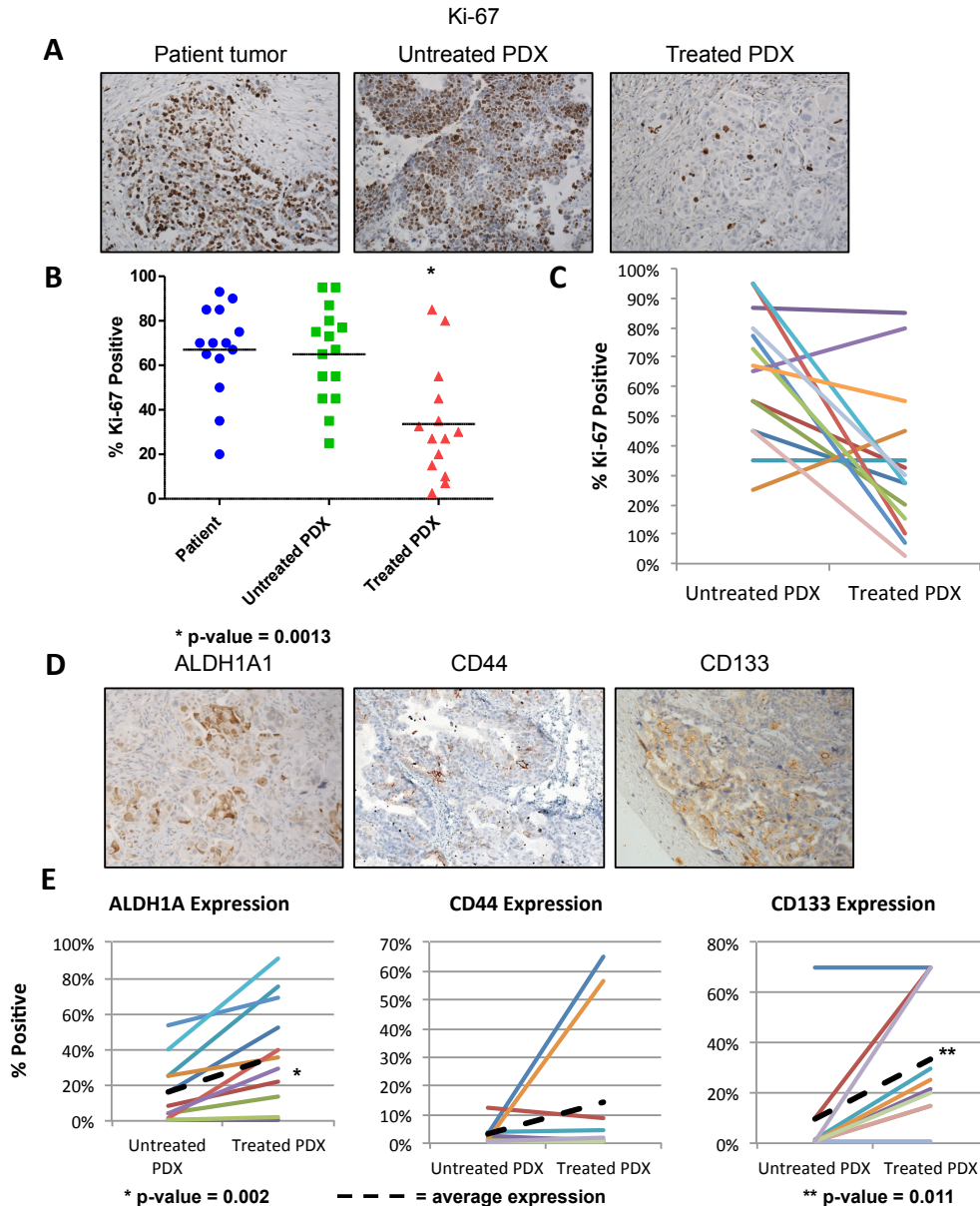


Figure 4: Chemotherapy treatment reduces proliferation and enriches the PDX for cancer stem cells. Tumor cell proliferation was quantified using the Ki67 marker on original patient samples, untreated PDX samples, and chemotherapy treated PDX samples. Change in cancer stem cell marker expression was analyzed after chemotherapy treatment. (A) Representative IHC of Ki67 staining in the patient sample, untreated PDX, and treated PDX. (B) On average, proliferation decreases with chemotherapy treatment in all PDX lines tested. There is no significant change in proliferation between the patient and the untreated PDX. (C) Proliferation rates for each treated and matched untreated pair show that the majority of tumors have a reduced proliferation rate after chemotherapy treatment (D) Representative IHC of CSC markers ALDH1A1, CD133, and CD44 of PDX treated with carboplatin and paclitaxel for 4 weeks. (E) In the treated PDX, expression of ALDH1A1 and CD133 are significantly increased (p-value = 0.0023 and p-value = 0.011 respectively).

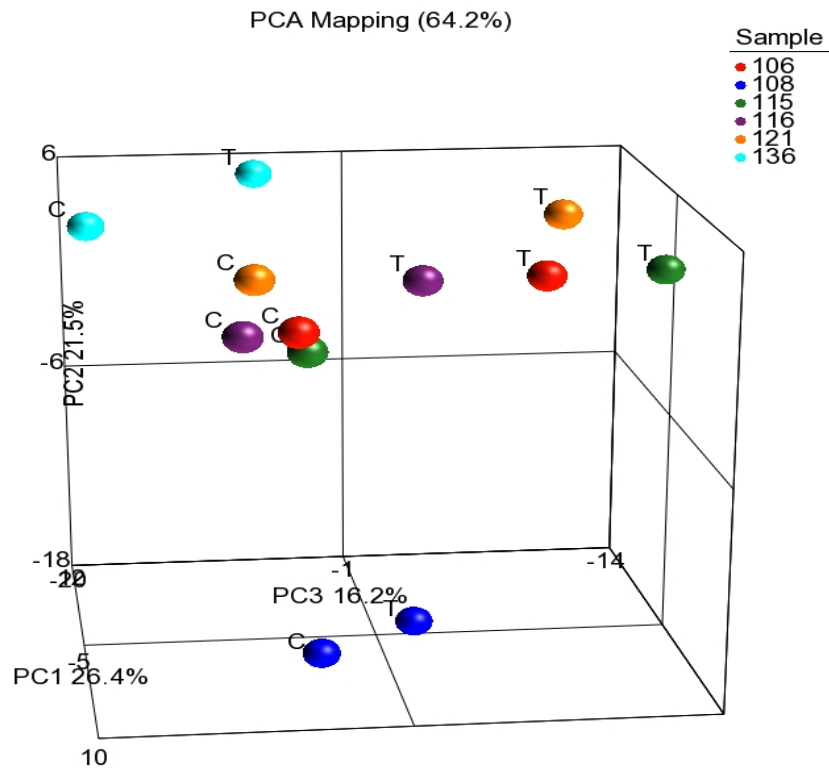


Figure 5: RNAseq comparing the treated PDX lines to the untreated PDX lines. Principal component analysis of genes expression in the treated and untreated PDX tumors. While matched treated and untreated PDX tumors clustered together, most treated PDX tumors had change of expression in the same direction indicating a small subset of genes responding to chemotherapy.

REFERENCES

1. Siegel, R., D. Naishadham, and A. Jemal, *Cancer statistics, 2013*. CA: A Cancer Journal for Clinicians, 2013. **63**(1): p. 11-30.
2. Romero, I. and R.C. Bast, *Minireview: Human Ovarian Cancer: Biology, Current Management, and Paths to Personalizing Therapy*. Endocrinology, 2012. **153**(4): p. 1593-1602.
3. Vaughan, S., et al., *Rethinking ovarian cancer: recommendations for improving outcomes*. Nat Rev Cancer, 2011. **11**(10): p. 719-725.
4. Bast, R.C., B. Hennessy, and G.B. Mills, *The biology of ovarian cancer: new opportunities for translation*. Nat Rev Cancer, 2009. **9**(6): p. 415-428.
5. Domcke, S., et al., *Evaluating cell lines as tumour models by comparison of genomic profiles*. Nat Commun, 2013. **4**.
6. Weroha, S.J., et al., *Tumorgrafts as in vivo surrogates for women with ovarian cancer*. Clinical Cancer Research, 2014.
7. Bjornsti, M.-A. and P.J. Houghton, *The tor pathway: a target for cancer therapy*. Nat Rev Cancer, 2004. **4**(5): p. 335-348.
8. Siolas, D. and G.J. Hannon, *Patient Derived Tumor Xenografts: transforming clinical samples into mouse models*. Cancer Research, 2013.
9. Sneddon, J.B. and Z. Werb, *Location, Location, Location: The Cancer Stem Cell Niche*. Cell Stem Cell, 2007. **1**(6): p. 607-611.
10. Rosen, J.M. and C.T. Jordan, *The increasing complexity of the cancer stem cell paradigm*. Science, 2009. **324**(5935): p. 1670-3.
11. Steg, A.D., et al., *Stem cell pathways contribute to clinical chemoresistance in ovarian cancer*. Clin Cancer Res, 2012. **18**(3): p. 869-81.
12. Press, J.Z., et al., *Xenografts of primary human gynecological tumors grown under the renal capsule of NOD/SCID mice show genetic stability during serial transplantation and respond to cytotoxic chemotherapy*. Gynecologic Oncology, 2008. **110**(2): p. 256-264.
13. Landen, C.N., et al., *Targeting Aldehyde Dehydrogenase Cancer Stem Cells in Ovarian Cancer*. Molecular Cancer Therapeutics, 2010. **9**(12): p. 3186-3199.
14. Silva, I.A., et al., *Aldehyde Dehydrogenase in Combination with CD133 Defines Angiogenic Ovarian Cancer Stem Cells That Portend Poor Patient Survival*. Cancer Res, 2011. **71**(11): p. 3991-4001.

15. Slomiany, M.G., et al., *Inhibition of Functional Hyaluronan-CD44 Interactions in CD133-positive Primary Human Ovarian Carcinoma Cells by Small Hyaluronan Oligosaccharides*. Clin Cancer Res, 2009. **15**(24): p. 7593-7601.
16. Curley, M.D., et al., *CD133 expression defines a tumor initiating cell population in primary human ovarian cancer*. Stem Cells, 2009. **27**(12): p. 2875-83.
17. Baba, T., et al., *Epigenetic regulation of CD133 and tumorigenicity of CD133+ ovarian cancer cells*. Oncogene, 2009. **28**(2): p. 209-18.
18. Zhang, S., et al., *Identification and characterization of ovarian cancer-initiating cells from primary human tumors*. Cancer Res, 2008. **68**(11): p. 4311-20.
19. Alvero, A.B., et al., *Targeting the Mitochondria Activates Two Independent Cell Death Pathways in Ovarian Cancer Stem Cells*. Molecular Cancer Therapeutics, 2011. **10**(8): p. 1385-1393.
20. Jordan, C.T., M.L. Guzman, and M. Noble, *Cancer Stem Cells*. New England Journal of Medicine, 2006. **355**(12): p. 1253-1261.
21. SABiosciences. *Human Cancer Drug Targets RT² Profiler PCR Array*. 2013; Available from: http://www.sabiosciences.com/rt_pcr_product/HTML/PAHS-507Z.html.
22. Sausville, E.A. and A.M. Burger, *Contributions of Human Tumor Xenografts to Anticancer Drug Development*. Cancer Research, 2006. **66**(7): p. 3351-3354.
23. Daniel, V.C., et al., *A Primary Xenograft Model of Small-Cell Lung Cancer Reveals Irreversible Changes in Gene Expression Imposed by Culture In vitro*. Cancer Research, 2009. **69**(8): p. 3364-3373.
24. Kim, M.P., et al., *Generation of orthotopic and heterotopic human pancreatic cancer xenografts in immunodeficient mice*. Nat. Protocols, 2009. **4**(11): p. 1670-1680.
25. Fleming, J.M., et al., *Local regulation of human breast xenograft models*. Journal of Cellular Physiology, 2010. **224**(3): p. 795-806.
26. Fichtner, I., et al., *Establishment of Patient-Derived Non-Small Cell Lung Cancer Xenografts as Models for the Identification of Predictive Biomarkers*. Clinical Cancer Research, 2008. **14**(20): p. 6456-6468.
27. Loukopoulos, P., et al., *Orthotopic Transplantation Models of Pancreatic Adenocarcinoma Derived From Cell Lines and Primary Tumors and Displaying Varying Metastatic Activity*. Pancreas, 2004. **29**(3): p. 193-203.

28. DeRose, Y.S., et al., *Tumor grafts derived from women with breast cancer authentically reflect tumor pathology, growth, metastasis and disease outcomes*. *Nat Med*, 2011. **17**(11): p. 1514-1520.
29. Zhao, X., et al., *Global gene expression profiling confirms the molecular fidelity of primary tumor-based orthotopic xenograft mouse models of medulloblastoma*. *Neuro-Oncology*, 2012. **14**(5): p. 574-583.
30. Houghton, P.J., et al., *The pediatric preclinical testing program: Description of models and early testing results*. *Pediatric Blood & Cancer*, 2007. **49**(7): p. 928-940.
31. Zhang, X., et al., *A Renewable Tissue Resource of Phenotypically Stable, Biologically and Ethnically Diverse, Patient-Derived Human Breast Cancer Xenograft Models*. *Cancer Research*, 2013. **73**(15): p. 4885-4897.
32. Kabos, P., et al., *Patient-derived luminal breast cancer xenografts retain hormone receptor heterogeneity and help define unique estrogen-dependent gene signatures*. *Breast Cancer Research and Treatment*, 2012. **135**(2): p. 415-432.
33. Nieman, K.M., et al., *Adipocytes promote ovarian cancer metastasis and provide energy for rapid tumor growth*. *Nat Med*, 2011. **17**(11): p. 1498-1503.
34. Rubio-Viqueira, B. and M. Hidalgo, *Direct In Vivo Xenograft Tumor Model for Predicting Chemotherapeutic Drug Response in Cancer Patients*. *Clinical Pharmacology & Therapeutics*, 2008. **85**(2): p. 217-221.
35. Fichtner, I., et al., *Anticancer drug response and expression of molecular markers in early-passage xenotransplanted colon carcinomas*. *European Journal of Cancer*, 2004. **40**(2): p. 298-307.
36. Fiebig, H.H., A. Maier, and A.M. Burger, *Clonogenic assay with established human tumour xenografts: correlation of in vitro to in vivo activity as a basis for anticancer drug discovery*. *European Journal of Cancer*, 2004. **40**(6): p. 802-820.
37. Shah, M.M. and C.N. Landen, *Ovarian cancer stem cells: Are they real and why are they important?* *Gynecol Oncol*, 2014. **132**(2): p. 483-489.
38. Bergamaschi, A., et al., *Molecular profiling and characterization of luminal-like and basal-like in vivo breast cancer xenograft models*. *Molecular Oncology*, 2009. **3**(5-6): p. 469-482.
39. Mattie, M., et al., *Molecular characterization of patient-derived human pancreatic tumor xenograft models for preclinical and translational development of cancer therapeutics*. *Neoplasia*, 2013. **15**(10): p. 1138-50.

40. Singh, A., et al., *Expression of ABCG2 (BCRP) Is Regulated by Nrf2 in Cancer Cells That Confers Side Population and Chemoresistance Phenotype*. *Molecular Cancer Therapeutics*, 2010. **9**(8): p. 2365-2376.
41. Morita, Y., et al., *Oocyte apoptosis is suppressed by disruption of the acid sphingomyelinase gene or by sphingosine -1-phosphate therapy*. *Nat Med*, 2000. **6**(10): p. 1109-1114.
42. Jurisicova, A., et al., *Molecular requirements for doxorubicin-mediated death in murine oocytes*. *Cell Death Differ*, 2006. **13**(9): p. 1466-1474.
43. Steg, A., et al., *Multiple Gene Expression Analyses in Paraffin-Embedded Tissues by TaqMan Low-Density Array: Application to Hedgehog and Wnt Pathway Analysis in Ovarian Endometrioid Adenocarcinoma*. *The Journal of Molecular Diagnostics*, 2006. **8**(1): p. 76-83.
44. Dobin, A., et al., *STAR: ultrafast universal RNA-seq aligner*. *Bioinformatics*, 2013. **29**(1): p. 15-21.
45. Trapnell, C., et al., *Transcript assembly and quantification by RNA-Seq reveals unannotated transcripts and isoform switching during cell differentiation*. *Nat Biotechnol*, 2010. **28**(5): p. 511-5.
46. Wagner, G.P., K. Kin, and V.J. Lynch, *Measurement of mRNA abundance using RNA-seq data: RPKM measure is inconsistent among samples*. *Theory Biosci*, 2012. **131**(4): p. 281-5.
47. Hochberg, Y. and Y. Benjamini, *More powerful procedures for multiple significance testing*. *Stat Med*, 1990. **9**(7): p. 811-8.

Supplementary Table 1: RNAseq revealed 299 genes that had significantly ($p < 0.05$) higher expression in the treated PDX samples versus the untreated PDX samples.

Gene	Chromosome	Start Location	Stop Location	Strand	Fold Change
VSTM4	10	50222290	50323578	-	2.88385
ZNF750	17	80787310	80797932	-	2.44072
RP11-193H5.1	1	238025475	238091620	+	2.38723
ACP5	19	11685475	11689802	-	2.29376
HIST1H2BC	6	26123695	26124133	-	2.14114
CPEB3	10	93808397	94050876	-	2.11674
DNM3	1	171810618	172381858	+	2.02791
MPC1	6	166778408	166796502	-	1.97979
PRPH	12	49688909	49692482	+	1.95466
ABCG1	21	43619799	43717355	+	1.93807
MGLL	3	127407905	127542094	-	1.92425
TLR5	1	223282748	223316625	-	1.88421
MMP14	14	23305742	23316809	+	1.87184
GPC4	X	132435064	132549206	-	1.86717
ITGB2	21	46305868	46348754	-	1.8659
EME2	16	1823229	1826240	+	1.80979
PTK2B	8	27168999	27316909	+	1.77717
FAM219A	9	34398182	34458569	-	1.7753
NMNAT2	1	183217372	183387635	-	1.73956
MOCOS	18	33767480	33848686	+	1.737
PLCB2	15	40580098	40600175	-	1.73671
GCLM	1	94352590	94375013	-	1.73021
ADSSL1	14	105190534	105213648	+	1.72613
LINC00957	7	44078648	44083896	+	1.71886
MKRN9P	12	88176663	88178489	-	1.70392
VAMP2	17	8062465	8066294	-	1.70315
CHST11	12	104850692	105155793	+	1.68861
PTPLAD2	9	21006365	21031636	-	1.68735
ADCY9	16	4012650	4166187	-	1.67735
ZNF727	7	63505821	63538928	+	1.676
PREX1	20	47240793	47444421	-	1.67126
MTSS1	8	125563011	125740749	-	1.66101
HERC2P3	15	20613650	20711434	-	1.65423
NAAA	4	76831808	76862167	-	1.64314
SCN5A	3	38589553	38691165	-	1.63118
MCEE	2	71336806	71357395	-	1.62541
FLCN	17	17115527	17140503	-	1.60288
HNRNPUL2-	11	62457734	62494857	-	1.59257

BSCL2					
ABCA7	19	1040102	1065571	+	1.58868
ZNF486	19	20278023	20311300	+	1.57838
ETV3	1	157094459	157108384	-	1.57332
TMEM200C	18	5890184	5892104	-	1.57315
UQCRHL	1	16133657	16134195	-	1.57235
RNASEL	1	182542769	182558395	-	1.55592
HTATIP2	11	20385231	20405330	+	1.55223
IER5	1	181057638	181059980	+	1.55116
RPRML	17	45055522	45056615	-	1.53476
TSSK6	19	19625028	19626470	-	1.53236
ANKRD18A	9	38571361	38620361	-	1.52864
TIMP2	17	76849059	76921473	-	1.52806
RASD1	17	17397753	17399710	-	1.5132
MYZAP	15	57884102	57977563	+	1.50081
STAG3L5P	7	99933702	99938952	+	1.4968
HPCA	1	33352098	33360248	+	1.48945
HSF4	16	67197288	67203849	+	1.47828
STIM1	11	3876933	4114441	+	1.45092
GNAI1	7	79764140	79848726	+	1.44357
MAPK7	17	19281034	19286858	+	1.44139
APOOP5	16	59788045	59789096	-	1.43991
HLA-A	6_ssto_hap7	1150098	29913662	+	1.43605
FAM84A	2	14772810	14780169	+	1.42164
SYNM	15	99645286	99675801	+	1.41178
PKIA	8	79428336	79517503	+	1.40459
STARD13	13	33677272	34250933	-	1.40261
DYX1C1- CCPG1	15	55647421	55790783	-	1.40222
EYA3	1	28296855	28415149	-	1.3939
MNT	17	2287354	2304259	-	1.38268
PRKAR2A	3	48788093	48885271	-	1.38138
SLC25A28	10	101370275	101380222	-	1.37891
SERINC3	20	43124864	43150727	-	1.37137
BLVRB	19	40953691	40971726	-	1.36946
ADIPOR1	1	202909960	202927701	-	1.35143
SEC22B	1	145096407	145116998	+	1.34893
PHF12	17	27232271	27278509	-	1.34879
KIAA1614	1	180882313	180915240	+	1.34765
ZDHHC1	16	67428322	67450340	-	1.34184
DYNLL2	17	56160780	56167619	+	1.33573

MFSD1	3	158519715	158547509	+	1.33549
KBTBD4	11	47593749	47600568	-	1.32875
ZBTB43	9	129567285	129600488	+	1.32686
ENTPD5	14	74433181	74486027	-	1.32495
C14orf142	14	93669237	93673460	-	1.32027
CHMP5	9	33264877	33282068	+	1.31782
RNF139	8	125487008	125500860	+	1.3174
DIRC2	3	122513901	122599987	+	1.31647
MID1IP1	X	38660685	38665784	+	1.30884
TM9SF2	13	100153628	100216303	+	1.30783
PLEKHM1	17_ctg5_hap1	128328	43568147	-	1.30503
ATP1B3	3	141595470	141645383	+	1.30497
PPT2	6_ssto_hap7	3382242	32131459	+	1.30378
CLIC2	X	154505496	154563991	-	1.30032
PRPF8	17	1553923	1588177	-	1.29751
TOM1	22	35695268	35743988	+	1.29725
PYGB	20	25228706	25278649	+	1.29328
ESYT3	3	138153415	138197257	+	1.29239
FAM129B	9	130267617	130341287	-	1.29145
PSMD1	2	231921578	232037541	+	1.28958
GABARAPL2	16	75600249	75611780	+	1.28721
ESRRA	11	64073000	64084213	+	1.28529
MEF2D	1	156433513	156470635	-	1.2823
TMBIM1	2	219138917	219157281	-	1.28031
CALCOCO2	17	46908350	46942608	+	1.2781
GOSR2	17	45000486	45018734	+	1.27738
S100A6	1	153507076	153508718	-	1.27694
WDR81	17	1619817	1641894	+	1.27622
FAM89A	1	231154704	231175996	-	1.27382
MCOLN1	19	7587496	7598896	+	1.27292
MAP3K10	19	40697651	40721483	+	1.27281
ZNF319	16	58028573	58033763	-	1.26794
ZAK	2	173940565	174132738	+	1.2671
OXNAD1	3	16306667	16347595	+	1.26545
TECPR1	7	97844755	97881564	-	1.26021
KLHL36	16	84682131	84695917	+	1.25481
LPIN3	20	39969560	39989223	+	1.24997
STAG3L2	7	74298092	74306732	-	1.24744
GPR137	11	64051811	64056973	+	1.23724
H2AFZ	4	100869244	100871513	-	1.23068
FAM27E3	9	67784944	67786626	-	1.2279

AFAP1L2	10	116054583	116164538	-	1.22724
RIN3	14	92980125	93155335	+	1.22721
KIF17	1	20990507	21044511	-	1.22185
SEC24C	10	75504131	75531934	+	1.21563
HECTD3	1	45468220	45477028	-	1.21411
COPA	1	160258377	160313355	-	1.21305
RSBN1L-AS1	7	77313168	77326663	-	1.20939
SQSTM1	5	179233388	179265078	+	1.20887
KLHL18	3	47324330	47388307	+	1.20439
ZNF555	19	2841433	2860473	+	1.20269
BCAS3	17	58755172	59470200	+	1.20016
KLC4	6	43027372	43042834	+	1.19962
PTPDC1	9	96793076	96872139	+	1.19953
C14orf37	14	58470808	58618848	-	1.19452
RXRA	9	137218316	137332432	+	1.19415
FTO	16	53737875	54148380	+	1.19311
LOC344967	4	40044537	40058820	-	1.19245
TLDC1	16	84509966	84538289	-	1.19096
CLPX	15	65442784	65477564	-	1.18712
YIPF5	5	143537723	143550279	-	1.18286
ENDOD1	11	94822974	94865816	+	1.18088
SURF4	9	136228325	136244821	-	1.1789
SCAMP2	15	75137197	75165671	-	1.17767
PSAP	10	73576055	73611083	-	1.17538
SLC25A44	1	156163723	156182588	+	1.16728
RAB7A	3	128444979	128533642	+	1.16442
ATXN7	3	63850233	63989137	+	1.15919
NUFIP2	17	27582854	27621167	-	1.15842
MKRN1	7	140152840	140179370	-	1.15465
LOC254896	8	22941868	22961071	+	1.14851
PIAS1	15	68346572	68480405	+	1.14763
RSPRY1	16	57220241	57272948	+	1.14671
HSPA9	5	137890571	137911319	-	1.1462
SKIV2L	6_ssto_hap7	3212164	31937533	+	1.13908
OSBP	11	59341871	59383618	-	1.13833
EMC3	3	10005636	10028523	-	1.13652
THAP6	4	76439654	76455237	+	1.13453
STX12	1	28099694	28150964	+	1.11803
HCCS	X	11129406	11141205	+	1.11749
TAF12	1	28929609	28969605	-	1.11704
MESDC1	15	81293295	81296346	+	1.11191

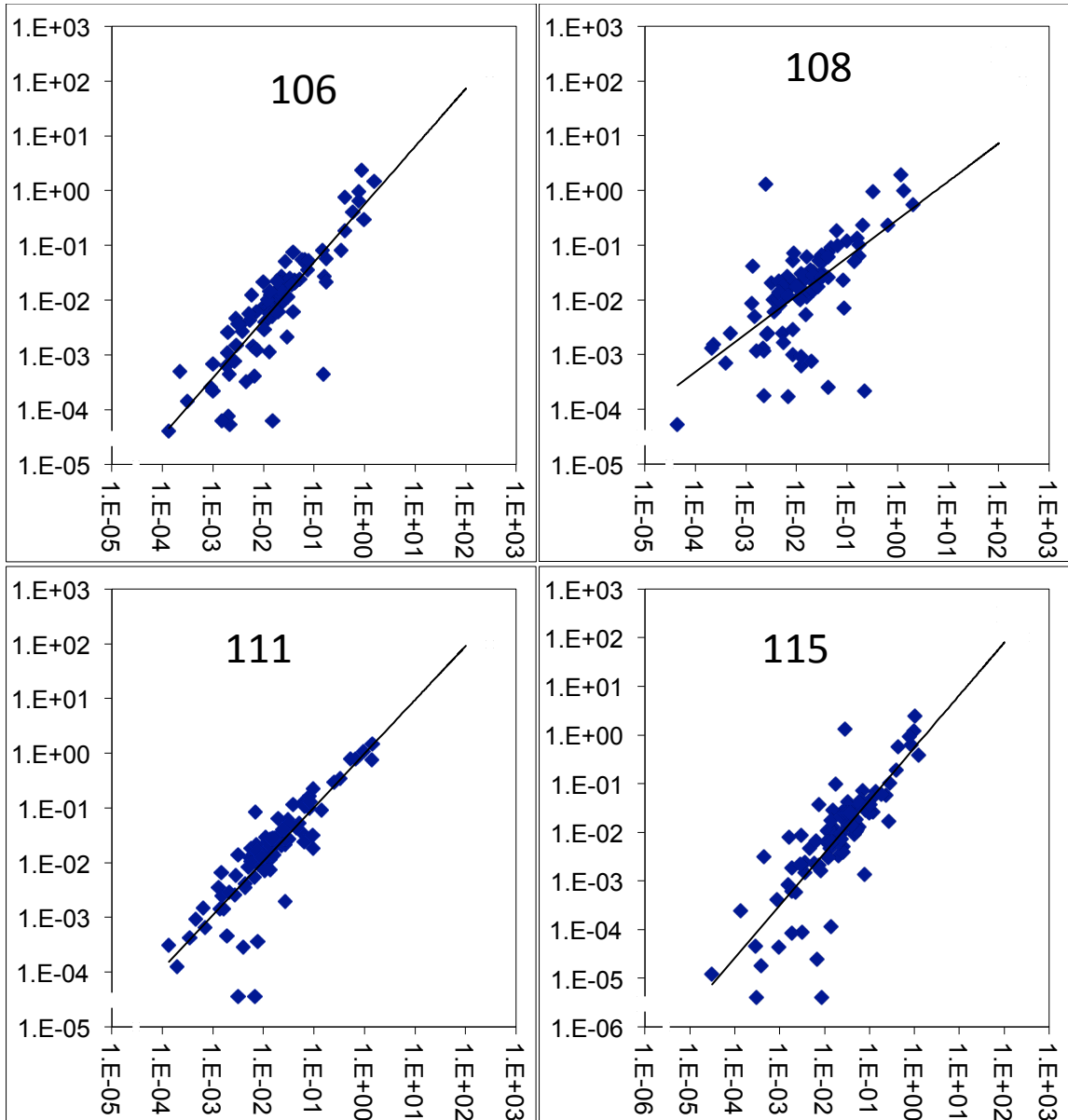
GADD45G	9	92219927	92221470	+	1.10348
RHOA	3	49396579	49449527	-	1.08749
ASTN1	1	176826441	177134041	-	1.08508
ECD	10	74894282	74927854	-	1.07666
LAMTOR3	4	100799495	100815704	-	-1.08305
RNF44	5	175953700	175964422	-	-1.08391
HNRNPDL	4	83343717	83351379	-	-1.09082
ZNF407	18	72342919	72777629	+	-1.09614
MAP7D3	X	135295379	135338642	-	-1.1053
LOC100129361	12	11323780	11328620	+	-1.12191
DZANK1	20	18364011	18447830	-	-1.13122
WWC2	4	184020463	184241930	+	-1.13131
ING5	2	242641456	242668897	+	-1.13132
GIT2	12	110367607	110434195	-	-1.13264
TM2D3	15	102182049	102192595	-	-1.13901
RUSC1-AS1	1	155290251	155293939	-	-1.13993
NADK2	5	36192691	36242382	-	-1.14161
RTEL1	20	62289163	62327607	+	-1.14575
TCEAL8	X	102507923	102510122	-	-1.14941
SPDL1	5	169010638	169031782	+	-1.15387
ZCCHC8	12	122956146	122985621	-	-1.16359
MDH1B	2	207602489	207630274	-	-1.16858
IFNGR2	21	34775202	34809829	+	-1.16925
CXorf23	X	19930980	19988383	-	-1.17025
FRG1	4	190861974	190884360	+	-1.1777
ZSCAN9	6	28193029	28201265	+	-1.18814
USP42	7	6144550	6201196	+	-1.18876
ATG12	5	115163894	115177549	-	-1.19193
CARF	2	203776941	203851209	+	-1.19386
HIST1H1C	6	26055968	26056700	-	-1.19716
PHC1	12	9067316	9094061	+	-1.19765
SECISBP2L	15	49280835	49338761	-	-1.2011
TOP2B	3	25639396	25705864	-	-1.20271
PIGB	15	55611133	55647847	+	-1.2065
GATAD1	7	92076762	92089382	+	-1.20707
PPHLN1	12	42719947	42842423	+	-1.20845
RBM19	12	114254543	114404177	-	-1.21448
CCDC88C	14	91737667	91884189	-	-1.21455
RNF138	18	29671818	29711525	+	-1.21865
MNAT1	14	61201459	61435399	+	-1.2339
FJX1	11	35639735	35642422	+	-1.23581

C1orf52	1	85715637	85725356	-	-1.23745
ZNF169	9	97021578	97065292	+	-1.24774
N6AMT1	21	30244513	30257696	-	-1.24812
LINC00998	7	112756773	112758638	-	-1.25062
UCK2	1	165796732	165880856	+	-1.25073
RSL1D1	16	11928055	11945443	-	-1.25096
RAB3IP	12	70132466	70216985	+	-1.25528
APAF1	12	99039078	99129212	+	-1.25549
TEKT4P2	21	9907189	9968594	-	-1.25804
POLR1C	6	43484777	43489247	+	-1.25846
ZNF74	22	20748405	20762754	+	-1.25997
HIST1H2BK	6	27106072	27114638	-	-1.26072
NPM1	5	170814708	170837889	+	-1.26122
EIF3C	16	28390903	28747051	+	-1.26145
NPHP3	3	132399453	132441304	-	-1.26174
DLG1	3	196769431	197025448	-	-1.26528
HCG8	6_ssto_hap7	1219726	29981700	-	-1.26818
TDRD3	13	60970591	61148014	+	-1.27252
WARS2	1	119573839	119683296	-	-1.2741
PHKA2	X	18910416	19002481	-	-1.27564
ALG10B	12	38710557	38723529	+	-1.27866
IDI1	10	1085964	1095062	-	-1.27877
PRKD2	19	47177573	47220385	-	-1.28338
ANAPC7	12	110810705	110841536	-	-1.28362
NEDD4L	18	55711610	56068773	+	-1.28409
IPO8	12	30781915	30848930	-	-1.28571
ZNHIT6	1	86115106	86174117	-	-1.29108
CROCC	1	17248445	17299475	+	-1.29865
NACA	12	57106211	57119327	-	-1.30339
MTX3	5	79272539	79287089	-	-1.30457
PTRHD1	2	25013136	25016252	-	-1.31352
TTC33	5	40711678	40756073	-	-1.31977
LRRC40	1	70610485	70671362	-	-1.32137
CCDC14	3	123632274	123680256	-	-1.32234
SUDS3	12	118814358	118855841	+	-1.33179
ZNF140	12	133657037	133684259	+	-1.33382
NDUFA5	7	123181083	123197959	-	-1.33767
PPA2	4	106290234	106395228	-	-1.33974
DCBLD2	3	98514814	98620534	-	-1.34346
IMMP2L	7	110303106	111202574	-	-1.34688
COMMD10	5	115420727	115628979	+	-1.35281

SEPHS1	10	13359438	13390299	-	-1.35534
NFATC2	20	50003494	50179371	-	-1.35748
CEP135	4	56814974	56899530	+	-1.3608
TMEM220	17	10616639	10633647	-	-1.36411
PGM2L1	11	74041361	74109503	-	-1.37177
L3MBTL3	6	130339728	130462595	+	-1.37235
TMA16	4	164415673	164441692	+	-1.3728
WDR77	1	111982512	111991831	-	-1.37912
LBR	1	225589204	225616558	-	-1.38056
NLN	5	65018023	65125112	+	-1.38189
FUT1	19	49251268	49258648	-	-1.38278
SERF1B	5	69321078	70214352	+	-1.38545
C12orf45	12	105380098	105388506	+	-1.38697
ADAM1A	12	112336867	112339707	+	-1.38905
NFKBIE	6	44225903	44233526	-	-1.38947
DPH5	1	101455180	101491363	-	-1.39075
ZNF681	19	23921997	23941694	-	-1.39198
TSHZ1	18	72922710	73001906	+	-1.39363
PRKCI	3	169940220	170023771	+	-1.40073
HSPG2	1	22148737	22263751	-	-1.40283
LONRF1	8	12579406	12612993	-	-1.40439
FAM161A	2	62051983	62081279	-	-1.40476
MCOLN2	1	85391266	85462797	-	-1.41279
C12orf60	12	14956506	14976792	+	-1.41351
ADM5	19	50191942	50194248	+	-1.41816
F2RL1	5	76114833	76131141	+	-1.41876
RSL24D1	15	55473512	55489232	-	-1.41939
TMEM183A	1	202976534	202993198	+	-1.42322
RTKN2	10	63952845	64028623	-	-1.43339
GLB1L2	11	134201768	134246219	+	-1.44439
ZNF596	8	182137	197341	+	-1.44515
PCDHB16	5	140561265	140565797	+	-1.4581
LOC100133091	7	76178658	76257300	+	-1.46254
DTWD1	15	49913226	49937334	+	-1.46696
SGTB	5	64961755	65017942	-	-1.46797
TFAP4	16	4307187	4323002	-	-1.47735
CAPS	19	5914193	5916223	+	-1.48887
FBRSL1	12	133067157	133161774	+	-1.49516
CHRNA10	11	3686817	3692615	-	-1.51081
ALKBH2	12	109525993	109531294	-	-1.51986
FAM86A	16	5134301	5147790	-	-1.52015

LOC100506548	5	40825365	40829245	-	-1.52016
SYCE1L	16	77233349	77246977	+	-1.53511
BEND3	6	107386385	107435637	-	-1.54651
DGKA	12	56324946	56347808	+	-1.54827
GPR125	4	22388997	22517678	-	-1.55067
KLF5	13	73629114	73651681	+	-1.55448
CKAP4	12	106631659	106641714	-	-1.56377
MECOM	3	168801287	169381564	-	-1.56982
ARNT2	15	80696692	80890278	+	-1.60687
FAM133B	7	92190072	92219709	-	-1.61605
PUS7	7	105096960	105162686	-	-1.61787
PLCE1	10	95753746	96088149	+	-1.73754
TES	7	115850547	115898838	+	-1.75919
POLR3G	5	89770681	89810370	+	-1.86241
EGFL8	6_ssto_hap7	3393402	32136063	+	-2.09768
GPHA2	11	64701943	64703361	-	-2.26238
APOC1	19	45417921	45422607	+	-2.48786

Supplementary Figure 1: The SABioSciences RT² qPCR array for cancer drug targets was run on the patient's tumor and their matched untreated PDX tumor. Differences in relative gene expression for each target was calculated and the 2^{ΔCt} value was determined. Correlation of expression is seen in each of the 4 pairs analyzed.



TARGETING RNA-POLYMERASE I USING CX-5461 AS A MECHANISM FOR
TREATING CHEMOTHERAPY RESISTANT EPITHELIAL OVARIAN CANCER

by

ZACHARY C. DOBBIN, ASHWINI A. KATRE, DAE HOON JEONG, ADAM D.
STEG, RONALD D. ALVAREZ, DAVID SCHNEIDER, AND CHARLES N. LANDEN

In preparation for *Gynecologic Oncology*

Format adapted for dissertation

ABSTRACT

Transcription of ribosomal RNA genes by RNA polymerase I and subsequent processing of the ribosomal RNA are fundamental control steps in the synthesis of functional ribosomes. Aberrant regulation of ribosomal RNA transcription by RNA polymerase I and ribosome biogenesis is associated with the etiology of a broad range of human diseases and especially is pervasive in cancer. Using a patient-derived xenograft model of ovarian cancer we discovered an increase in ribosome number after chemotherapy treatment. Using CX-5461, a selective inhibitor for ribosomal RNA synthesis, we determined the potential of Pol I inhibition as a therapeutic strategy for ovarian cancer. Chemotherapy resistant ovarian cancer cell lines SKOV3TR and HeyA8MDR were more sensitive to Pol I inhibition as compared to their sensitive parental lines. Also, CX-5461 has activity as a single agent in 3 out of 5 PDX models tested indicating a role for targeting Pol I as a treatment option for ovarian cancer.

INTRODUCTION

Ovarian cancer represents the greatest clinical challenge of all the gynecologic malignancies because it has highest mortality rate. [1] The optimal treatment for ovarian cancer is debulking surgery followed by platinum-based combination chemotherapy [1]. Although response rates to adjuvant chemotherapy with carboplatin and paclitaxel in advanced disease are higher) as many as 80% of patients will ultimately develop tumor recurrence [2]. Most of these recurrent tumors are resistant to or eventually become resistant to all available chemotherapy drugs. [1, 3]. Although in recent years evaluation of multiple chemotherapeutic and target agents alone or in combination has yielded modest

improvement in survival, drug resistance remains the major cause of death of ovarian cancer patients. [3, 4]

Increase in size and number of nucleoli is the prominent marker of aggressive tumor. The nucleolus is site of ribosomal RNA synthesis and enlarged nucleolus correlates with accelerated ribosomal RNA synthesis by RNA polymerases [5, 6]. RNA polymerase I (Pol I) transcribes multiple copies of genes encoding the pre-rRNA precursor that is processed into 18S, 5.8S and 28S rRNAs. RNA polymerase II (pol II) transcribes mRNAs which encode protein synthesis. RNA polymerase III (pol III) transcribes remaining non-coding proteins for ribosomal synthesis. Together pol I and pol III contribute to 80 % of nuclear transcription [6]. An increase of ribosomal RNA transcription in the nucleolus by RNA polymerase I correlates with an adverse prognosis in cancer [7].

A number of clinically approved chemotherapeutic drugs act, at least in part, through inhibition of ribosomal RNA synthesis [8]. However, none of these drugs directly target the ribosomal RNA polymerase I [8-10]. Recently, small molecule inhibitors such as CX-3543 and CX-5461, which target preferentially ribosomal RNA polymerase I transcription, were developed [9]. Especially, CX-5461 is potent and selective inhibitor for ribosomal RNA synthesis by RNA polymerase I in nucleolus of cancer cells. But, CX-5461 does not inhibit mRNA synthesis by RNA polymerase II and does not inhibit DNA replication or protein synthesis [11]. Interestingly, Bywater et al. showed that small molecule CX-5461 exhibits inhibition of ribosomal DNA transcription dependent on p53 mutational status and induces p53-dependent apoptotic cell death of hematologic malignancies, while maintaining normal cells [12].

In our study, we investigated the effects of CX-5461 on the viability of ovarian cancer cells, both alone and in combination with chemotherapy. We show that CX-5461 has activity alone on ovarian cancer cells and more effectively can kill taxane-resistant ovarian cancer cells independent of p53 mutational status. In addition, we found that while ovarian PDXs show an increase in RNA Polymerase I genes after chemotherapy treatment they have a variable response to Pol I inhibition. These findings suggest that targeting Pol I might be a viable option in treating ovarian cancer.

MATERIALS AND METHODS

Reagents and Cell Culture

CX-5461 was purchased from ChemScene and dissolved in 50 mmol/L NaH₂PO₄ (pH 4.5) to make 10mmol/L stock solution. The ovarian cancer cell lines A2780ip2, A2780cp20, HeyA8, HeyA8MDR, SKOV3ip1, and SKOV3TRip2 [13-18] were maintained in RPMI-1640 medium supplemented with 10% FBS (Hyclone). A2780cp20 (platinum resistant), HeyA8MDR (paclitaxel resistant), and SKOV3TRip2 (paclitaxel resistant, a kind gift of Dr. Michael Seiden; [19] were generated by sequential exposure to increasing concentrations of chemotherapy. HeyA8MDR and SKOV3TRip2 were maintained with the addition of 150 ng/mL of paclitaxel in RPMI-1640 medium. All ovarian cancer cell lines were routinely screened for Mycoplasma species (GenProbe Detection Kit; Fisher) with experiments carry out at 70% to 80% confluent cultures. Purity of cell lines was confirmed with short tandem repeat genomic analysis, and all cell lines were used within 20 passages from stocks.

Ovarian Cancer Patient Derived Xenograft Model

An ovarian cancer PDX model was developed and characterized by our group [20]. Briefly, established models of ovarian cancer PDX were subjected to 4 weeks of carboplatin (90 mg/kg) and paclitaxel (20 mg/kg). This comprised a treated and untreated cohort of matched PDX tumors. Tumors were collected and analyzed for expression of RNA polymerase I genes comparing matched PDX models before and after treatment. A further 5 ovarian cancer PDX models were treated with single-agent CX-5461 (50 mg/kg q3d) and response was followed using caliper measurements. Tumor volume was calculated using the formula $(\text{Length} \times \text{Width}^2)/2$.

Assessment of cell viability and cell cycle analysis

2,000 cells/well were plated on 96-well plates and treated the next day with increasing concentrations of CX-5461, alone or in combination with carboplatin or paclitaxel, in triplicate. Viability was assessed by 2-hour incubation with 0.15% MTT (Sigma) and spectrophotometric analysis at OD570 (optical density at 570 nm). IC50 of the agent of CX-5461 was determined by finding the dose at which the drug had 50% of its effect, calculated by the equation $[(\text{OD}_{570_{\text{MAX}}} - \text{OD}_{570_{\text{MIN}}})/2] + \text{OD}_{570_{\text{MIN}}}$. For cell-cycle analysis, cells were treated with vehicle alone or CX-5461 at the IC50 and IC90 dose for 48 hours, trypsinized, and fixed in 100% ethanol overnight. Cells were then centrifuged, washed in PBS, and suspended in PBS containing 0.1% Triton X-100 (v/v) 200 µg/ml DNase-free RNase A, and 20 µg/mL propidium iodide (PI). PI fluorescence was assessed by flow cytometry and the percentage of cells in sub-G₀, G₀-G₁, S-, and G₂-M phases was calculated by the cell-cycle analysis module for Flow Cytometry Analysis Software (FlowJo v7.6.1).

RNA Extraction and Reverse Transcription

Total RNA was extracted from the ovarian cancer cell lines and ovarian cancer PDX using the RNeasy Mini kit per the manufacturer's instructions (Qiagen, Frederick MD). The concentrations of all RNA samples were quantified using spectrophotometric absorbance at 260/280 nm. cDNA was prepared using the High Capacity Reverse Transcription Kit (Applied Biosystems, Foster City, CA). The resulting cDNA samples were analyzed using quantitative PCR.

Quantitative PCR

Primer and probe sets for *UBTF* (Hs01115792_g1), *18S* (Hs99999901_s1), *RNA28S* (Hs03654441_s1), *β -Actin* (Hs01060665_g1, Housekeeping Gene), *POLR1B* (Hs00219263_m1), and *RRN3* (Hs01592557_m1) were obtained from Applied Biosystems and used according to manufacturer's instructions. *ITS1*, pre-rRNA, was custom ordered from Applied Biosystems (Forward Primer: CCGCGCTCTACCTTACCTACCT, 3'-Primer: GCATGGCTTAATCTTTGAGACAAG, Probe: TTGATCCTGCCAGTAGC) [21] PCR amplification was performed on an ABI Prism 7900HT and gene expression was calculated using the comparative C_T method as previously described [22].

RESULTS

Increase in expression of ribosomal proteins by chemotherapy

Previously, 6 matched pairs of ovarian cancer PDX were treated with a combination of carboplatin and paclitaxel and subjected to RNA-seq [20]. IPA pathway analysis when comparing matched treated and untreated PDX in each pair found an increase in genes related to ribosomal synthesis. Specifically, the up regulation of *RPS6* indicates an

increase in ribosomal synthesis by Pol I. To confirm the RNA-seq data, qPCR was conducted on the matched treated-untreated ovarian cancer PDX for *UBTF*, *POLR1B*, and *RRN3*. These 3 genes are part of the complex that makes up Pol 1 and are a measure of Pol I abundance [12]. In addition, the amount of 18S rRNA and 28S rRNA was determined. In the 6 pairs of ovarian cancer PDX that were subjected to RNA-seq, the majority showed an increase of expression of *UBTF* and *POLR1B* of at least 2-fold in the treated PDX compared to untreated PDX (Figure 1A,B). *RRN3* was increased in PDX 115 and PDX 121 at least two-fold as well (Figure 1C).

When the total amount of 18S and 28S rRNA was measured, there was a surprising increase in the amount of ribosomes after chemotherapy treatment. 18S levels increased 37.9-fold ($p=0.010$) and 28S levels increased 39.0-fold ($p=0.19$) (Figure 1D). The reliance of the surviving cell populations after chemotherapy treatment to be expressing high levels of ribosomal content led to the hypothesis that inhibiting ribosomal synthesis may be a method for targeting ovarian cancer and specifically the cell populations surviving primary chemotherapy.

CX-5461 diminish cell viability in ovarian cancer cell lines

CX-5461 has recently been reported as a selective inhibitor of Pol 1 with the ability to inhibit solid tumor growth [11, 12] however it is more effective in cells with wild-type *TP53*. In high-grade serous ovarian cancer, *TP53* mutations have been identified in 96% of tumors [23]. However, based on the RNA-seq and follow up qPCR data, we endeavored to examine the response of 3 ovarian cancer cell lines with their matched chemoresistant variants. A2780ip/A2780cp20, SKOV3ip1/SKOV3TR, and HeyA8/HeyA8MDR were treated with CX-5461 in a single agent setting *in vitro*.

A2780ip2 had an IC₅₀ of 22 nM compared to 92 nM in A2780cp20 (Table 1, Figure 2A). SKOV3ip1 had an IC₅₀ of 510 nM compared to 48 nM in SKOV3TR (Table 1, Figure 2B). Also HeyA8 had an IC₅₀ of 1900 nM that dropped to 67 nM in the chemoresistant HeyA8MDR (Table 1, Figure 2C). The increase in resistance in A2780cp20 follows what has been previously reported as A2780ip2 is wild-type for *TP53* while A2780cp20 has a mutation in *TP53* [24, 25]. However, both SKOV3ip1 and SKOV3TR have a mutated *TP53* and HeyA8 and HeyA8MDR are wild-type for *TP53* (Table 1). This potentially indicates that the mechanism of action for CX-5461 in these later cell lines is independent of *TP53 status*. A2780cp20, HeyA8MDR, and SKOV3TRip2 cells were exposed to either NaH₂PO₄ (vehicle control) or CX-5461 (10, 50, 100 nmol/L) in combination with increasing concentrations of carboplatin or paclitaxel. But, they did not show synergic effect between CX-5461 and carboplatin or paclitaxel (data not shown).

CX-5461 causes cell cycle arrest in G2/S

All six cell lines were treated with either vehicle control, the IC₅₀, or IC₉₀ of CX-5461 for 48 hours. Cells were fixed, stained with PI and sorted to determine where in the cell cycle the drug was having an effect. The IC₉₀ dose did cause an increase in the amount of cell death for A2780ip2, A2780cp20, SKOV3ip1, SKOV3TRip2, and HeyA8 compared to control treatment (Figure 2D-F). In addition, there was pronounced G2/S arrest in both SKOV3 cell lines with the IC₉₀ dose, from 24.48% to 37.89% in SKOV3ip1, and 36.45% to 56.16% in SKOV3TRip2 (Figure 2E). This was also observed with the IC₉₀ dose in A2780cp20 (38.86% to 69.61%), HeyA8MDR (31.75% to 51.49%) and the IC₅₀ dose in A2780ip2 (26.31% to 42.71%) (Figure 2D,F). An arrest in G2/S makes sense as Pol I activity is the highest in the G2/S phase [26].

Ovarian Cancer PDXs have variable response to Pol I inhibition

Based on the activity of CX-5461 *in vitro* even in the presence of *TP53* mutations, and the RNA-seq data, the response of five different ovarian cancer PDXs were treated with single-agent CX-5461 at 50mg/kg q3d for 45 days. Response was varied with PDX 208 and 182 growing on treatment, PDX 127 having stable disease, and PDX 153 and 225 showing response, with PDX 225 having a complete regression of tumor (Figure 3A). Untreated PDX 208, 182, 127, 153, and 225 were analyzed using qPCR for the genes *POLR1B*, *RRN3*, and *UBTF*. *RRN3* is an essential Pol I initiation factor, *POLR1B* is the second largest subunit of Pol 1, and *UBTF* is a factor involved in the pre-initiation complex formation and chromatin remodeling [12]. The ΔC_T was graphed against the percent change in tumor volume. There was a positive correlation between *RRN3* and *POLR1B* expression and percent change in tumor volume. As *RRN3* and *POLR1B* mRNA expression increase, there is a greater reduction of tumor volume ($R=0.7562$ and $R=0.7696$, respectively)(Figure 3B-D). This correlation was not observed in *UBTF* expression (Figure 3E). These data suggests that sensitivity to Pol I inhibition is dependent on the level of expression of the factors comprising initiation complex of Pol I and its related transcription factors.

Next, qPCR was conducted on the treated PDXs 208, 182, 127, and 153 for *ITSI*, *POLR1B*, *RRN3*, and *UBTF*. Since PDX 225 had a complete response to CX-5461, there was no tumor to analyze and compare to the untreated sample. For PDX 208, 182, and 153, the expression of *ITSI* decreased in the treated as compared to control, with no detectable expression in PDX 153 (Figure 4A). *ITSI* is a read-out of pre-rRNA. The decrease of *ITSI* indicates that CX-5461 prevents the translation of rRNA [12, 21]. Interest-

ingly, PDX 127 had no change in *ITSI* expression even though the tumor neither grew nor regressed on treatment. This possibly indicates that CX-5461 had a mechanism of action of PDX 127 unrelated to ribosome translation, and future studies are needed to evaluate these potential alternatives. Except in PDX 153, which should a decrease of *POLR1B* and *RRN3* with CX-5461 treatment, there were only minor differences in expression levels of the initiation factors of Pol I after CX-5461 treatment (Figure 4B, C). These leads support to the idea that CX-5461 is acting on Pol I after the recruitment of initiation factors.

DISCUSSION

Ovarian cancer unfortunately has limited chemotherapeutic options after patients develop resistant to the standard regiment of platinum- and taxane-based therapy. Therefore it is imperative to identify novel targets that could be used in conjunction with standard therapy to hopefully improve patient outcomes. Previously, our group has developed and characterized an ovarian cancer PDX model that recapitulates the complexity of a patient's tumor in terms of heterogeneity and biological activity [20]. In addition, when we conducted RNA-seq comparing matched chemotherapy treated and untreated PDXs, we found that genes related to ribosomal synthesis were significantly up-regulated in the tumor cells surviving a platinum and taxane based therapy. This led us to the hypothesis that targeting ribosomal synthesis maybe be a potential strategy for treatment in ovarian cancer in addition to standard chemotherapy.

Transcription of ribosomal RNA genes by RNA polymerase I and subsequent processing of the ribosomal RNA are fundamental control steps in the synthesis of functional ribosomes [6, 8, 9]. If ribosomal RNA synthesis is upregulated, cell proliferation

rate is increased [8]. If ribosomal RNA transcription in the nucleolus is inhibited, cells undergo cell cycle arrest associated with apoptosis, senescence or autophagy [8]. Aberrant regulation of ribosomal RNA transcription by RNA Polymerase I and ribosome biogenesis (the complex and highly coordinated cellular process leading to the production of ribosomes) is associated with the etiology of a broad range of human diseases and especially is pervasive in cancer [8, 27, 28].

There have been numerous chemotherapeutic drugs developed with an impact on disrupting ribosome biogenesis including cisplatin, actinomycin D, camptothecin (irinotecan/topotecan), mitomycin C, 5-fluorouracil, and doxorubicin [8-10]. However, none of these chemotherapeutic drugs are selective enough for ribosomal RNA transcription by RNA polymerase I to allow definitive conclusions on what degree their therapeutic effect is mediated through ribosome biogenesis [29]. But, CX-5461 which was developed by Cylene Pharmaceuticals, is an oral small molecule targeting RNA polymerase I that selectively inhibits RNA polymerase I transcription [8, 29]. CX-5461 impairs initiation of RNA polymerase I transcription by disrupting the binding of the RNA polymerase I transcription initiation factor SL-1 to the ribosomal DNA promoter [11, 12, 29]. CX-5461 selectively inhibits a 300–400 fold more RNA polymerase I than RNA polymerase II or RNA polymerase III [11].

Bywater *et al.* demonstrated that human hematologic cancer cells (leukemia and lymphoma) with p53 wild type are more sensitive to CX-5461 than p53 mutant cells in vitro and in vivo. As the result, they suggested that CX-5461 has therapeutic effect for hematologic malignancies by p53 mutational status dependent apoptosis [12]. But, in solid tumor cell lines, CX-5461 inhibits the initiation stage of rRNA synthesis by RNA pol-

ymerase I and induces both senescence and autophagy by a p53-independent process [11]. These differential responses between the nucleolar stress and cell death according to different types of cancer may mean that hematological malignancies have unique nucleolar biology susceptible to activation of p53 dependent apoptosis following acute perturbations of ribosome biogenesis [12]. However, we showed that CX-5461 is more sensitive in A2780ip2 with *TP53* wild type than in A2780cp20 with a *TP53* mutation. This finding may mean that CX-5461 may have a therapeutic effect for ovarian cancer through p53 activation. Conversely, we found that the taxane resistant lines SKOV3TRip2 and HeyA8MDR were more sensitive to Pol I inhibition than their parental lines, even though SKOV3 has a mutation in *TP53* in both lines, while HeyA8 is wild-type for *TP53* in both lines.

Based on our RNAseq data and the *in vitro* cell line data, we moved forward with treating 5 PDX lines with CX-5461 in a single agent setting. If up-regulation of ribosomal synthesis is a hallmark of aggressive cancer and is required for cellular proliferation, inhibition may lead to a novel treatment approach. In a single agent setting, we found a variable response to CX-5461 treatment with each PDX having a different level of response to treatment. In our investigation the only unifying feature is that higher basal levels of Pol I initiation factors *RRN3* and *POLR1B* correlated with a greater response to therapy.

However, the data are too preliminary to be able to identify a level of expression of these factors that would predict CX-5461 response. More importantly, two out of five of the PDX models had regression of tumor, with 1 having a complete clinical response. One PDX had stable disease, while two PDXs grew. While preliminary, this would indi-

cate a 40-60% response rate to CX-5461 in a single agent setting. The ovarian PDX model more accurately replicates the biology of the original patients' tumor and this level of response provides strong evidence for moving CX-5461 into a more expansive pre-clinical trials and potentially clinical trials.

Table 1: Mutational status and IC₅₀ of CX-5461 in the ovarian cancer cell lines tested. A2780ip2, SKOV3ip1, and HeyA8 are the chemotherapy sensitive ovarian cancer cell lines. A2780cp20, SKOV3TRip2, and HeyA8MDR are the corresponding chemotherapy resistant lines, respectively. P53 mutation status was determined for each line based and compared to the IC₅₀ of CX-5461.

Cell lines	P53 state	CX-5461 IC50
A2780ip2	WT	22nM
A2780cp20	MT	92nM

SKOV3ip1	MT	510nM
SKOV3TRip2	MT	48nM

HeyA8	WT	1900nM
HeyA8MDR	WT	67nM

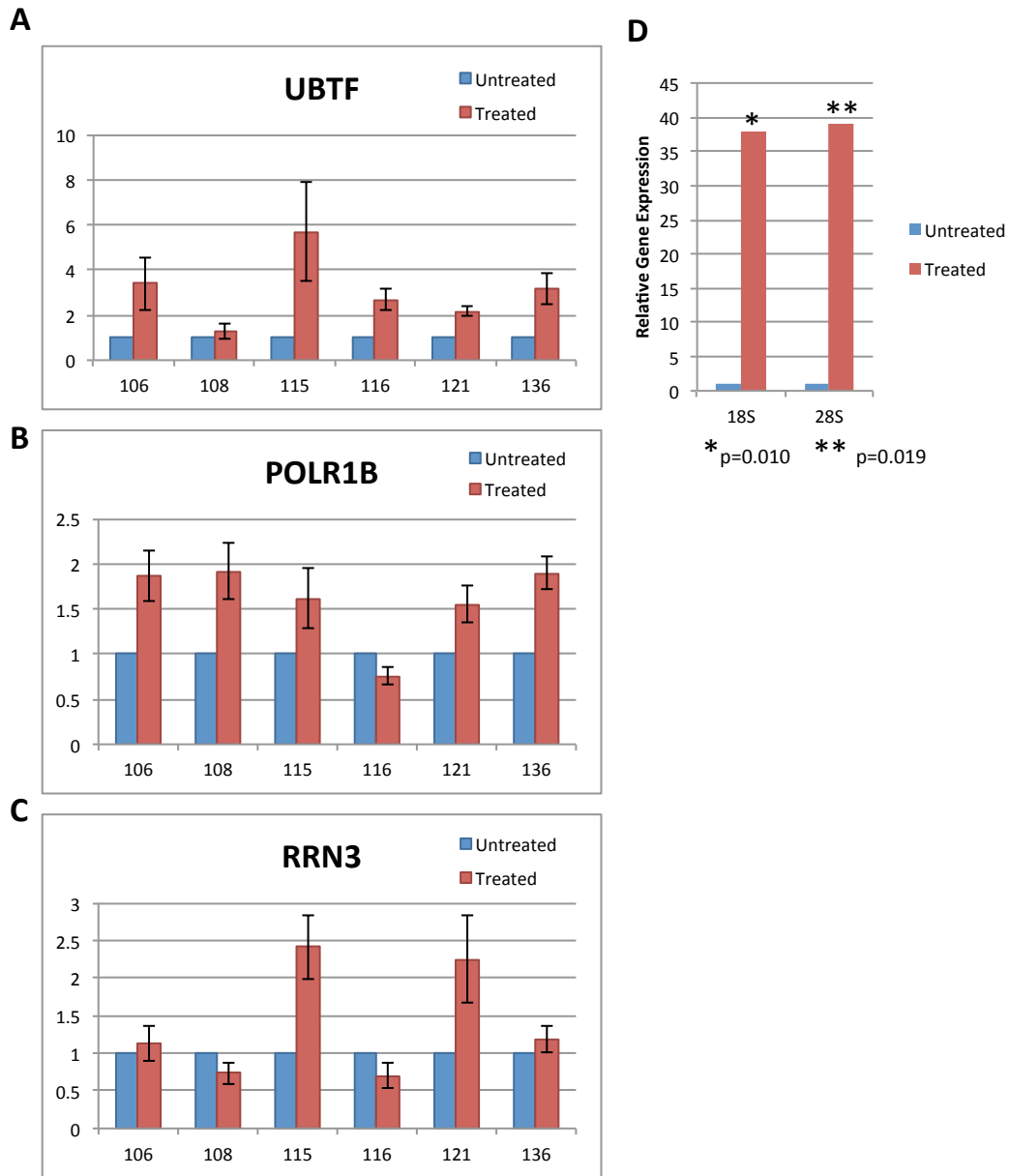


Figure 1: Expression of RNA Polymerase I initiation factors in ovarian cancer PDX models. (A,B,C) qPCR was conducted on 6 pairs of ovarian cancer PDX treated with carboplatin and paclitaxel or control for *UBTF*, *POLR1B*, and *RRN3* and gene expression was compared to the untreated matched PDX. The tumor cell population surviving initial chemotherapy generally had a greater expression of *UBTF*, *POLR1B*, and *RRN3*. (D) Total level of ribosomal subunits 18S and 28S was determined. Treated ovarian cancer PDXs had a 37.9-fold increase of 18S ($p=0.010$) and a 39.0-fold increase of 28S ($p=0.019$).

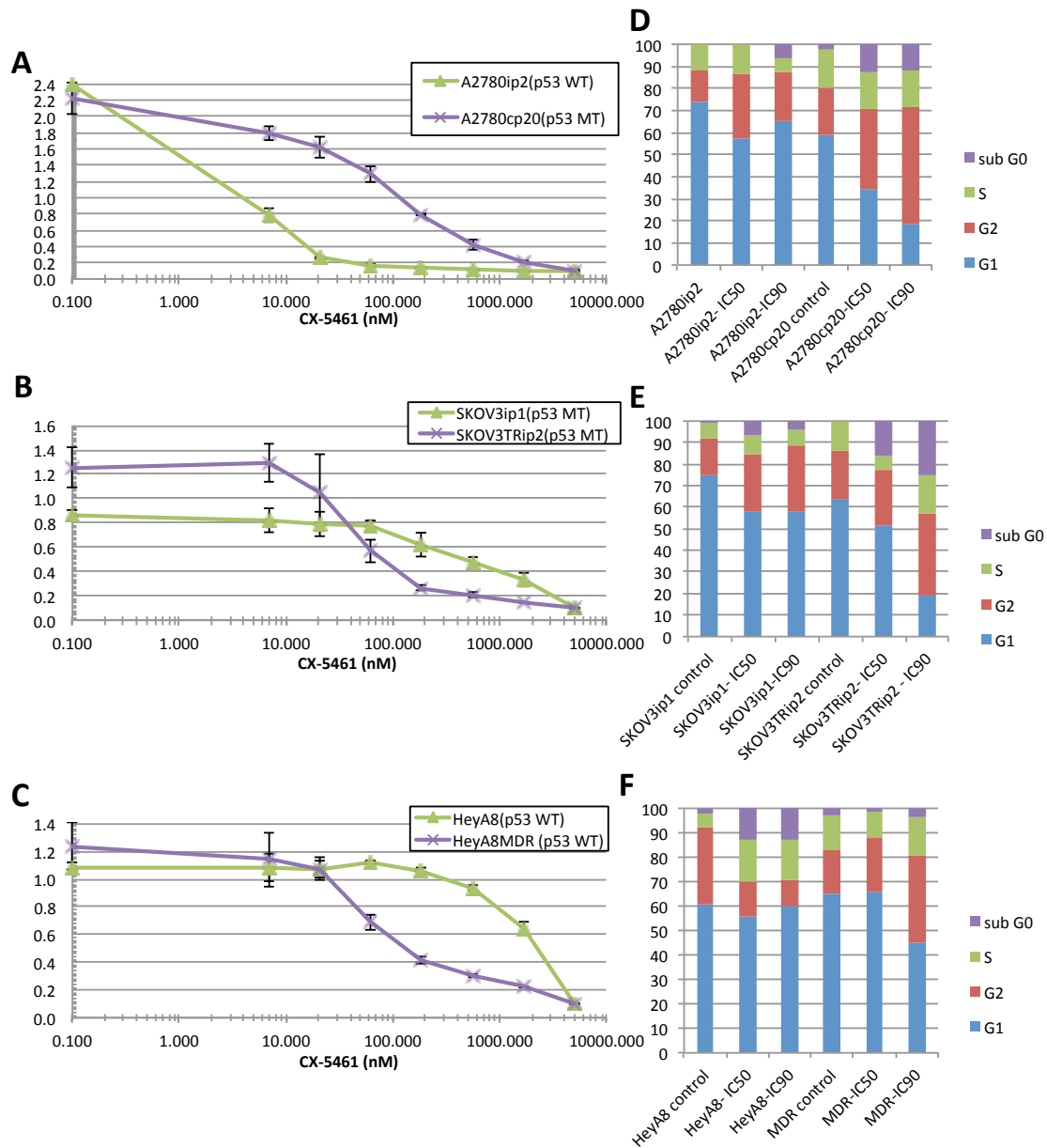


Figure 2: Response of ovarian cancer cell lines to CX-5461. Cell viability and cell cycle analysis was conducted on 6 pairs of chemo-sensitive and chemo-resistant ovarian cancer cell lines. (A) MTT assay of A2780ip2 and chemoresistant A2780cp20 and A2780cp55 showed that the *TP53* wild-type A2780ip2 was more sensitive than A2780cp20 and A2780cp55 to CX-5461. (B) MTT assay of SKOV3ip1 and SKOV3TRip2 after treatment with CX-5461 indicates that SKOV3TRip2 has a lower IC₅₀ for CX-5461. (C) MTT assay of HeyA8 and HeyA8MDR after treatment with CX-5461. HeyA8MDR was more sensitive than chemo-sensitive HeyA8. (D-F) Cell cycle analysis of A2780ip2, A2780cp20, SKOV3ip1, SKOV3TRip2, HeyA8, and HeyA8MDR using propidium iodide after 48 hr treatment with the control, IC₅₀, or IC₉₀ dose of CX-5461. In general, treatment with CX-5461 resulted in an increase in sub-G₀ fraction and a portion of cells in the S/G₂ phase.

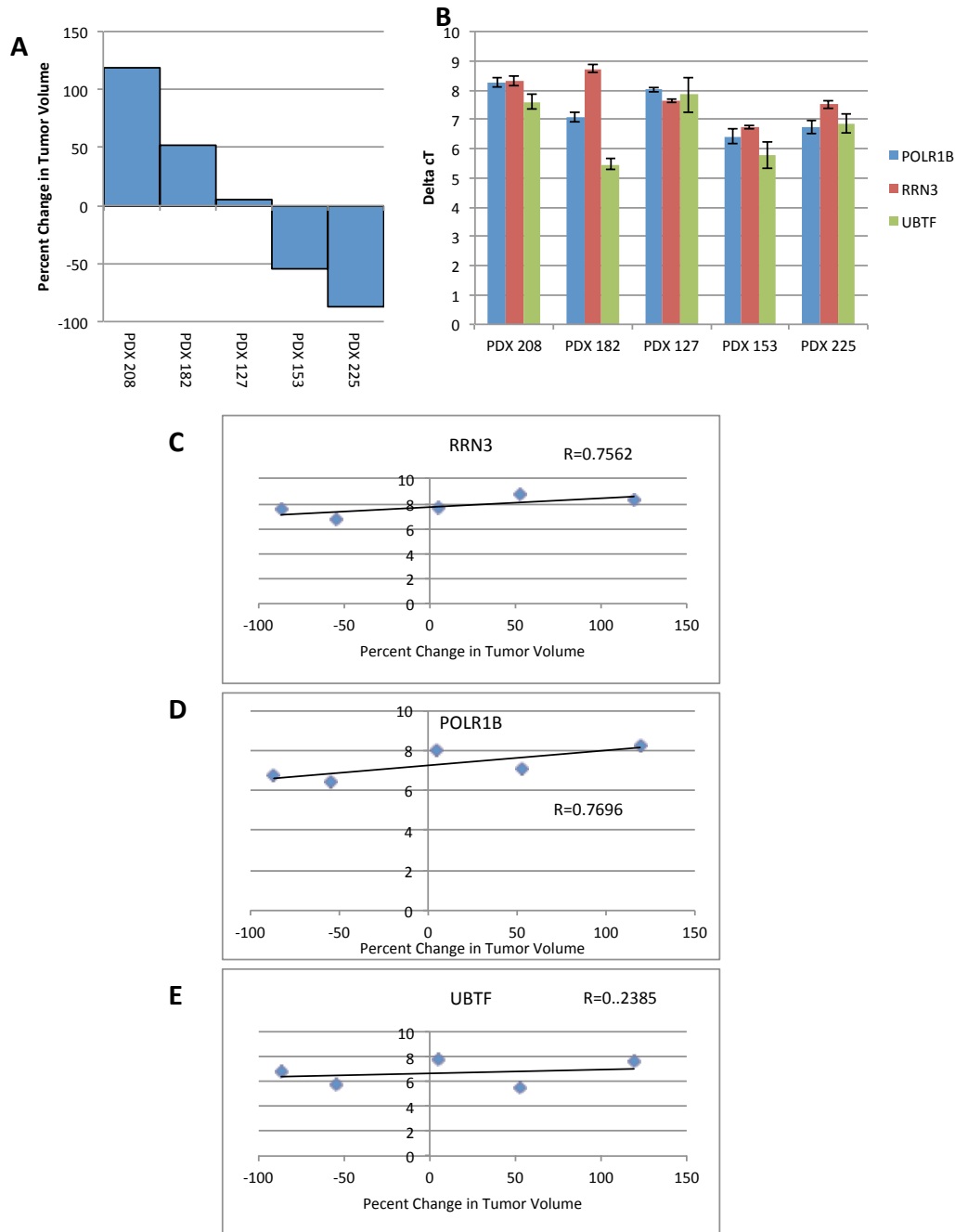


Figure 3: Treatment of ovarian cancer PDX with CX-5461. (A) Waterfall plot displaying percent change of tumor volume in PDXs 208, 182, 127, 153, and 225 after 45 days of treatment with 50mg/kg CX-5461 q3D. (B) qPCR of Pol I initiation factors *RRN3*, *POLR1B*, and *UBTF*. ΔC_T was calculated. There was an increase in expression of *RRN3*, *POLR1B*, and *UBTF* in PDX models that had a greater response to CX-5461. (C,D,E) ΔC_T of *RRN3*, *POLR1B*, and *UBTF* was plotted against the percent change in tumor volume. There was a strong positive correlation of *RRN3* ($R=0.7562$) and *POLR1B* ($R=0.7696$) expression and reduction in tumor volume. *UBTF* expression did not correlate with tumor reduction.

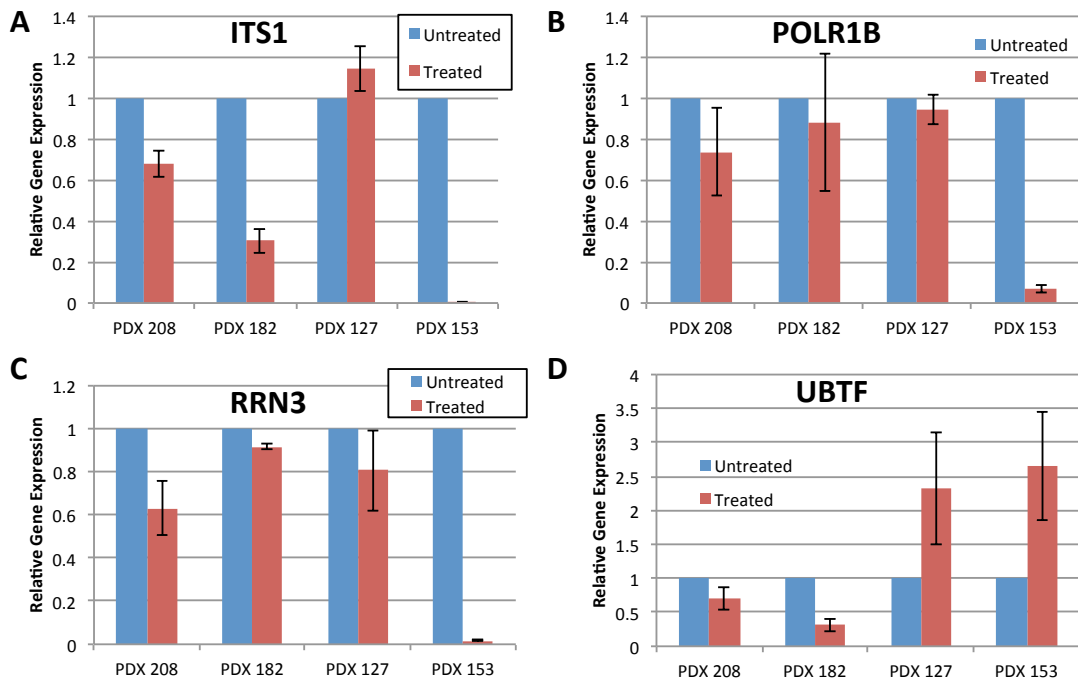


Figure 4: Response of ribosomal translation factors after CX-5461 treatment. (A) *ITS1* expression was measured using qPCR and relative gene-expression was determined. In PDX 208, 182, and 153 there was a decrease in expression of *ITS1* after CX-5461 treatment. However, PDX 127 did not show a decrease but had a stable tumor size on CX-5461. (B-D) Relative gene expression of *POLR1B*, *RRN3*, and *UBTF* using qPCR in PDX treated with CX-5461 compared to untreated PDXs. There was no significant pattern of response indicating CX-5461 is acting downstream of Pol I initiation factors act but before ribosomal translation begins.

REFERENCES

1. Berek, J.S., T.A. Longacre, and M. Friedlander, *Chapter 37. Ovarian, fallopian tube, and peritoneal cancer*. 15th ed. Berek and Novaks Gynecology. 2012, Philadelphia: Lippincott Williams and Wilkins.
2. Armstrong, D.K., *Relapsed ovarian cancer: challenges and management strategies for a chronic disease*. *Oncologist*, 2002. **7 Suppl 5**: p. 20-8.
3. Borst, P., *Cancer drug pan-resistance: pumps, cancer stem cells, quiescence, epithelial to mesenchymal transition, blocked cell death pathways, persists or what?* *Open Biology*, 2012. **2**(5).
4. Rubin, S.C., et al., *Ten-year follow-up of ovarian cancer patients after second-look laparotomy with negative findings*. *Obstet Gynecol*, 1999. **93**(1): p. 21-4.
5. Shiue, C.N., A. Arabi, and A.P. Wright, *Nucleolar organization, growth control and cancer*. *Epigenetics*, 2010. **5**(3): p. 200-5.
6. White, R.J., *RNA polymerases I and III, non-coding RNAs and cancer*. *Trends Genet*, 2008. **24**(12): p. 622-9.
7. Williamson, D., et al., *Nascent pre-rRNA overexpression correlates with an adverse prognosis in alveolar rhabdomyosarcoma*. *Genes Chromosomes Cancer*, 2006. **45**(9): p. 839-45.
8. Hannan, K.M., et al., *Dysregulation of RNA polymerase I transcription during disease*. *Biochim Biophys Acta*, 2013. **1829**(3-4): p. 342-60.
9. Drygin, D., W.G. Rice, and I. Grummt, *The RNA polymerase I transcription machinery: an emerging target for the treatment of cancer*. *Annu Rev Pharmacol Toxicol*, 2010. **50**: p. 131-56.
10. Burger, K., et al., *Chemotherapeutic drugs inhibit ribosome biogenesis at various levels*. *J Biol Chem*, 2010. **285**(16): p. 12416-25.
11. Drygin, D., et al., *Targeting RNA Polymerase I with an Oral Small Molecule CX-5461 Inhibits Ribosomal RNA Synthesis and Solid Tumor Growth*. *Cancer Research*, 2011. **71**(4): p. 1418-1430.
12. Bywater, Megan J., et al., *Inhibition of RNA Polymerase I as a Therapeutic Strategy to Promote Cancer-Specific Activation of p53*. *Cancer Cell*, 2012. **22**(1): p. 51-65.

13. Louie, K.G., et al., *Radiation survival parameters of antineoplastic drug-sensitive and -resistant human ovarian cancer cell lines and their modification by buthionine sulfoximine*. *Cancer Res*, 1985. **45**(5): p. 2110-5.
14. Landen, C.N., et al., *Tumor-selective response to antibody-mediated targeting of alphavbeta3 integrin in ovarian cancer*. *Neoplasia*, 2008. **10**(11): p. 1259-67.
15. Halder, J., et al., *Focal adhesion kinase targeting using in vivo short interfering RNA delivery in neutral liposomes for ovarian carcinoma therapy*. *Clin Cancer Res*, 2006. **12**(16): p. 4916-24.
16. Buick, R.N., R. Pullano, and J.M. Trent, *Comparative properties of five human ovarian adenocarcinoma cell lines*. *Cancer Res*, 1985. **45**(8): p. 3668-76.
17. Moore, D.H., et al., *Collagenase expression in ovarian cancer cell lines*. *Gynecol Oncol*, 1997. **65**(1): p. 78-82.
18. Yu, D., et al., *Enhanced c-erbB-2/neu expression in human ovarian cancer cells correlates with more severe malignancy that can be suppressed by E1A*. *Cancer Res*, 1993. **53**(4): p. 891-8.
19. Duan, Z., et al., *TRAG-3, a novel gene, isolated from a taxol-resistant ovarian carcinoma cell line*. *Gene*, 1999. **229**(1-2): p. 75-81.
20. Dobbin, Z.C., et al., *Using heterogeneity of the patient-derived xenograft model to identify the chemoresistant population in ovarian cancer*. 2014. 2014.
21. Drygin, D., et al., *Anticancer activity of CX-3543: a direct inhibitor of rRNA biogenesis*. *Cancer Res*, 2009. **69**(19): p. 7653-61.
22. Steg, A., et al., *Multiple Gene Expression Analyses in Paraffin-Embedded Tissues by TaqMan Low-Density Array: Application to Hedgehog and Wnt Pathway Analysis in Ovarian Endometrioid Adenocarcinoma*. *The Journal of Molecular Diagnostics*, 2006. **8**(1): p. 76-83.
23. Cancer Genome Atlas Research, N., *Integrated genomic analyses of ovarian carcinoma*. *Nature*, 2011. **474**(7353): p. 609-15.
24. Forbes, S., et al., *COSMIC 2005*. *Br J Cancer*, 2006. **94**(2): p. 318-22.
25. Skilling, J.S., et al., *p53 gene mutation analysis and antisense-mediated growth inhibition of human ovarian carcinoma cell lines*. *Gynecol Oncol*, 1996. **60**(1): p. 72-80.
26. Klein, J. and I. Grummt, *Cell cycle-dependent regulation of RNA polymerase I transcription: The nucleolar transcription factor UBF is inactive in mitosis and early G1*. *Proceedings of the National Academy of Sciences*, 1999. **96**(11): p. 6096-6101.

27. Narla, A. and B.L. Ebert, *Translational medicine: ribosomopathies*. Vol. 118. 2011. 4300-4301.
28. Bywater, M.J., et al., *Dysregulation of the basal RNA polymerase transcription apparatus in cancer*. Nat Rev Cancer, 2013. **13**(5): p. 299-314.
29. Hein, N., et al., *The nucleolus: an emerging target for cancer therapy*. Trends Mol Med, 2013. **19**(11): p. 643-54.

GENERAL DISCUSSION

Summary of Key Findings

In this dissertation, works were presented on the establishment of an ovarian cancer PDX model for the purposes of attempting to identify the population of cells responsible for chemotherapy resistance. In Section 2 (pp. 19 – 45), a description of the role of the PI3K/AKT/MTOR pathway in not only the tumorigenesis of ovarian cancer, but its progression, proliferation, and potential roles in survival after chemotherapy.

PI3K/AKT/MTOR alterations can be initializing events for high-grade serous ovarian carcinoma. Additionally, changes to outside inputs in the PI3K/AKT/MTOR pathway, such as AMPK, sMEK, or FASN can result in deregulation of this pathway resulting in an increase in tumor cell survival, invasion and migration. While there has been clinical correlation of members of the PI3K/AKT/mTOR pathway predicting patient response to chemotherapy, targeting the pathway is difficult due to the numerous inputs and outputs that can be altered. However, there has been promise with the use of some PI3K/AKT/MTOR pathway inhibitors in recent clinical studies [81].

Section 3 (pp. 46 – pp. 85) focused on the development and characterization of the ovarian cancer PDX model. We showed that the ovarian PDX model can be established with a high engraftment of 85% when using the subcutaneous compartment. This rate is the highest reported in a large cohort of ovarian cancer PDX, with the Werhoa *et al* group reporting 74% with the IP model [71, 73]. While there were concerns about using the heterotopic site versus the orthotopic site, our PDX model showed a strong correla-

tion of oncogene expression between matched SQ PDX tumors and IP PDX tumors, including a strong correlation between the SQ PDX tumors and the original patient sample. This indicates, that at least in ovarian cancer, the use of the heterotopic location does not dramatically affect the key genetic make up of the tumor [73]. Our results were confirmed in the IP ovarian PDX model where Werhoa *et al* also saw a strong correlation of gene expression between the PDX and the original patient [71]. In addition to genetic expression, our model demonstrated a statistically significant correlation in response to primary combination therapy of carboplatin and paclitaxel. Patients that had a complete response to primary therapy corresponded to PDX models that had the greatest reduction in volume. These findings indicate that our PDX model has biological and clinical relevance to the disease afflicting the patient population, allowing for a platform that can potentially investigate ovarian cancer with greater fidelity than the use of clonal cells. When the PDX model was interrogated for expression of CSC cells, we saw that while the treated tumor was enriched for expression of CD133 and ALDH1A1, like what is seen in persistent disease in the patients, they did not make up the majority of the surviving tumor. When RNAseq was conducted on the treated and untreated PDX models, we discovered that chemotherapy induces the expression of ribosomal synthesis genes (explored in Section 4) and one of the top altered pathways was the Sphingosine-1-phosphate pathway.

One of the interesting findings from the RNAseq conducted on the ovarian cancer PDX models was the upregulation of ribosomal synthesis genes. In Section 4 (pp. 86 – pp. 106) we tested the effect of inhibiting Pol I on the survival of ovarian cancer cells and in the ovarian cancer PDX model. When examining the chemotherapy treated ovarian

cancer PDX models, we found that there was an ~30-fold increase in expression of rRNA 18S and 28S, indicating a higher amount of ribosomes after chemotherapy treatment. Coupled with the RNAseq data, this led to the hypothesis that if Pol I was targeted, the polymerase responsible for synthesizing ribosomes, ovarian cancer cells could be killed. The Pol I inhibitor CX-5461 was used as it has been shown to be selective for Pol I and had the ability to kill ovarian cancer cell lines [82]. Interestingly, we found that our chemotherapy resistant cell lines SKOV3TR and HeyA8MDR were more sensitive to Pol I inhibition compared to their chemotherapy sensitive parental lines SKOV3ip1 and HeyA8. When treating the ovarian cancer PDX models, we found a variable response with some models showing complete regression on single agent and some growing. While a 100% response rate was not expected, we conclude that further studies using CX-5461 in a treatment regimen for ovarian cancer needs to be explored.

Current and Future Directions

Development of a Fully Chemotherapy Resistant Ovarian Cancer PDX

The work presented in Section 3 (pp. 47 – pp. 86) focused on the initial characterization and response to chemotherapy of the ovarian PDX model. What the PDX models provides is a platform for the development of chemotherapy resistant phenotype there a “natural” evolution. The PDX models were treated with a combination of carboplatin and paclitaxel until the original tumor regressed to no evidence of disease (NED). In the first study of the PDX model, chemotherapy treatment was stopped at 4 weeks to allow for a sample to analyze. After the PDX model reached NED, the model was placed on observation until recurrence of tumor (Figure 1). Due to the age of the animal at the time of recurrence, the tumor was harvested and re-implanted into new mice to allow for continued

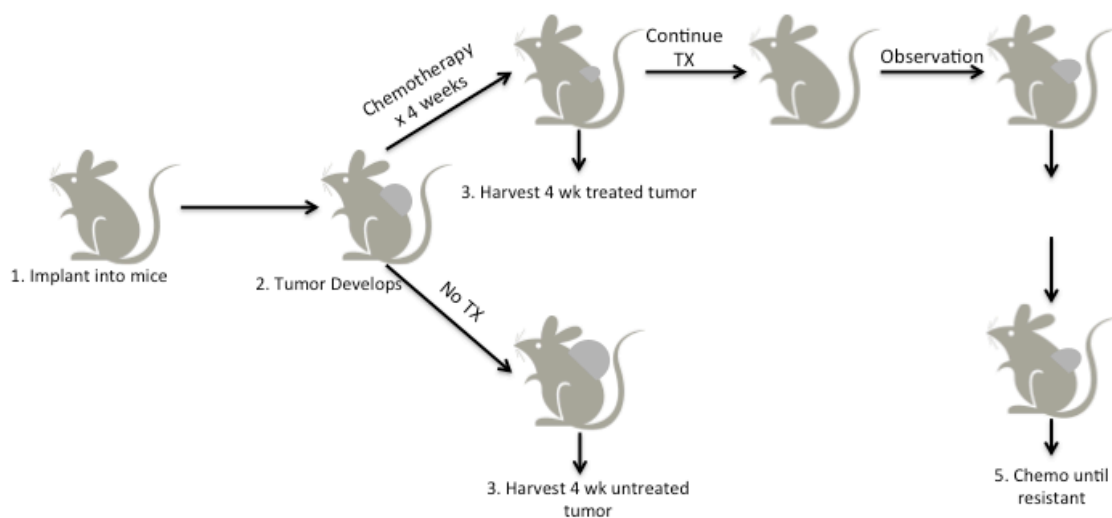


Figure 1: *Model of development for a chemotherapy-resistant PDX.* In the original study design, after 4 weeks of chemotherapy treatment in the PDX, tumors were harvested and examined. In order to develop a chemotherapy resistant PDX, treatment was continued until the mouse had no evidence of disease or stopped responding to therapy. At that point, the PDX was placed on observation and once tumor recurred, it was extracted and expanded into new mice and re-challenged with chemotherapy until resistant.

development. Once the new generation of PDX tumor grew, it was challenged with chemotherapy to demonstrate resistance (Figure 2). Typically, chemotherapy resistance developed after the first recurrence, though in PDX 208, resistance development has required multiple exposures to chemotherapy. The advantage of developing resistance in this method is it replicates the clinical process. It is our hypothesis that the mechanism the PDX tumor uses to gain chemotherapy resistance will be similar to the mechanisms in the patient's tumor. This would allow for novel targets and therapeutics interventions to be developed to target the resistant population.

Targeting Cancer Stem Cells in the Chemotherapy Resistant PDX

As work by Steg *et al* showed, chemotherapy resistant ovarian cancer clinical specimens were significantly enriched for at least one of the CSC markers ALDH1A1 or CD133 [48]. If CSC are responsible for recurrence and chemotherapy resistance, targeting this population is necessary to improve survival [20, 38]. Methods for targeting CSC include targeting the CSC marker directly, targeting the pathways involved in “stemness” or conjugating standard chemotherapy to an aptamer that targets CSC resulting in both the non-CSC and CSC population being targeted [20, 83]. In conjunction with our collaborators at the University of Michigan, we used a small molecule to target ALDH+/CD133+ populations. 673A was identified by Dr. Ronald Buckanovich's group by screening a library of compounds that had confirmed or potential anti-ALDH activity based on molecular homology to the ALDH inhibitor DEAB [84]. 673A was found to deplete ovarian cancer cell line A2780 of ALDH activity as measured by the ALDEFLUOR assay and also depleted the CD133⁺ population. In our hands, we took the

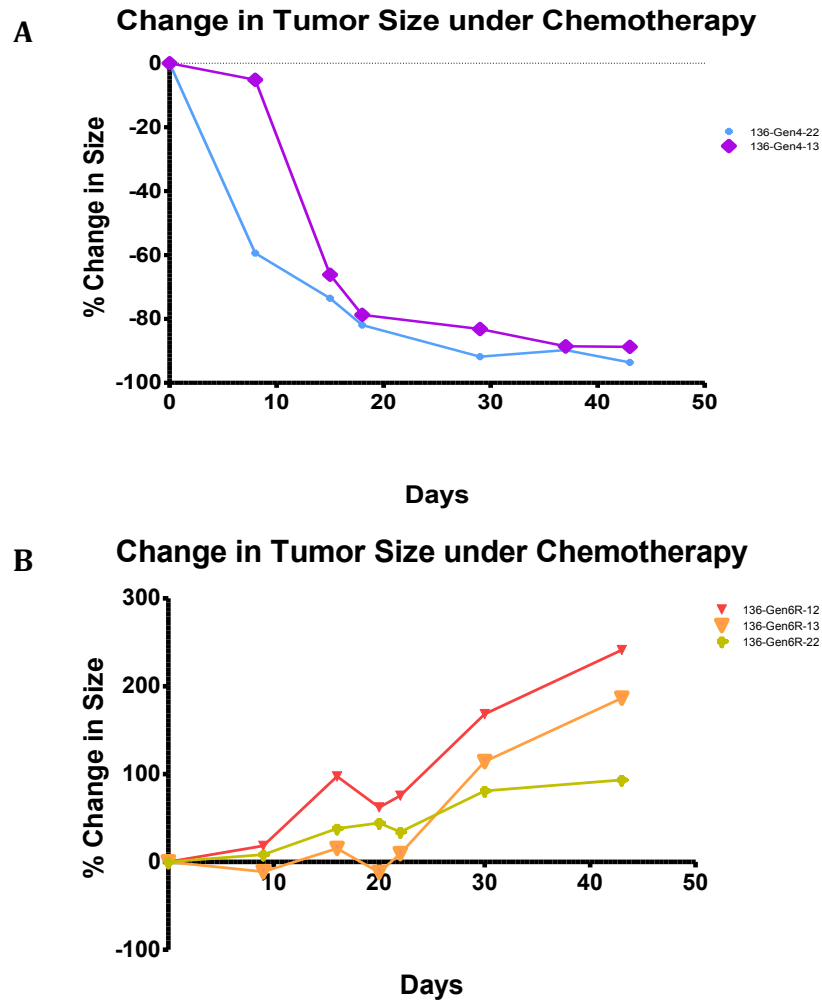


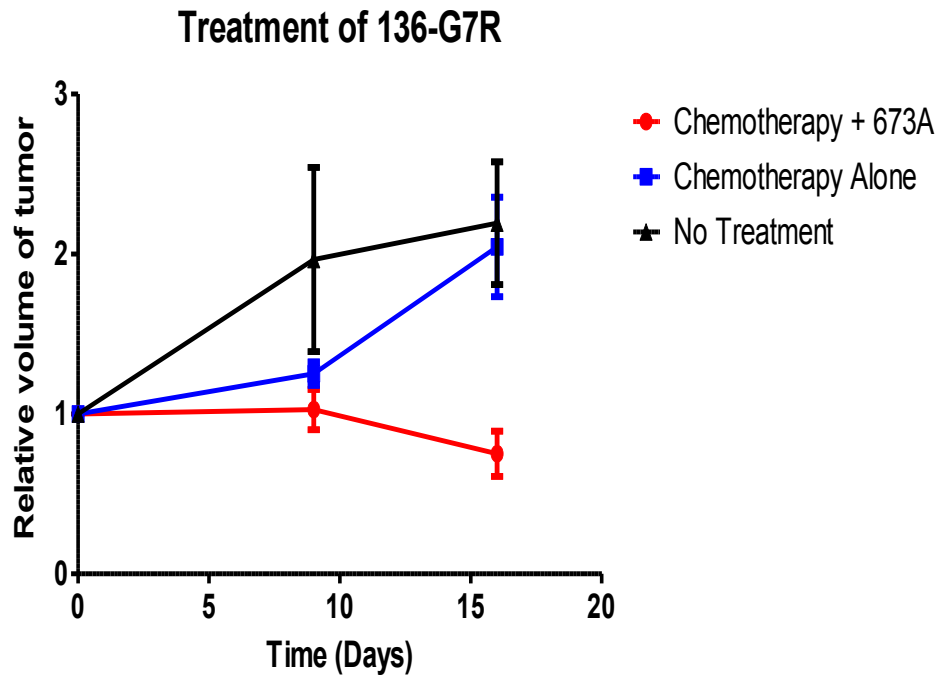
Figure 2: Comparison between chemotherapy sensitive and resistant PDX. (A) PDX 136 was initially chemosensitive and showed complete regression of the tumor after approximately 40 days of chemotherapy. After the tumor recurred and was expanded into new mice, PDX 136 was re-treated with chemotherapy. (B) PDX-136-Resistant grows on chemotherapy demonstrating the development of complete resistance to carboplatin and paclitaxel as compared to PDX-136-Sensitive.

chemotherapy-resistant PDX 136R and the corresponding sensitive line PDX 136S. Both lines were treated with vehicle, carboplatin, or carboplatin + 673A. Carboplatin was administered at 90 mg/kg injection IP weekly while 673A was injected daily IP at 2.23 mg/kg. In PDX-136R, tumor volume increased on vehicle treatment and carboplatin, while carboplatin plus 673A resulted in stable disease that started regressing (Figure 3). The difference in tumor volume was significantly reduced in the carboplatin + 673A treatment group ($p < 0.05$). However, in the chemosensitive PDX-136S, vehicle treatment resulted in tumor growth, but carboplatin and carboplatin + 673A had similar regression (Figure 4).

The responses seen in PDX 136S make sense, as the ALDH+/CD133+ population is in the minority therefore the majority of the tumor volume is comprised of the chemotherapy sensitive cells. In PDX 136R it needs to be evaluated what was the composition of the tumor before and after treatment with 673A in terms of the CSC markers ALDH1A1 and CD133. In addition, future experiments need to be conducted in the other PDX models to make sure this response isn't limited to the one PDX. However, these preliminary results are promising in that directly targeting the CSC with a molecular target could reverse chemotherapy resistance.

Identifying novel pathways to target chemotherapy resistance in ovarian cancer

By subjecting the ovarian cancer PDX tumors to a combination of paclitaxel and carboplatin, we were able to recreate the clinical regimen patients undergo. This created a cohort of treated with matched untreated PDX tumors that could be examined for molecular changes that could provide insight into how the tumor cells are surviving chemotherapy. One of the first methods that were used was Ki-67 staining to understand



Change in tumor volume at end of treatment

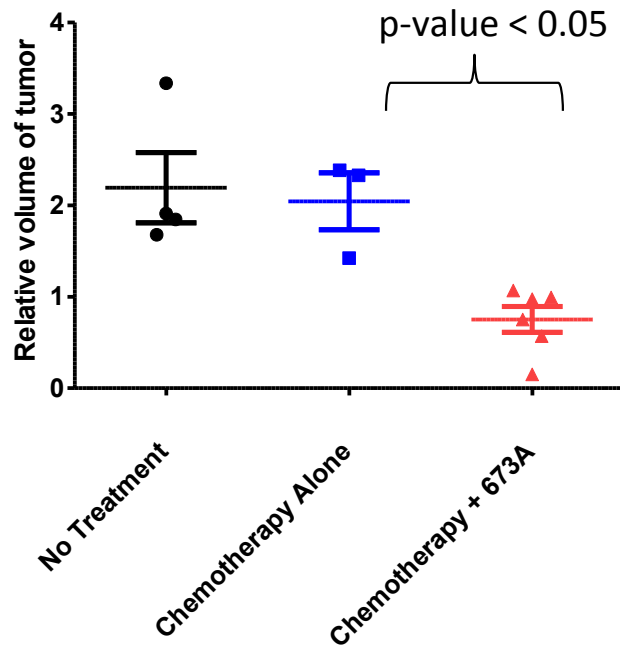


Figure 3: *Treatment of PDX-136-Resistant with 673A and Chemotherapy.* 673A is a compound that specifically depletes tumors of the ALDH1A1 and CD133 positive CSC populations. When used in combination with chemotherapy in the chemotherapy resistant PDX-136, there was a significant decrease in volume of the tumor at the end of treatment as compared to chemotherapy alone, which grew similar to the untreated PDX.

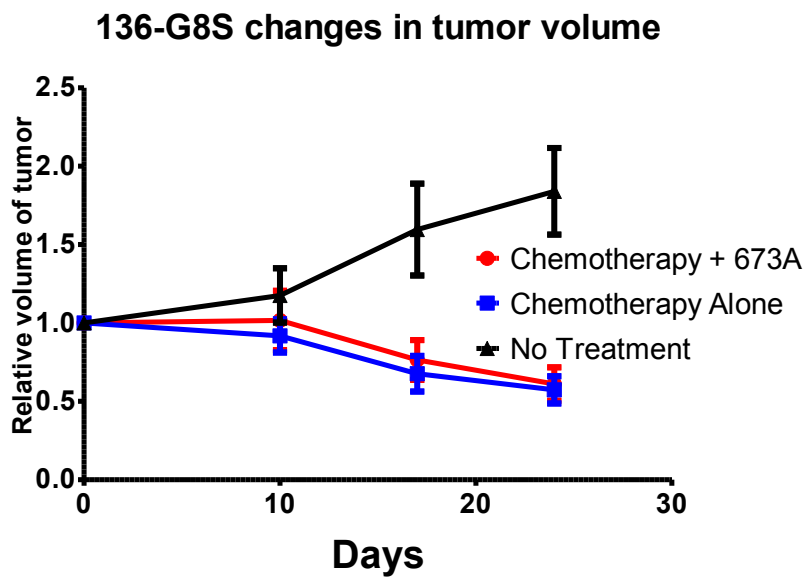


Figure 4: *Treatment of PDX-136 Sensitive with 673A and Chemotherapy.* When the original chemosensitive PDX 136 was treated with the CSC-targeting 673A and chemotherapy, there was no difference in reduction of tumor volume as compared to chemotherapy alone. This is expected as the CSC should be a minority of the tumor population in the sensitive model as compared to the resistive, with the bulk of the tumor being killed by the chemotherapy.

how proliferation was changing due to chemotherapy. Interestingly, a significant decrease in proliferation was noted in the treated PDX tumors compared to the untreated PDX. However, on histological examination, there were still normal looking tumor cells in appearance. This led to the idea that a dormancy phenotype was being deployed to allow the cells to survive.

Autophagy in ovarian cancer PDX

Chemotherapy treated and untreated ovarian cancer PDX models were stained for microtubulue-associated protein 1 light change 3 (LC3) using immunohistochemistry. LC3, a mammalian orthologue of yeast ATG8 is a marker for autophagosome formation [85, 86]. In autophagy, the cytosolic precursor, LC3-I undergoes proteolytic cleavage at the C-terminal end followed by the lipidation of the exposed glycine residue with a phosphatidylethanolamine group, called LC3-II [85]. LC3-II, which is incorporated into the autophagosome membrane and is in combination with p62, which is degraded in autophagy, is a measure of autophagosome activity [85, 87, 88]. After determining intensity of staining by scoring for percent expression of LC3 on the specimens (Figure 5A), the treated specimens had an average staining of 64 % while the untreated PDX had an average of 58% expression (p-value = 0.640) (Figure 5B) While the change in expression of LC3 was not significant when all PDX models were combined, there were some pairs of PDX samples that did show an increase in LC3 expression. For example, PDX 108 increased from 22.5% to 95% and PDX 135 increased from 20% to 85%. Analysis of the conversion of LC3-I to LC3-II using Western Blot showed similar results, with the amount of LC3-II, a marker of autophagosomes, increasing in a few PDX samples, but unchanged in others (Figure 5C). This indicates that autophagy does occur

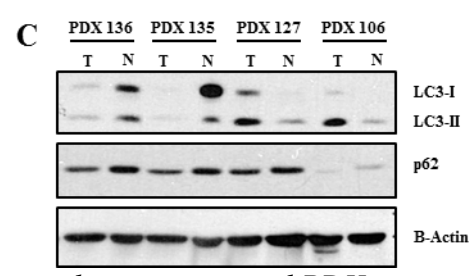
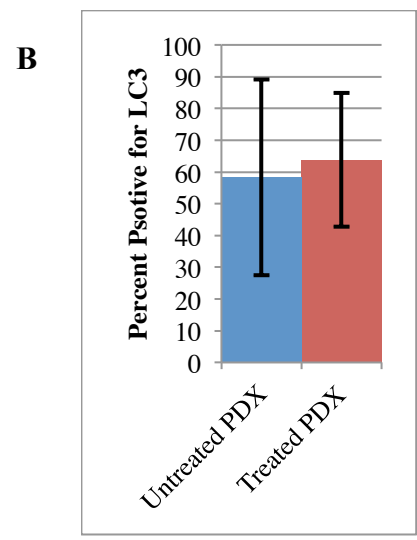
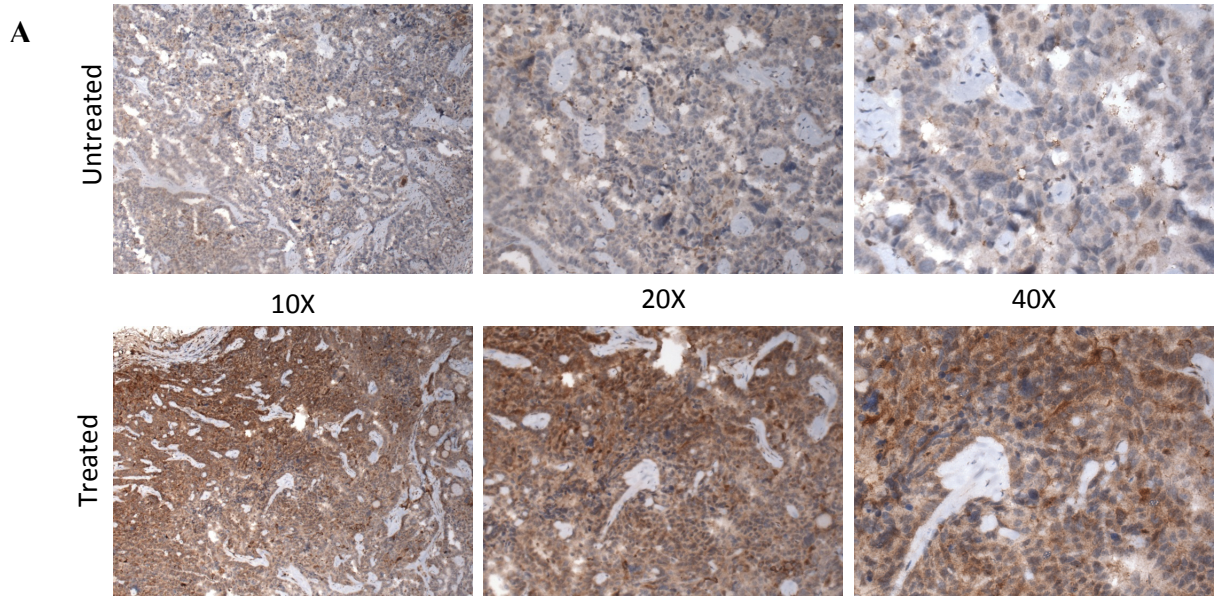


Figure 5: Analysis of autophagy induction in treated PDX tumors. (A) Using IHC for LC3-II, some PDX models showed an increase in expression of LC3-II after treatment with chemotherapy. (B) However, quantification of LC3-II expression was not significantly different between the treated and untreated PDX models. (C) On Western Blot, there was variable induction of autophagy as measured by an increase in the LC3-II vs LC3-I fragment and decrease in p62 levels. T =treated, N = no treatment.

in some specimens in response to therapy, it is not a universal response. A key question that requires further study is if the autophagy seen in some of the PDX samples is an example of pro-tumorigenic autophagy, where the cells are using the dormancy of autophagy for survival. In ovarian cancer, the gene *ARHI* has been shown to induce autophagic cell death *in vitro*, however, in an *in vivo* setting, *ARHI* expression results in the cells surviving as dormant cells that are able to regrow tumors [89]. In addition, these *ARHI*-expressing dormant cells can only be killed when the autophagy inhibitor chloroquine is used [89]. This provides evidence that autophagy can induce a protective dormant phenotype for ovarian cancer allowing the tumor to recur at a later date.

In addition, the RNAseq data showed that 3rd most altered pathway was Sphingosine-1-phosphate signaling (S1P). This pathway has a role in the initiation of autophagy that appears to be protective for cells undergoing stress through the inhibition of mTOR signaling pathway [90]. In two studies, it was shown that S1P pathway induction of autophagy resulted in protecting normal oocytes from chemotherapy/radiation used in treatment of other non-ovarian malignancies [91, 92]. In ovarian cancer, one group found that by treating with a sphingosine analog, FTY-720, resulted in protective autophagy, antagonizing the activity of cisplatin [93]. This information, including the fact that some of the PDX models did show an increase in autophagy, provides the groundwork for exploring the role of the Sphingosine-1-phosphate pathway in ovarian cancer chemotherapy resistance.

Conflict between induction of autophagy and ribosome translation

In the initial analysis of the data, it appeared that we were observing both a global increase in the amount of autophagy and the amount of ribosome translation. These func-

tions are normally considered to be on the opposite side of physiological activities for cells. In addition, one of the frequent roles of autophagy is to degrade mature ribosomes [94]. However, there is a possible connection between the autophagy and increase in ribosomal synthesis that was observed. The gene *MYC* is mutated in approximately 25% of epithelial ovarian cancers [19, 95]. *MYC* is an interesting oncogene that after chromosomal translocation and gene amplification can cause both increased proliferation and apoptosis depending on the cellular context [96-99]. c-Myc functions as a transcription factor that induces proliferations and importantly ribosome biogenesis, which is associated with an increased rate of protein synthesis [96, 100]. This sets the stage for *MYC* alteration causing an increase in ribosome biogenesis, especially under states of stress, as the cell is trying to manufacture proteins needed for survival.

In normal cells, there is the unfolded protein response (UPR), which is a homeostasis program initiated by an excess of unfolded/misfolded proteins [96]. When the UPR is activated by microenvironmental conditions, such as lack of nutrients or hypoxia, the process of autophagy is activated in order for the cell to dispose of misfolded/unused proteins and generate the nutrients needed for survival. However in cancer, the UPR response is frequently found to be with the concurrent activation of pro-survival pathways, including *MYC* activation [101, 102]. A recent study has shown that c-Myc activation in a lymphoma model causes an increase in protein synthesis, such as ribosomal synthesis, that triggers the UPR to induce ER-autophagy as noticed by an increase in LC3-II and p62 degradation [96]. The increase in autophagy results in cell survival by avoiding apoptotic pathways and when autophagy was inhibited by using a *Perk*^{-/-} mutant and by autophagy inhibitors, cell viability decreased with a correlative increase in apoptosis activi-

ty [96]. Therefore, c-Myc activation by causing an increase in proliferation of proteins induces a protective autophagy for tumor cells.

Therefore it is the hypothesis that in the ovarian cancer PDX, treatment is causing cellular stress that is inducing c-Myc activity to increase protein proliferation. This increase in cellular proliferation is increasing ribosome biogenesis, as noted by the observed increase in total ribosomes, while also inducing the UPR to cause a protective autophagy for the surviving cells. This potential pathway activation needs to be explored to determine to what level the PDX models tested have *MYC* amplification or mutation, including examining the levels of ULK1 and Atg5 as the mediators of this protective autophagy.

Final Conclusions

This dissertation described the development and characterization of an ovarian cancer PDX model that recapitulates the heterogeneity of the patients' tumor and has biological and clinical relevance to the patient's tumor. The generation of the PDX creates a platform that can be used to delve into the mechanisms and pathways that ovarian cancer employs to survive primary chemotherapy and eventually develop chemotherapy resistance. While the generation and characterization of the fully chemotherapeutic resistant PDX models are in the infancy, preliminary data have identified a few interesting strategies for overcoming chemotherapy resistance. The most promising seems to be the direct targeting of the CSC ALDH1A1 and CD133, though this needs further exploration. Also, this dissertation work has demonstrated that targeting ribosome synthesis by Pol I inhibition is a therapeutic strategy that could have potential benefit for ovarian cancer patients. The generation, characterization, and maintenance of a PDX model is both a la-

bor and financial intensive process, however the benefits are immense for the advancement of understanding chemotherapy resistance. It is a resource that should be a priority for UAB to further develop and expand for all cancer types.

GENERAL REFERENCES

1. DeSantis, C.E., et al., *Cancer treatment and survivorship statistics, 2014*. CA Cancer J Clin, 2014. **64**(4): p. 252-71.
2. Chan, J.K., et al., *Patterns and progress in ovarian cancer over 14 years*. Obstet Gynecol, 2006. **108**(3 Pt 1): p. 521-8.
3. Morgan, R.J., et al., *Epithelial Ovarian Cancer*. Journal of the National Comprehensive Cancer Network, 2011. **9**(1): p. 82-113.
4. Siegel, R., D. Naishadham, and A. Jemal, *Cancer statistics, 2013*. CA: A Cancer Journal for Clinicians, 2013. **63**(1): p. 11-30.
5. Armstrong, D.K., *Relapsed ovarian cancer: challenges and management strategies for a chronic disease*. Oncologist, 2002. **7 Suppl 5**: p. 20-8.
6. Olson, S.H., et al., *Symptoms of ovarian cancer*. Obstet Gynecol, 2001. **98**(2): p. 212-7.
7. Vine, M.F., et al., *Types and duration of symptoms prior to diagnosis of invasive or borderline ovarian tumor*. Gynecol Oncol, 2001. **83**(3): p. 466-71.
8. Goff, B.A., et al., *Ovarian carcinoma diagnosis*. Cancer, 2000. **89**(10): p. 2068-75.
9. Buys, S.S., et al., *Effect of screening on ovarian cancer mortality: the Prostate, Lung, Colorectal and Ovarian (PLCO) Cancer Screening Randomized Controlled Trial*. Jama, 2011. **305**(22): p. 2295-303.
10. Bristow, R.E., et al., *Survival Effect of Maximal Cytoreductive Surgery for Advanced Ovarian Carcinoma During the Platinum Era: A Meta-Analysis*. Journal of Clinical Oncology, 2002. **20**(5): p. 1248-1259.
11. Elattar, A., et al., *Optimal primary surgical treatment for advanced epithelial ovarian cancer*. Cochrane Database Syst Rev, 2011(8): p. Cd007565.
12. Hoskins, W.J., et al., *The effect of diameter of largest residual disease on survival after primary cytoreductive surgery in patients with suboptimal residual epithelial ovarian carcinoma*. Am J Obstet Gynecol, 1994. **170**(4): p. 974-9; discussion 979-80.

13. Romero, I. and R.C. Bast, *Minireview: Human Ovarian Cancer: Biology, Current Management, and Paths to Personalizing Therapy*. *Endocrinology*, 2012. **153**(4): p. 1593-1602.
14. Vaughan, S., et al., *Rethinking ovarian cancer: recommendations for improving outcomes*. *Nat Rev Cancer*, 2011. **11**(10): p. 719-725.
15. Bast, R.C., B. Hennessey, and G.B. Mills, *The biology of ovarian cancer: new opportunities for translation*. *Nat Rev Cancer*, 2009. **9**(6): p. 415-428.
16. Tone, A.A., et al., *The role of the fallopian tube in ovarian cancer*. *Clin Adv Hematol Oncol*, 2012. **10**(5): p. 296-306.
17. Bast, R.C. and G.B. Mills, *Dissecting "PI3Kness": The Complexity of Personalized Therapy for Ovarian Cancer*. *Cancer Discovery*, 2012. **2**(1): p. 16-18.
18. Kurman, R.J., et al., *Early detection and treatment of ovarian cancer: shifting from early stage to minimal volume of disease based on a new model of carcinogenesis*. *Am J Obstet Gynecol*, 2008. **198**(4): p. 351-6.
19. Cancer Genome Atlas Research, N., *Integrated genomic analyses of ovarian carcinoma*. *Nature*, 2011. **474**(7353): p. 609-15.
20. O'Connor, M.L., et al., *Cancer stem cells: A contentious hypothesis now moving forward*. *Cancer Lett*, 2014. **344**(2): p. 180-7.
21. Nowell, P.C., *The clonal evolution of tumor cell populations*. *Science*, 1976. **194**(4260): p. 23-8.
22. Nguyen, L.V., et al., *Cancer stem cells: an evolving concept*. *Nat Rev Cancer*, 2012. **12**(2): p. 133-43.
23. Hamburger, A.W. and S.E. Salmon, *Primary bioassay of human tumor stem cells*. *Science*, 1977. **197**(4302): p. 461-3.
24. Singh, S.K., et al., *Identification of human brain tumour initiating cells*. *Nature*, 2004. **432**(7015): p. 396-401.
25. Dobbin, Z.C. and C.N. Landen, *Isolation and characterization of potential cancer stem cells from solid human tumors--potential applications*. *Curr Protoc Pharmacol*, 2013. **63**: p. Unit 14.28.
26. Kelly, P.N., et al., *Tumor growth need not be driven by rare cancer stem cells*. *Science*, 2007. **317**(5836): p. 337.
27. Puglisi, M.A., et al., *Colon cancer stem cells: controversies and perspectives*. *World J Gastroenterol*, 2013. **19**(20): p. 2997-3006.

28. Dalerba, P., et al., *Phenotypic characterization of human colorectal cancer stem cells*. Proc Natl Acad Sci U S A, 2007. **104**(24): p. 10158-63.
29. Lapidot, T., et al., *A cell initiating human acute myeloid leukaemia after transplantation into SCID mice*. Nature, 1994. **367**(6464): p. 645-648.
30. Reynolds, B. and S. Weiss, *Generation of neurons and astrocytes from isolated cells of the adult mammalian central nervous system*. Science, 1992. **255**(5052): p. 1707-1710.
31. Galli, R., et al., *Isolation and characterization of tumorigenic, stem-like neural precursors from human glioblastoma*. Cancer Res, 2004. **64**(19): p. 7011-21.
32. Dalerba, P., R.W. Cho, and M.F. Clarke, *Cancer stem cells: models and concepts*. Annu Rev Med, 2007. **58**: p. 267-84.
33. Dontu, G., et al., *Stem cells in normal breast development and breast cancer*. Cell Prolif, 2003. **36 Suppl 1**: p. 59-72.
34. O'Brien, C.A., et al., *A human colon cancer cell capable of initiating tumour growth in immunodeficient mice*. Nature, 2007. **445**(7123): p. 106-10.
35. Zhang, S., et al., *Identification and characterization of ovarian cancer-initiating cells from primary human tumors*. Cancer Res, 2008. **68**(11): p. 4311-20.
36. Holohan, C., et al., *Cancer drug resistance: an evolving paradigm*. Nat Rev Cancer, 2013. **13**(10): p. 714-26.
37. Alison, M.R., et al., *Cancer stem cells: in the line of fire*. Cancer Treat Rev, 2012. **38**(6): p. 589-98.
38. Shah, M.M. and C.N. Landen, *Ovarian cancer stem cells: Are they real and why are they important?* Gynecol Oncol, 2014. **132**(2): p. 483-489.
39. Sundfeldt, K., et al., *E-cadherin expression in human epithelial ovarian cancer and normal ovary*. Int J Cancer, 1997. **74**(3): p. 275-80.
40. Auersperg, N., et al., *E-cadherin induces mesenchymal-to-epithelial transition in human ovarian surface epithelium*. Proc Natl Acad Sci U S A, 1999. **96**(11): p. 6249-54.
41. Szotek, P.P., et al., *Normal ovarian surface epithelial label-retaining cells exhibit stem/progenitor cell characteristics*. Proc Natl Acad Sci U S A, 2008. **105**(34): p. 12469-73.
42. Bowen, N.J., et al., *Gene expression profiling supports the hypothesis that human ovarian surface epithelia are multipotent and capable of serving as ovarian cancer initiating cells*. BMC Med Genomics, 2009. **2**: p. 71.

43. Humphries, A., et al., *Lineage tracing reveals multipotent stem cells maintain human adenomas and the pattern of clonal expansion in tumor evolution*. Proc Natl Acad Sci U S A, 2013. **110**(27): p. E2490-9.
44. Abitorabi, M.A., et al., *Presentation of integrins on leukocyte microvilli: a role for the extracellular domain in determining membrane localization*. J Cell Biol, 1997. **139**(2): p. 563-71.
45. Qian, X., et al., *Prognostic significance of ALDH1A1-positive cancer stem cells in patients with locally advanced, metastasized head and neck squamous cell carcinoma*. J Cancer Res Clin Oncol, 2014. **140**(7): p. 1151-8.
46. A, D.A.C.P., et al., *Co-expression of stem cell markers ALDH1 and CD44 in non-malignant and neoplastic lesions of the breast*. Anticancer Res, 2014. **34**(3): p. 1427-34.
47. Deng, Y., et al., *ALDH1 is an independent prognostic factor for patients with stages II-III rectal cancer after receiving radiochemotherapy*. Br J Cancer, 2014. **110**(2): p. 430-4.
48. Landen, C.N., et al., *Targeting Aldehyde Dehydrogenase Cancer Stem Cells in Ovarian Cancer*. Molecular Cancer Therapeutics, 2010. **9**(12): p. 3186-3199.
49. Silva, I.A., et al., *Aldehyde Dehydrogenase in Combination with CD133 Defines Angiogenic Ovarian Cancer Stem Cells That Portend Poor Patient Survival*. Cancer Res, 2011. **71**(11): p. 3991-4001.
50. Kryczek, I., et al., *Expression of aldehyde dehydrogenase and CD133 defines ovarian cancer stem cells*. Int J Cancer, 2011.
51. Zoller, M., *CD44: can a cancer-initiating cell profit from an abundantly expressed molecule?* Nat Rev Cancer, 2011. **11**(4): p. 254-67.
52. Alvero, A.B., et al., *Molecular phenotyping of human ovarian cancer stem cells unravels the mechanisms for repair and chemoresistance*. Cell Cycle, 2009. **8**(1): p. 158-66.
53. Shi, M.F., et al., *Identification of cancer stem cell-like cells from human epithelial ovarian carcinoma cell line*. Cell Mol Life Sci, 2010. **67**(22): p. 3915-25.
54. Gao, M.Q., et al., *CD24+ cells from hierarchically organized ovarian cancer are enriched in cancer stem cells*. Oncogene, 2010. **29**(18): p. 2672-80.
55. Deng, S., et al., *Distinct expression levels and patterns of stem cell marker, aldehyde dehydrogenase isoform 1 (ALDH1), in human epithelial cancers*. PLoS One, 2010. **5**(4): p. e10277.

56. Steffensen, K.D., et al., *Prevalence of epithelial ovarian cancer stem cells correlates with recurrence in early-stage ovarian cancer*. J Oncol, 2011. **2011**: p. 620523.
57. Curley, M.D., et al., *CD133 expression defines a tumor initiating cell population in primary human ovarian cancer*. Stem Cells, 2009. **27**(12): p. 2875-83.
58. Baba, T., et al., *Epigenetic regulation of CD133 and tumorigenicity of CD133+ ovarian cancer cells*. Oncogene, 2009. **28**(2): p. 209-18.
59. Zhang, J., et al., *CD133 expression associated with poor prognosis in ovarian cancer*. Mod Pathol, 2012. **25**(3): p. 456-64.
60. Rizzo, S., et al., *Ovarian cancer stem cell-like side populations are enriched following chemotherapy and overexpress EZH2*. Mol Cancer Ther, 2011. **10**(2): p. 325-35.
61. Kulkarni-Datar, K., et al., *Ovarian tumor initiating cell populations persist following paclitaxel and carboplatin chemotherapy treatment in vivo*. Cancer Lett, 2013. **339**(2): p. 237-46.
62. Steg, A.D., et al., *Stem cell pathways contribute to clinical chemoresistance in ovarian cancer*. Clin Cancer Res, 2012. **18**(3): p. 869-81.
63. Begley, C.G. and L.M. Ellis, *Drug development: Raise standards for preclinical cancer research*. Nature, 2012. **483**(7391): p. 531-533.
64. Gillet, J.-P., et al., *Redefining the relevance of established cancer cell lines to the study of mechanisms of clinical anti-cancer drug resistance*. Proceedings of the National Academy of Sciences, 2011. **108**(46): p. 18708-18713.
65. Domcke, S., et al., *Evaluating cell lines as tumour models by comparison of genomic profiles*. Nat Commun, 2013. **4**.
66. Sausville, E.A. and A.M. Burger, *Contributions of Human Tumor Xenografts to Anticancer Drug Development*. Cancer Research, 2006. **66**(7): p. 3351-3354.
67. Frese, K.K. and D.A. Tuveson, *Maximizing mouse cancer models*. Nat Rev Cancer, 2007. **7**(9): p. 645-58.
68. Kim, M.P., et al., *Generation of orthotopic and heterotopic human pancreatic cancer xenografts in immunodeficient mice*. Nat. Protocols, 2009. **4**(11): p. 1670-1680.
69. Rubio-Viqueira, B. and M. Hidalgo, *Direct In Vivo Xenograft Tumor Model for Predicting Chemotherapeutic Drug Response in Cancer Patients*. Clin Pharmacol Ther, 2008. **85**(2): p. 217-221.

70. Bergamaschi, A., et al., *Molecular profiling and characterization of luminal-like and basal-like in vivo breast cancer xenograft models*. *Molecular Oncology*, 2009. **3**(5–6): p. 469-482.
71. Weroha, S.J., et al., *Tumorgrafts as in vivo surrogates for women with ovarian cancer*. *Clinical Cancer Research*, 2014.
72. Dangles-Marie, V., et al., *Establishment of human colon cancer cell lines from fresh tumors versus xenografts: comparison of success rate and cell line features*. *Cancer Res*, 2007. **67**(1): p. 398-407.
73. Dobbin, Z.C., et al., *Using heterogeneity of the patient-derived xenograft model to identify the chemoresistant population in ovarian cancer*. 2014. 2014.
74. Zhao, X., et al., *Global gene expression profiling confirms the molecular fidelity of primary tumor-based orthotopic xenograft mouse models of medulloblastoma*. *Neuro-Oncology*, 2012. **14**(5): p. 574-583.
75. Houghton, P.J., et al., *The pediatric preclinical testing program: Description of models and early testing results*. *Pediatric Blood & Cancer*, 2007. **49**(7): p. 928-940.
76. Siolas, D. and G.J. Hannon, *Patient Derived Tumor Xenografts: transforming clinical samples into mouse models*. *Cancer Research*, 2013.
77. Sausville, E.A., *Contributions of Human Tumor Xenografts to Anticancer Drug Development*. *Cancer Research*, 2006. **66**(7): p. 3351-3354.
78. Press, J.Z., et al., *Xenografts of primary human gynecological tumors grown under the renal capsule of NOD/SCID mice show genetic stability during serial transplantation and respond to cytotoxic chemotherapy*. *Gynecologic Oncology*, 2008. **110**(2): p. 256-264.
79. Shiue, C.N., A. Arabi, and A.P. Wright, *Nucleolar organization, growth control and cancer*. *Epigenetics*, 2010. **5**(3): p. 200-5.
80. White, R.J., *RNA polymerases I and III, non-coding RNAs and cancer*. *Trends Genet*, 2008. **24**(12): p. 622-9.
81. Li, H., J. Zeng, and K. Shen, *PI3K/AKT/mTOR signaling pathway as a therapeutic target for ovarian cancer*. *Arch Gynecol Obstet*, 2014.
82. Drygin, D., et al., *Targeting RNA Polymerase I with an Oral Small Molecule CX-5461 Inhibits Ribosomal RNA Synthesis and Solid Tumor Growth*. *Cancer Research*, 2011. **71**(4): p. 1418-1430.
83. Shigdar, S., et al., *Clinical applications of aptamers and nucleic acid therapeutics in haematological malignancies*. *Br J Haematol*, 2011. **155**(1): p. 3-13.

84. Chefetz, I., et al., *Targeting ovarian cancer stem cells using a novel ALDH inhibitor*. Cancer Research, 2013. **73**(8 Supplement): p. 3731.
85. Lee, H.S., et al., *Clinical utility of LC3 and p62 immunohistochemistry in diagnosis of drug-induced autophagic vacuolar myopathies: a case-control study*. PLoS One, 2012. **7**(4): p. e36221.
86. Kabeya, Y., et al., *LC3, a mammalian homologue of yeast Apg8p, is localized in autophagosome membranes after processing*. Embo j, 2000. **19**(21): p. 5720-8.
87. Klionsky, D.J., et al., *Guidelines for the use and interpretation of assays for monitoring autophagy in higher eukaryotes*. Autophagy, 2008. **4**(2): p. 151-75.
88. Komatsu, M. and Y. Ichimura, *Physiological significance of selective degradation of p62 by autophagy*. FEBS Lett, 2010. **584**(7): p. 1374-8.
89. Lu, Z., et al., *The tumor suppressor gene ARHI regulates autophagy and tumor dormancy in human ovarian cancer cells*. J Clin Invest, 2008. **118**(12): p. 3917-29.
90. Pyne, N.J. and S. Pyne, *Sphingosine 1-phosphate and cancer*. Nat Rev Cancer, 2010. **10**(7): p. 489-503.
91. Morita, Y., et al., *Oocyte apoptosis is suppressed by disruption of the acid sphingomyelinase gene or by sphingosine -1-phosphate therapy*. Nat Med, 2000. **6**(10): p. 1109-1114.
92. Jurisicova, A., et al., *Molecular requirements for doxorubicin-mediated death in murine oocytes*. Cell Death Differ, 2006. **13**(9): p. 1466-1474.
93. Zhang, N., et al., *Combination of FTY720 with cisplatin exhibits antagonistic effects in ovarian cancer cells: role of autophagy*. Int J Oncol, 2013. **42**(6): p. 2053-9.
94. Beau, I., A. Esclatine, and P. Codogno, *Lost to translation: when autophagy targets mature ribosomes*. Trends in Cell Biology, 2008. **18**(7): p. 311-314.
95. Ross, J.S., et al., *Comprehensive genomic profiling of epithelial ovarian cancer by next generation sequencing-based diagnostic assay reveals new routes to targeted therapies*. Gynecol Oncol, 2013. **130**(3): p. 554-9.
96. Hart, L.S., et al., *ER stress-mediated autophagy promotes Myc-dependent transformation and tumor growth*. The Journal of Clinical Investigation, 2012. **122**(12): p. 4621-4634.
97. Ruggero, D., et al., *The translation factor eIF-4E promotes tumor formation and cooperates with c-Myc in lymphomagenesis*. Nat Med, 2004. **10**(5): p. 484-6.

98. Hemann, M.T., et al., *Evasion of the p53 tumour surveillance network by tumour-derived MYC mutants*. Nature, 2005. **436**(7052): p. 807-11.
99. Pelengaris, S., M. Khan, and G.I. Evan, *Suppression of Myc-induced apoptosis in beta cells exposes multiple oncogenic properties of Myc and triggers carcinogenic progression*. Cell, 2002. **109**(3): p. 321-34.
100. van Riggelen, J., A. Yetil, and D.W. Felsher, *MYC as a regulator of ribosome biogenesis and protein synthesis*. Nat Rev Cancer, 2010. **10**(4): p. 301-309.
101. Dang, C.V., *Enigmatic MYC Conducts an Unfolding Systems Biology Symphony*. Genes Cancer, 2010. **1**(6): p. 526-531.
102. Hanahan, D. and R.A. Weinberg, *The hallmarks of cancer*. Cell, 2000. **100**(1): p. 57-70.

APPENDIX A: INSTITUTIONAL REVIEW BOARD APPROVAL

OMB No. 0990-0263
Approved for use through 1/31/2012

Protection of Human Subjects Assurance Identification/IRB Certification/Declaration of Exemption (Common Rule)

Policy: Research activities involving human subjects may not be conducted or supported by the Departments and Agencies adopting the Common Rule (56FR28003, June 18, 1991) unless the activities are exempt from or approved in accordance with the Common Rule. See section 101(b) of the Common Rule for exemptions. Institutions submitting applications or proposals for support must submit certification of appropriate Institutional Review Board (IRB) review and approval to the Department or Agency in accordance with the Common Rule.

Institutions must have an assurance of compliance that applies to the research to be conducted and should submit certification of IRB review and approval with each application or proposal unless otherwise advised by the Department or Agency.

1. Request Type <input type="checkbox"/> ORIGINAL <input type="checkbox"/> CONTINUATION <input type="checkbox"/> EXEMPTION	2. Type of Mechanism <input type="checkbox"/> GRANT <input type="checkbox"/> CONTRACT <input type="checkbox"/> FELLOWSHIP <input type="checkbox"/> COOPERATIVE AGREEMENT <input type="checkbox"/> OTHER: _____	3. Name of Federal Department or Agency and, if known, Application or Proposal Identification No.
4. Title of Application or Activity Characterization and Targeting of the Aldehyde Dehydrogenase Subpopulation in Ovarian Cancer		5. Name of Principal Investigator, Program Director, Fellow, or Other LANDEN JR., CHARLES N.

6. Assurance Status of this Project (*Respond to one of the following*)

- This Assurance, on file with Department of Health and Human Services, covers this activity:
 Assurance Identification No. FWA00005960, the expiration date 10/26/2010 IRB Registration No. IRB00000196
- This Assurance, on file with (*agency/dept*) _____, covers this activity.
 Assurance No. _____, the expiration date _____ IRB Registration/Identification No. _____ (*if applicable*)
- No assurance has been filed for this institution. This institution declares that it will provide an Assurance and Certification of IRB review and approval upon request.
- Exemption Status: Human subjects are involved, but this activity qualifies for exemption under Section 101(b), paragraph _____.

7. Certification of IRB Review (*Respond to one of the following IF you have an Assurance on file*)

- This activity has been reviewed and approved by the IRB in accordance with the Common Rule and any other governing regulations.
 by: Full IRB Review on (date of IRB meeting) _____ or Expedited Review on (date) 12/22/09
 If less than one year approval, provide expiration date _____
- This activity contains multiple projects, some of which have not been reviewed. The IRB has granted approval on condition that all projects covered by the Common Rule will be reviewed and approved before they are initiated and that appropriate further certification will be submitted.

8. Comments Protocol subject to Annual continuing review.	Title X091119014 Characterization and Targeting of the Aldehyde Dehydrogenase Subpopulation in Ovarian Cancer
--	--

IRB Approval Issued: 12/23/09

9. The official signing below certifies that the information provided above is correct and that, as required, future reviews will be performed until study closure and certification will be provided. 11. Phone No. (<i>with area code</i>) (205) 934-3789 12. Fax No. (<i>with area code</i>) (205) 934-1301 13. Email: smoores@uab.edu	10. Name and Address of Institution University of Alabama at Birmingham 701 20th Street South Birmingham, AL 35294
14. Name of Official Marilyn Doss, M.A.	15. Title Vice Chair, IRB
16. Signature	17. Date <u>12-22-09</u>

Authorized for local Reproduction Sponsored by HHS

Public reporting burden for this collection of information is estimated to average less than an hour per response. An agency may not conduct or sponsor, and a person is not required to respond to, a collection of information unless it displays a currently valid OMB control number. Send comments regarding this burden estimate or any other aspect of this collection of information, including suggestions for reducing this burden to: OS Reports Clearance Officer, Room 503 200 Independence Avenue, S.W., Washington, DC 20201. Do not return the completed form to this address.

APPENDIX B: INSTITUTIONAL ANIMAL CARE AND USE COMMITTEE APPROVAL




THE UNIVERSITY OF ALABAMA AT BIRMINGHAM

Institutional Animal Care and Use Committee (IACUC)

NOTICE OF APPROVAL

DATE: June 9, 2010

TO: Landen, Charles N. Jr.
SHEL-505
934-0473

FROM: 
Judith A. Kapp, Ph.D., Chair
Institutional Animal Care and Use Committee

SUBJECT: Title: Examination of the True Mediators of Chemoresistance in Ovarian Cancer
Sponsor: Internal
Animal Project Number: 100609077

On June 9, 2010, the University of Alabama at Birmingham Institutional Animal Care and Use Committee (IACUC) reviewed the animal use proposed in the above referenced application. It approved the use of the following species and numbers of animals:

Species	Use Category	Number in Category
Mice	C	250

Animal use is scheduled for review one year from June 2010. Approval from the IACUC must be obtained before implementing any changes or modifications in the approved animal use.

Please keep this record for your files, and forward the attached letter to the appropriate granting agency.

Refer to Animal Protocol Number (APN) 100609077 when ordering animals or in any correspondence with the IACUC or Animal Resources Program (ARP) offices regarding this study. If you have concerns or questions regarding this notice, please call the IACUC office at 934-7692.

Institutional Animal Care and Use Committee
CH19 Suite 403
933 19th Street South
205.934.7692
FAX 205.934.1188

Mailing Address:
CH19 Suite 403
1530 3RD AVE S
BIRMINGHAM AL 35294-0019